

ROLE OF HISTONE METHYLATION AND VARIANTS IN GENOME FUNCTION

Deepak Kumar Jha

A dissertation submitted to the faculty of the University of North Carolina at Chapel Hill in partial fulfillment of the requirements for the degree of Doctor of Philosophy in the Department of Biochemistry and Biophysics in the School of Medicine.

Chapel Hill
2014

Approved by:

Brian Strahl

Dale Ramsden

Kerry Bloom

Jean Cook

Scott Bultman

© 2014
Deepak Kumar Jha
ALL RIGHTS RESERVED

ABSTRACT

Deepak Kumar Jha: Role of histone methylation and variants in genome function
(Under the direction of Brian Strahl)

The eukaryotic genome is compacted in the form of chromatin, which is a complex of DNA and histone proteins. Regulation of chromatin structure influences all aspects of cellular processes, especially the DNA –dependent processes. The basic unit of chromatin is composed of DNA wrapped around a core of octameric histones, forming what is called the nucleosome core particle. The dynamic nature of this structure implies that there will be well-regulated processes and pathways that help in the interchanges between one form of chromatin and another. In *chapter 1*, I outline the current state of literature for mechanisms that regulate chromatin structure, with special emphasis on histone modifications and histone variants. I also review the literature for genome maintenance and how chromatin regulates genomic integrity.

One of the most critical histone modifications that regulate chromatin structure is the methylation of histone H3 at lysine 36 (H3K36me). Set2 catalyzes H3K36me and its function is well established in regulation of chromatin structure during transcription elongation, but its function in maintaining the integrity of yeast genome was not known. In *chapter 2*, I describe its novel function in regulating chromatin structure after double strand break (DSB). Work from chapter 2 reveals that Set2-dependent H3K36me (2/3) and its interaction with RNA polymerase

II (RNAPII) is critical for surviving DSBs after phleomycin. It also shows that H3K36me is critical for full activation of a DSB checkpoint. Furthermore, I show that H3K36me is also important for chromatin remodeling around a DSB, abrogation of which subsequently facilitates inappropriate end-processing. In *chapter 3*, I describe our ongoing efforts to delineate the dynamic incorporation/eviction of the histone variant Htz1 in yeast. I show that deletion of *NAPI* and *CHZ1* results in increased retention of Htz1 in yeast chromatin, and show that there are two non-overlapping surfaces on the Htz1-H2B nucleosome. Furthermore we show that specific point mutations of these residues have biochemical and biological effects on cells. In *chapter 4*, I describe the implications of my research, place it in the wider context of chromatin research and discuss the contribution of H3K36me and Htz1 in tumorigenesis.

To my parents

ACKNOWLEDGEMENTS

I would like to thank my family for supporting all of my endeavors: my mother, my two elder sisters and my wife.

My friends from the All India Institute of Medical Sciences: Jaideep, Angshuman Mandal, Tathagat Duttaray, Suvenu Lomash, Suryadeep Dash, Suvi Jain, Samarpita Sengupta, Sohini Mukherjee, Sandhya Pande, N. Govindrajan, Neha Dikshit, Swarna Mehrotra, Seema Mittal, Debabrata Panja, Subhanjan Mondal, and Shikhar Agarwal.

My friends from Jawaharlal Nehru University: Sayantan Bose, Dipti Karmarkar, Manish Kushwaha, Surendra Shukla, Praveen Kumar Singh, Tribhuvan Yadav, Deepak Kumar, Nitesh Kumar, and Sutirtha Dutta.

My friends from UNC-Chapel Hill: Robert Sons, Brent Hehl, Kelly Watson, Liz Lessey-Morillon, Maria Aleman, Dileep Varma, Anita Nair-Varma, Daniel Dominguez, Justin English, Lindsay-Faircloth Rizzardi, Aaron Nile, Kate Coleman and all of the office staff in the Department of Biochemistry and Biophysics.

I would like to thank current and past members of the Strahl Lab, in particular: Raghuvar Dronamraju, for always coming up with interesting ideas and having insightful discussions; Steve Fuchs, for initiating me onto yeast genetics; Kate Gardner, for encouragement and expectations; Krzysztof Krajewski, for tolerating me as a neighbor and scientific and political discussions; Scott Rothbart, for coffee trips and maintaining a fun environment.

I would also like to thank the 3rd floor GMB neighbors- members of the Cook lab (especially Lindsay Rizzardi, Kate Coleman, Karen Reidy, and Srikrupa) and the Dohlman lab (especially Steve Cappell, Michal Nagiec, Matt Torres and Justin English).

This work and my own graduate education would not be complete without the help of my thesis committee: Dale (for his incisive comments and high expectations, and especially for pointing me to relevant literatures early on); Kerry (for scientific and career advice and allowing me to audit his microscopy class); Jean (for her comments on my work and science in general, and numerous career advice sessions in the 3rd floor GMB team area) and Scott (for his enthusiasm and support- inside and outside the committee meetings). In addition, UNC allowed me to interact and benefit from numerous faculties in the department of Biochemistry and Biophysics, as well as Genetics and Pharmacology. Specifically, interactions with Henrik Dohlman, Richard Wolfenden, Bill Marzluff, Zefeng Wang, Vytas Bankaitis, Bob Duronio (also my first rotation mentor), Beverly Errede, Greg Wang, and Jeremy Purvis have been fun, informative, and always gave me the extra push to succeed.

To Brian, for giving me the freedom and opportunities that I needed to succeed.

PREFACE

Chapter 2 is an extended version of work published in *Nature Communications*, June 9th 2014 titled ‘**An RNA Polymerase II-coupled function for histone H3K36 methylation in checkpoint activation and DSB repair**’ (Jha & Strahl, 2014; Nature Communications; June 9th 1).

Chapter 3 is derived from a manuscript being prepared for *Nature Structural and Molecular Biology*. This will be co-first authored with Srinivas Ramachandran and Michael Parra.

Parts of figures and text in Chapter 4 were modified with permission from an article published in *Nature Structural and Molecular Biology* (2014) titled “**SET-ting the stage for DNA repair**” (Jha, Strahl *et.al* 2014)².

TABLE OF CONTENTS

LIST OF TABLES	xiv
LIST OF FIGURES	xiv
LIST OF ABBREVIATIONS.....	xvi
CHAPTER 1- REGULATION OF CHROMATIN STRUCTURE AND ITS INFLUENCE ON GENOME FUNCTION	1
1.1 Introduction to chromatin structure	1
1.2 Mechanisms of regulating chromatin structure.....	2
1.3 Lysine Methylation of Histones.....	7
1.4 Description of Set2/H3K36me from yeast to man.....	9
1.5 Regulation of chromatin structure by Htz1/H2A.Z	14
1.6 Maintenance of genomic integrity in eukaryotes.....	15
1.7 DNA damage Checkpoint Activation.....	19
1.8 Interplay of chromatin with DSB signaling and DSB repair	20
CHAPTER 2: AN RNA POLYMERASE II-COUPLED FUNCTION FOR HISTONE H3K36 METHYLATION IN CHECKPOINT ACTIVATION AND DSB REPAIR.....	27
2.1 Overview.....	27
2.2 Introduction.....	27
2.3 Results.....	29

2.3.1 Set2/H3K36me is required for resistance to DSB	29
2.3.2 <i>SET2</i> is functionally connected to DSB response and repair.....	30
2.3.3 Set2/H3K36me regulates checkpoint activation after DSB.....	34
2.3.4 H3K36me2 and me3 are DSB-inducible and present at DSBs.....	39
2.3.5 Interplay between Set2 and chromatin regulators after DSB.....	43
2.3.6 Set2 regulates chromatin dynamics around a DSB.....	45
2.3.7 Set2 regulates DSB repair in the context of transcription.....	50
2.4 Discussion	55
2.5 Methods.....	59
CHAPTER 3: RATIONAL DESIGN OF H2A.Z MUTANTS UNCOVER DIFFERENTIAL CHAPERONE INTERACTIONS AND FUNCTION.....	64
3.1 Abstract	64
3.2 Introduction.....	65
3.3 Results.....	
3.3.1 Chz1 and Nap1 function in H2A.Z eviction	66
3.3.2 Constraint-driven CZB structural ensemble generated by DMD simulations.....	67
3.3.3 Diverse interactions drive specific recognition of H2A.Z-H2B by Chz1	68
3.3.4 Interrogating the H2A.Z-H2B binding surface of Chz1	70
3.3.5 H2A.Z-Chz1 destabilizing mutants result in impairment of H2A.Z levels in chromatin	70

3.3.6 H2A.Z mutations disrupt specific chaperone interactions	72
3.3.7 Mutations predicted to affect H2A.Z-chaperone interactions disrupt H2A.Z function	73
3.3.8 Characterization of a novel and toxic H2A.Z form that is dependent on chromatin deposition	74
3.4 Discussion	78
3.5 Materials and methods	81
CHAPTER 4: CONCLUSIONS, UNANSWERED QUESTIONS AND DISEASE RELEVANCE	85
4.1 Conclusion for Chapter 2	85
4.2 Outstanding Questions	93
4.3 Disease Relevance	95
4.4. Conclusion for chapter 3	97
4.5 Unanswered Questions and Perspective	100
LIST OF YEAST STRAINS USED IN CHAPTER 2	102
LIST OF YEAST STRAINS USED IN CHAPTER 3	106
REFERENCES.....	114

LIST OF TABLES

Table 1: Major histone variants across eukaryotes and their functions	5
Table 2: Chapter one summary	26
Table 3: Chapter two summary	63
Table 4: Chapter three summary	84
Table 5: Yeast strains used in Chapter 2	102
Table 6: Yeast strains used in Chapter 3	107

LIST OF FIGURES

Figure 1: A schematic model the function of yeast Set2/H3K36me.	11
Figure 2. Methylation by Set2 at H3K36 and RNAPII–Set2 interaction is required for cellular resistance against double strand break (DSB).	31
Figure 3. <i>set2Δ</i> is sensitive to persistent but reparable DSB at ADH4 locus and <i>set2Δ</i> does not alter yKu80 protein levels.	32
Figure 4. <i>SET2</i> functionally interacts with DNA damage response and repair genes.	37
Figure 5. DNA damage signaling is attenuated in <i>set2Δ</i>	39
Figure 6. <i>set2Δ</i> leads to reduced DNA damage checkpoint activation.	39
Figure 7. Temporal regulation of H3K36me3 and H3K36me2 is driven by regulated down-regulation of Set2.	41
Figure 8. Regulation of Set2 and Rpb1 after DSB.	45
Figure 9. Set2 regulates chromatin remodeling after DSB induction.	50
Figure 10. Set2 primarily functions in DSB repair in the context of a transcribing unit.	53
Figure 11. A simplified model depicting a function of Set2 and H3K36me in regulating DNA damage response and repair.	54
Figure 12. <i>nap1Δ</i> and <i>chz1Δ</i> result in increased Htz1 levels in the chromatin.	67

Figure 13. Molecular recognition of H2A.Z-H2B by Chz1.....	69
Figure 14. Protein (A) and RNA (B) levels of Htz1 mutants and their ability to get incorporated into the chromatin.....	71
Figure 15. Unique mutations disrupt Nap1-Htz1 interactions.....	73
Figure 16. Biological consequences of the point mutants of Htz1.....	76
Figure 17. Inappropriate incorporation of Htz1 mutants results in defects in cell growth.....	77
Figure 18. Hypothetical model for the basis of “separation-of-function” between different H2A.Z-specific chaperones.....	81
Figure 19. H3K36 methylation functions in DSB sensing and repair.....	91

LIST OF ABBREVIATIONS AND SYMBOLS

°	Degree
Δ	Deletion
Å	Angstrom(10^{-10} meter)
aa	Amino acid
ATP	Adenosine triphosphate
BSA	Bovine serum albumin
CEN	Centromeric plasmid
CHX	Cycloheximide
DMSO	Dimethyl sulfoxide
EDTA	Ethylenediaminetetraacetic acid
GO	Gene ontology
hr	Hour
kDa	Kilodalton
M	Molar
m	10^{-3}
m	Meter

mg	Milligram
min	Minute
mm	Millimolar
MS	Mass spectrometry
MW	Molecular weight
NaCl	Sodium chloride
n	10^{-9}
nM	Nanomolar
nm	Nanometer
NMR	Nuclear magnetic resonance
OD	Optical density
p	10^{-12}
PAGE	Polyacrylamide gel electrophoresis
PDB	Protein databank file
PMSF	Phenylmethanesulfonyl fluoride
RNA	Ribonucleic acid
RNAi	RNA interference

Rpm	Rotations/minute
s.d	Standard deviation
SDS	Sodium doadecyl sulfide
s.e.m	Standard error mean
SGA	Synthetic genetic array
siRNA	Small interfering RNA
TCA	Trichloroacetic acid
<i>ts</i>	Temperature sensitive
UV	Ultra violet light
μ	10^{-6}
μ l	Microliter
μ M	Micro molar
WT	Wild-type
wt	Weight
YPD	Yeast peptone dextrose
vol	Volume

CHAPTER 1: REGULATION OF CHROMATIN STRUCTURE AND ITS INFLUENCE ON GENOME FUNCTIONS

1.1 Introduction to chromatin structure

Prokaryotes and eukaryotes are the two major branches of life on earth. The fundamental difference between the two classes is the presence of a nucleus, a central organelle tasked with storing the genetic material in the form of DNA. In the case of eukaryotes, the DNA is packaged with histone proteins inside the nucleus³. In the case of humans, the total genome size is about 3 billion base-pairs, which has to fit into a nucleus of about 10 micron in diameter – a packaging ratio of about 10^6 ⁴. To accomplish that cells compact the genome by wrapping the DNA around the core of 8 histone proteins. Histone proteins are highly basic proteins and typically they consists of two copies each of histone H2A, H2B, H3 and H4. One-hundred and forty-seven base pair of DNA double helix wraps around the core octamer of histone proteins, forming what is called the nucleosome core particle (NCP)⁴. The NCPs are the fundamental building blocks of chromatin and serve multiple purposes in regulating the genome activity and integrity⁴. NCPs package the genome to accommodate it in the nuclei, restrict access to the DNA to prevent DNA damage, hide or expose regulatory sequences for appropriate modulation of genome function. In addition to the well-established role of nucleosomes in chromatin compaction, eukaryotic genomes also undergo several long-range interactions that further pack the genome and organize the nuclei in specific domains based on access to DNA, transcription activity, and association with the nuclear membrane^{5,6}. Such three-dimensional organizations have come to occupy a central focus in our understanding of nuclear architecture and function^{5,6}.

1.2 Mechanisms of regulating chromatin structure:

During the life cycle of a cell, it has to grow by acquiring nutrients, divide and reproduce and maintain a relatively error free genome while braving a variety of stresses- both endogenous and exogenous. In terms of the cell's life, it needs to obtain nutrients and grow (G1- phase of the cell cycle), divide and reproduce (S-G2, M) and maintain the fidelity of its genome ^{7,8}. All these processes necessitate a dynamic chromatin transactions- alteration of chromatin structure between various levels of access, both at the local (G1, S and during DNA repair) and global (G2-M and DNA repair) levels. To accomplish this, cells have a variety of mechanisms that include: modification of histone proteins, using the energy of ATP to remodel the chromatin structure, using variant histones with altered biochemical and biophysical properties, and using RNA-based mechanisms ⁹⁻¹². All these mechanisms will be described in the following sub-sections:

a) *Histone Modifications*: Histone proteins are highly basic proteins that bind, rather tightly, to DNA through electrostatic interactions ^{3,4}. Addition of covalent chemical moieties to histone proteins can alter the biochemical/ biophysical properties of histone proteins and disrupt either general DNA-histone contact or locally alter the histone-DNA interaction ¹³. For example, addition of a negatively charged acetyl group on lysine residues of histone proteins can disrupt the strong electrostatic interactions between DNA and histone proteins ¹⁴⁻¹⁶. The early stage of chromatin research was primarily reliant on this simplistic interpretation of histone modifications. Additionally, it was also assumed that the modifications would generally occur on the unstructured tails of the histone protein and leave the central structured part of histone untouched. Discovery of histone methylation, and in particular modification of core residues in histones (H3 Lysine 79 methylation; H3K79me) (van Leeuwen, 2002 #24) and acetylation of

lysine 56 of histone H3; H3K56Ac¹⁷) challenged the afore-mentioned simplistic idea. To date, a large number of histone modifications have been discovered that span a vast chemical space such as acetylation, methylation, phosphorylation, ubiquitination, palmitoylation, crotonylation and sumoylation^{11,18-21}. The underlying mechanism that seems to provide a reasonable explanation for these modifications comes from the ‘histone code’ hypothesis²²⁻²⁵. The ‘Histone code’ hypothesis, as proposed about a decade ago, expounded on the possibility that individual histone modifications or their combinations will act as a sign-post for the genome and recruit protein(s) that can subsequently possess enzymatic activity capable of dynamically altering chromatin structure and effecting biological functions²²⁻²⁵. Retrospectively, although quite simplistic, the histone code hypothesis serves as a useful way to understand how these myriad histone modifications can result in multiple biological outcomes. Given the complexity of these histone modifications, lack of strict ‘keys’ that can deduce their downstream function, histone modifications should be (and are to some extent) thought of more as a ‘language’ than ‘code’ – since downstream function of several of these histone modifications are dependent on context similar to words having different meaning in different contexts²⁶⁻²⁸. The array of histone modifications that have been discovered in model organisms as well as human cells is quite large and complex and with the technological advancements in discovery of cellular post-translational modifications (PTMs), the field has exploded in recent times²⁹. The study of histone PTMs has impacted our understanding of gene regulation, DNA repair, cell division, and organismal development²⁹.

b) *ATP-dependent chromatin remodelers*: An attractive way of accessing the underlying the DNA sequence of the chromatin is to disrupt the nucleosome, either partially or completely^{9,30-34}. Cells have enzymes that use the energy stored in ATP, and accomplish exactly that. These

enzymes belong to the class of ATP-dependent chromatin remodelers. Some of the defining features of proteins belonging to this class are: i) Ability to bind to DNA and nucleosomal components, including histone modifications ii) DNA-dependent ATPase activity, albeit the DNA structures that activate the ATPase can vary depending upon the class of remodeler and iii) presence of multiple domains in the proteins, some of which can be used for protein-protein interactions and modulation of ATPase activity⁹.

Essentially, all ATP-dependent remodelers perform one of the following functions: a) reposition nucleosomes to either unravel the underlying DNA sequence or hide it and b) disrupt the nucleosome structure either by eviction of histone dimers or altering the octamer composition by incorporating histone variants^{9,35,36}. Many of these ATP-dependent remodelers exist as multi-protein complexes and are required for multiple cellular functions involving dynamic changes in chromatin structures^{9,36}. For example, the INO80 ATP-dependent remodeler functions during double strand break (DSB) repair, transcription regulation, DNA replication³⁷ and the SWR1 complex is similarly required for maintenance of chromatin organization during gene expression and DNA repair³⁸. In higher organisms, various ATP-dependent remodelers are crucial for appropriate developmental progression. For example, the Brg1 null mouse is embryonically inviable³⁹. An interesting mechanism to regulate the function of these remodelers is to alter their subunit composition- resulting in widely different cellular outcomes. For example, work from the Crabtree lab has shown that a critical exchange of subunits in hSWI/SNF occurs during vertebrate development⁴⁰. For example, appropriate neural differentiation is dependent upon incorporation of different versions of BAF45 and BAF53 subunits (BAF45 and 53a in the neuronal progenitors vs. BAF45/53b in post-mitotic neurons)⁴⁰. In sum, ATP-dependent

chromatin remodelers function, both in isolation and in combination with histone modifications to dynamically alter the chromatin structure and influence cellular processes.

c) *Histone variants*: A typical nucleosome consists of two copies each of histones H2A, H2B, H3 and H4. Additionally, in higher eukaryotes, there exists histone H1, which acts as linker histone between NCPs ⁴. However, there are a large number of atypical histones, called histone variants that differ in sequence, genomic location and functions ^{41,42}. Some of the more ubiquitous variants for the histones are listed below:

Variant	Species	Function
MacroH2A	All vertebrates	X-chromosome inactivation
H2ABbd	All vertebrates	Transcription
H2A.X	All eukaryotes	Genome integrity, Transcription
H2A.Z	All eukaryotes	Transcription, genome integrity
CenH3	All eukaryotes	Centromere
H3.3	All eukaryotes	Transcription

Besides these more common histone variants, there are species-specific variants such as histone H1⁰ in mouse ⁴³. Typically, these histones are regulated in a manner quite different from the canonical histones. Canonical histones are synthesized in an S-phase dependent manner while the variants may not be subjected to the same set of regulatory mechanisms ^{44,45}. Histone variants are also differentially incorporated into the chromatin- temporally or spatially. For example, H2A.Z containing nucleosomes are present around the transcription start sites (TSS)

and in the sub-telomeric heterochromatin⁴⁶⁻⁴⁸. They are specifically excluded from within the gene bodies⁴⁶⁻⁴⁸. Another example is incorporation of H2A.X around a DNA damage sites in eukaryotes⁴⁹. Presence of H2A.X (and its subsequent phosphorylation) acts as one of the first signals of DNA damage response in cells. Another recently described function of H2A.X is its ability to function as a ‘bookmark’ during stem cell differentiation⁵⁰. Presence of histone variants alters the biophysical characters of the nucleosomes as well. For example the H2A.Z containing nucleosome is substantially more prone to salt-dependent dissociation than an H2A-containing nucleosome⁵¹. Another layer of complexity arises when the histone variants are also modified (H2A.X phosphorylation at Serine 139 is described above; sumoylation of H2A.Z is critical for relocation of a double strand break to the nuclear periphery) [Kalocsay, 2009 #62]. Recently, a large number of histone variants and their mutations have been associated with different kinds of cancers. Most notably, mutation at lysine 36 or lysine 9 of the histone variant H3.3 to methionine (H3.3K36M or H3.3K9M) have been shown as drivers of pediatric glioblastomas^{42,52-54}, again reinforcing the idea that histone variants perform critical functions in regulating chromatin structure and genome function.

d) Non-coding RNA: Biochemical purification of chromatin results in recovery of about twice as much RNA as DNA, which led to the conception that RNA can regulate chromatin structure and function⁵⁵. Over the past few years, a large number of RNAs have been isolated that directly impact chromatin structure, and chromatin-templated processes in cells⁵⁵. These RNAs comprise the now famous long non-coding RNAs (lncRNAs). One of the most famous lncRNAs is the Xist RNA that regulates X-chromosome inactivation^{55,56}. Xist is synthesized from one of the two X-chromosomes and then results in recruitment of the chromatin modifier, Polycomb repressor complex (PRC2), to the silenced X-chromosome^{55,56}. PRC2 catalyzes

H3K27me3, which is associated with transcriptional silencing and thereby promotes X-chromosome inactivation in higher humans^{55,56}. PRC2 also associates with another lncRNA, HOTAIR, which recruits it to several sites in the genome to control gene-silencing⁵⁷. A new class of RNAs has been recently discovered, called enhancer RNAs (eRNAs), which are lncRNAs that emanate from enhancer regions marked with H3K4me1, H3K27Ac and p300 histone acetyltransferase protein⁵⁸. Such eRNAs were shown to be critical for gene activation of nearby genes⁵⁸. In sum, non-coding RNAs in general and lncRNAs in particular have become increasingly important in regulation of chromatin structure and function.

1.3 Lysine Methylation of Histones

A major class of histone modifications in eukaryotes is the methylation of lysines and arginines in histones, predominantly histone H3 and histone H4. Methylation of histone H3 and H4 have been extensively studied and these modifications have been shown to be critical for regulation of transcription, replication, DNA replication, mitosis, meiosis and appropriate developmental progression. For histone H3, the most well studied methylation involves methylation of histone H3 lysine 4, 9, 27, 36 and 79 while for histone H4 the most well studied methylation is at lysine 20.

Two classes of methyltransferases catalyze lysine methylation of histones: SET domain and non-SET domain methyltransferase. SET domain stands for SuVar3–9, Enhancer of Zeste, Trithorax and forms the largest class of histone methyltransferase (HMTs)⁵⁹. There are seven main families, across all eukaryotes, for the SET domain containing lysine methyltransferases- SET1, SET2, SUV39, EZ, RIZ, SMYD and SUV4-20⁵⁹. In addition, PR-Set7/Set8 and Set7/9 are two additional HMTs, which do not belong to a particular class. Some SET domain containing HMTs can act on peptides (e.g. G9a), while others prefer nucleosomal substrates

(e.g. Set2)⁵⁹. HMTs have specificity in terms of the methylation states (mono-, di- and tri-) that they can achieve on the lysine residues. Different methylation states tend to have different localization in the genome and hence different functions as well. In budding yeast, the major SET domain containing HMTs are Set1, Set2 and Set5, while the non-SET domain containing HMT is Dot1.

Set1 is required for methylation of lysine 4 on histone H3 (H3K4me1/2/3)⁶⁰. H3K4me is associated with active transcription, where H3K4me3 is present in the promoter and 5' end of genes while H3K4me2 is spread across the gene body⁶¹. In contrast, H3K4me1 is enriched towards the 3' end of genes⁶¹. *In vitro* experiments support the idea that presence of H3K4me3 activates transcription⁶². In human cells, H3K4me1 is associated with enhancers regions of the gene⁶³. Beyond regulation of transcription elongation, H3K4me2 has also been associated with positive regulation of replication initiation in budding yeast⁶⁴. Consistent with the yeast data, H3K4me is also critical for replication in human cells⁶⁵. Set1 and H3K4me has also been recently linked with maintenance of genome integrity, specifically with the regulation of DSB sensing and repair⁶⁶. Interestingly, H3K4me is also associated with initiation and regulation of meiotic double strand break and overall efficiency of meiosis- both in yeast and humans^{67,68}.

Set5 is a newly discovered HMT, responsible for mono methylation of H4 K5, 8 and 12⁶⁹. It was proposed that Set5 is required for maintenance of appropriate chromatin structure along with global regulators of chromatin structure like NuA4 and COMPASS (Set1-containing complex)⁶⁹. This regulation of chromatin structure by Set5 was linked to stress response in budding yeast, but no clear mechanism was elucidated⁶⁹. Dot1 is the sole non-SET domain HMT in budding yeast. Dot1 is responsible for methylation of H3K79 (all three forms of methylation)⁷⁰. Dot1 stands for Disruptor of Telomeric silencing, derived from its function in

regulating telomeric silencing of genes ⁷⁰. H3K79me is also present in the gene bodies but its specific function and proteins that can recognize it are not clearly understood ⁶³. H3K79me has significant role in maintenance of genomic integrity- stabilizing Rad9 on the chromatin around DSBs, activating DNA damage response in response to MMS and replication stress, and negatively regulating resection ⁷¹. In human cells, Dot1L (human homolog of Dot1) is required for H3K79me1/2 and is necessary for embryonic development ^{72,73}. Tissue specific loss of Dot1L revealed that Dot1 is critical for cardiac development ⁷³.

Set2 and methylation of H3K36 will be dealt with in detail in the following section.

1.4 Description of Set2/H3K36me from yeast to man:

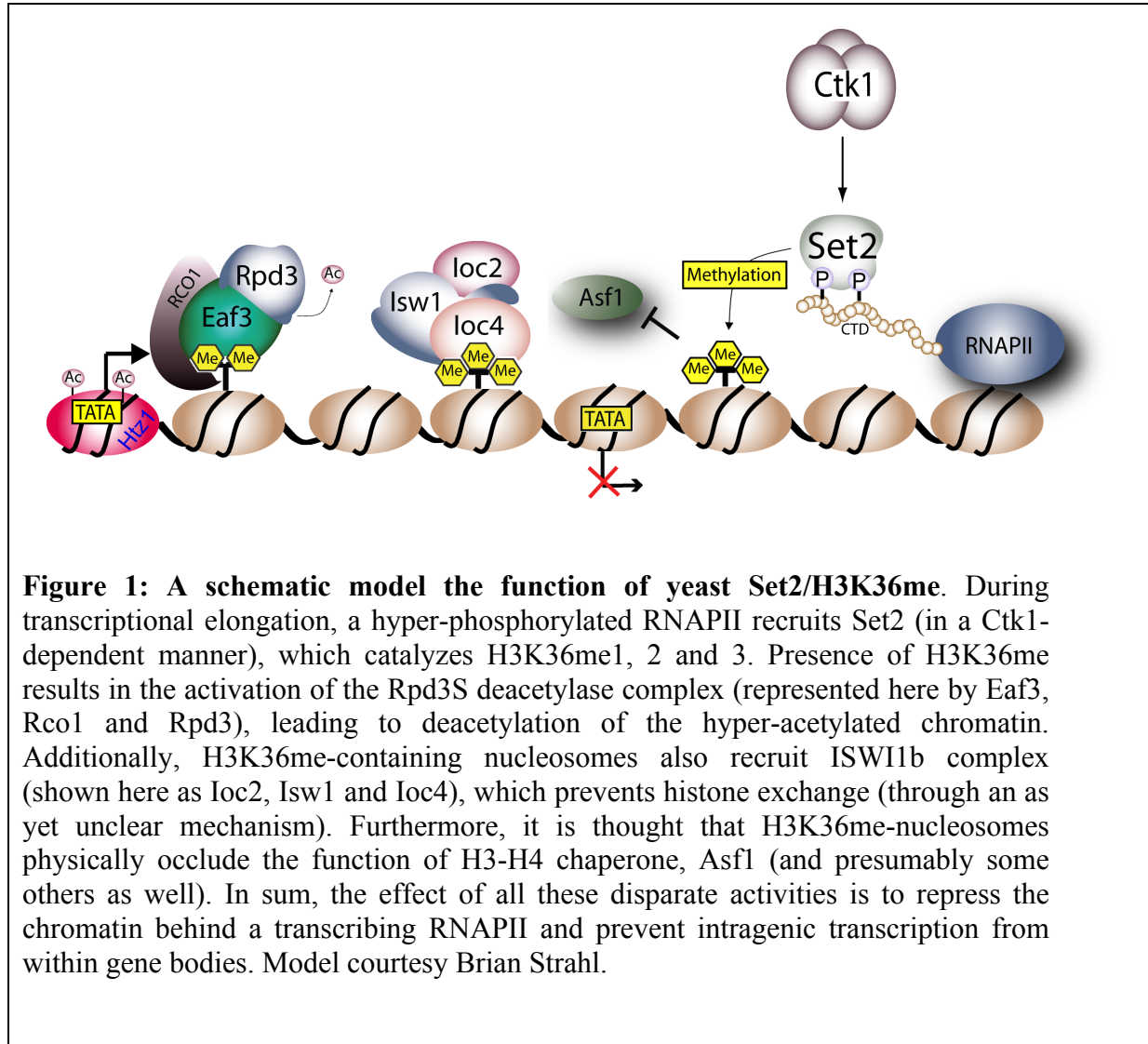
As mentioned before, methylation of lysine 36 (H3K36me) is a highly conserved histone methylation from yeast to humans ⁷⁴. This modification occurs at position 36 of histone H3, a rather interesting position from the structural perspective. Lysine 36 is close to the entry- and exit- points of DNA in a nucleosome core particle. Therefore, any modification of this position will likely influence the structure of nucleosome as well, besides the modifications acting as recruitment platform for various protein complexes. H3K36me was discovered in budding yeast and Set2 was the enzyme that was implicated for this histone modification ⁷⁵. Set2 (and its homologs and orthologs) are present from yeast to human ⁷⁴.

Set2 is a nucleosomal histone methyltransferase belonging to the SET-domain class of methyltransferases ⁷⁴. The human homolog of yeast Set2 is SETD2, which is frequently mutated in clear cell renal cell carcinoma, and some classes of breast cancer and glioblastoma ^{74,76}. In yeast, Set2 is capable of all forms of H3K36 methylation

(H3K36me1/2 and 3) while in higher organisms (primarily metazoans) the capability is restrictive ⁷⁴. Human SETD2 can only catalyze H3K36me3 while there are multiple H3K36me1/2 methyltransferase (NSD (1-3), Ash1L, Setd3, SMYD2 and SETMAR) ⁷⁴. Yeast Set2 is a 733 amino acid long protein and has multiple domains that help in catalysis, recruitment to chromatin and protein-protein interactions. The definitive catalytic domain (SET) along with accessory domains exists in the extreme N-terminus (from residue 1-261) and is capable of catalyzing H3K36me1 and H3K36me2 ⁷⁷. In addition, Set2 contains a unique domain in its extreme C-terminus called the Set2-RNA Polymerase II (RNAPII) interaction domain (SRI domain) ^{78,79}. It spans from residue 619-718 and is responsible for recruiting Set2 to the elongating form of RNAPII (hyperphosphorylated at serine2 and serine 5 in the CTD of RNAPII) ^{78,79}. Furthermore, there is a coiled-coil and a WW domain in the yeast Set2, the functions of which is not clearly understood ⁷⁸.

In terms of its function, yeast Set2 is very reliant on the presence of hyperphosphorylated RNAPII for realizing its full catalytic potential (H3K36me3). During transcription cycle, the RNAPII is bound to a gene promoter and is phosphorylated on Serine5 of the C-terminal domain of the largest subunit (Rpb1) ⁸⁰. Subsequently, Bur1 (and Ctk1) phosphorylate Serine2 in the heptapeptide repeat, YSPTSPS, resulting in promoter clearance and productive elongation of RNAPII-dependent transcription ⁸⁰. This elongating RNAPII recruits Set2 to transcribed regions, which results in H3K36me1/2/3 in gene bodies ⁷⁸. The distribution of H3K36me1, me2 and me3 is stereotypical: H3K36me1 near the 5' end of genes, H3K36me2 distributed across gene bodies and H3K36me3 increases towards the 3' end of genes ⁷⁴. To date, the majority of functions of

Set2 have been shown to be driven by H3K36me2/3 and no clear function has emerged for H3K36me1. For the most part, H3K36me2/3 function in regulating chromatin structure in transcribed regions, the mechanisms are described underneath (**Figure 1**).



For a vast majority of histone modifications, the downstream function is typically dependent on protein(s) or complex(es) that recognize the modification and get recruited to chromatin. These proteins themselves contain enzymatic functions or protein-protein

interaction motifs that result in modulation of chromatin structure- an idea that was the cornerstone of the ‘histone code’ hypothesis^{22,23,25}. In the case of H3K36me, multiple groups discovered that H3K36me_{2/3} is recognized by the Rpd3(S) complex, using the methyl-recognizing (chromo and PHD) domains of Eaf3 and Rco1 subunits. Rpd3(S) complex contains the Rpd3 histone deacetylase, which removes histone acetylation from the open reading frames of genes thereby repressing the chromatin structure⁸¹⁻⁸³. Subsequently, it was clarified that the recruitment of Rpd3S was not dependent on H3K36me but its activity was⁸⁴. It was also shown that Rpd3S can bind to the CTD of RNAPII, and hence a modified model included an RNAPII-dependent recruitment of Rpd3S and its activation by H3K36me⁸⁴. Additionally, binding of Eaf3 and Rco1 to H3K36me_{2/3} acts to increase their affinity to the transcribing region of the genome⁸⁴. Furthermore, it was shown that presence of H3K36me *per se* is inhibitory to the function of transcription associated histone chaperones, primarily Asf1⁸⁵. H3K36me₃ and to some extent H3K36me₂ physically inhibited the binding of Asf1 (and to some extent FACT (Spt16) and Spt6) to nucleosomes and therefore transcription associated histone exchange was diminished⁸⁵. Further reduction in histone exchange occurred due to combined action of the ISWI1b ATP-dependent remodeling complex (that can bind to H3K36me-nucleosomes) and Chd1 protein⁸⁶. In sum, due to the activation of the Rpd3S deacetylase complex, and inhibition of histone exchange (by the combined action of Chd1 and the ISWI1b ATP-dependent remodeler and physical occlusion by H3K36me₃), H3K36me maintains a repressed chromatin structure in the wake of a transcribing RNAPII^{85,86}. Consequently, loss of either Set2 (*set2Δ*) from cells or mutation of H3K36 results in a relatively permissive chromatin structure, as evidenced by generation of intragenic

transcripts, and resistance to transcriptional stress induced by 6-Azauracil (which reduces the GTP pool in cells, resulting in slower transcription) (**Figure 1**)^{85,86}. In addition to the well-established function of H3K36me during transcription elongation, it was suggested that H3K36me1 in budding yeast might positively impact replication initiation, albeit the mechanism for this observation is completely unclear⁸⁷. Besides the described functions of Set2/H3K36me in budding yeast, it was not understood or known, before the publication of a part of this dissertation, if Set2 or any of its downstream methylation state contributed to genome stability in budding yeast.

In other eukaryotes, there have been reports of Set2/H3K36me (or Set2 orthologs) functioning in diverse arrays of functions. For examples, in humans, the SETD2 protein, which catalyzes H3K36me3, was shown to be crucial for regulation of alternative splicing of FGF receptor⁸⁸ and subsequently shown that even global regulation of alternative splicing was dependent on H3K36me3 (and SETD2)⁸⁹. In addition, SETD2 was shown to regulate the recruitment of MSH6, a repair protein that functions in mismatch repair, to chromatin during S-phase⁹⁰. Consistent with this notion, clear cell renal carcinoma patients showed increased mutation rate when SETD2 was non-functional^{90,91}. In *Drosophila melanogaster*, H3K36me2 catalyzed by Mes-4 and H3K36me3 catalyzed by dSetd2 have opposing effects on histone acetylation, specifically H4K16Ac⁹². The opposing activity of H3K36me2 vs. H3K36me3 results in fine-tuned H4K16Ac levels during transcription elongation⁹². Recently, Mes4 has been shown to co-purify with dCTCF and another insulator binding protein in *Drosophila melanogaster*, Beaf2⁹³. The co-purification of Mes4 and its requirement for subsequent transcription-associated H3K36me3 (which is dependent upon dSetd2) led authors to

conclude that H3K36me3 helps in maintaining H3K27me3 repressive domains in flies ⁹³.

In conclusion, H3K36me is a highly conserved histone modification, from yeast to humans, which regulate chromatin structure during transcription as well as other DNA-templated processes.

1.5 Regulation of chromatin structure by Htz1/H2A.Z:

A typical nucleosome consists of 2 copies each of core histones –H2A, H2B, H3 and H4. However, depending upon the genomic location, transcription status, cell cycle and stress signaling, atypical histones can get incorporated into the chromatin. These atypical histones, called histone variants, change the physico-chemical properties of nucleosomes and thus dynamically regulate chromatin structure and function ⁴¹. One of the most critical histone variants is Htz1 (in yeast) and H2A.Z in humans ⁴¹. Htz1/H2A.Z is a variant of histone H2A, with about 60% sequence identity with H2A but the amino acid sequence in the C-terminus of Htz1/H2A.Z is more acidic than the H2A ⁹⁴. The resulting change in the amino acids in the C-terminus is critical for its specific deposition in the chromatin ⁹⁴. The crystal structure of H2A.Z-containing nucleosomes, along with salt-dialysis experiments, show that H2A.Z renders the nucleosome unstable and therefore amenable for further disruption ⁹⁴. In line with this thinking, H2A.Z/Htz1 is present at the -1 and +1 nucleosome around the TSS, hence providing a more conducive nucleosome structure for transcription activation and regulation ⁴⁶⁻⁴⁸.

Htz1/H2A.Z is incorporated in an orchestrated manner, with the help of several multi-protein complexes such as the SWR1 and INO80 complexes ⁹⁴. SWR1 is thought to be the major complex that regulates Htz1 deposition in yeast chromatin ⁹⁴. SWR1 relies on both the direct binding to linker DNA ^{95,96} and interaction of one of its subunits, Bdf1, to hyper-acetylated histone H4 ^{48,96}. Bdf1 contains bromo-domains that recognize acetylated histones ^{48,96}. This is

probably a major reason why Htz1-containing nucleosomes are present at -1 and +1 nucleosomes- an area with free DNA available at the nucleosome free region (NFRs) and a hyper acetylated promoter. Consistent with a major role of SWR1 in depositing Htz1, loss of Swr1 or any of its critical subunits, results in a significant reduction in Htz1 in the chromatin⁹⁷. SWR1 shares a number of subunits with the NuA4 complex, which is an H4-specific histone acetyltransferase complex (HAT)- another intriguing connection between histone acetylation and Htz1⁹⁴. In addition to the SWR1 complex, INO80 has been shown to regulate the levels of Htz1 in the chromatin.

Consistent with the function of INO80 complex in regulating Htz1 levels in the chromatin, partial or complete loss of Ino80 results in increase in the Htz1 levels in the chromatin- in a manner that does not increase the total amount of Htz1 in chromatin, but rather mis-localizes them³⁷. For example, there is more Htz1 in the gene bodies and towards the 3' end of genes in an *ino1* delete than in WT³⁷. Further analysis revealed that Htz1 eviction from specific genomic locations is dependent on Ino80³⁷, similar to the role of SWI/SNF in removing mis-localized Cse4 (the centromeric histone H3)⁹⁸. Additionally, two other chaperone proteins are involved in Htz1 dynamics- Nap1 and Chz1. Nap1 is a histone H2A-H2B and Htz1-H2B chaperone, and for the purposes of Htz1, it imports the Htz1-H2B dimer into the nucleus and then hands it off to SWR1 complex⁹⁷. In contrast, Chz1 is a Htz1-H2B specific chaperone, that has been shown to regulate incorporation of Htz1 in yeast chromatin⁹⁹. Both these chaperones and the dynamic incorporation and eviction of Htz1 will be discussed in greater detail in chapter 3. Work from this dissertation shows, for the first time, that Nap1 and Chz1 have non-overlapping functions in terms of Htz1 dynamics, interaction with Htz1-containing nucleosomes and eviction of Htz1 from chromatin.

1.6 Maintenance of genomic integrity in eukaryotes:

Maintenance of an accurate genome is critical for the survival of any cell. Cells face a large number of challenges to their genome. Some of these sources of damage include intrinsic such as the reactive oxygen species generated from oxidative respiration while others are exogenous such as the ultra violet rays from the sun ¹⁰⁰. Irrespective of the source of genomic insults, cells have elaborate machineries devoted to repair specific kinds of DNA damage. Broadly speaking, one can classify DNA damage in following classes: i) base damage ii) nucleotide damage iii) replication induced DNA damage and iv) DNA breaks- single- and double-stranded ¹⁰⁰. Depending upon the kinds of DNA damage, cells will recruit one (or many) of the following pathways to repair those damages. I will describe some of these pathways, briefly, in the following section:

i) Base damage- Base Excision repair, which involves removal of the mutated/altered base by a DNA glycosylase resulting in an abasic site. This abasic site is then cleaved by an AP endonuclease or an AP lyase followed by gap-filling by a DNA polymerase and ligation of the nick by a ligase ¹⁰¹.

ii) Nucleotide damage: Nucleotide Excision Repair (NER) is the pathway of choice for fixing nucleotide damage to DNA ¹⁰¹. NER can be broadly divided into global genomic NER (GG-NER) and transcription-coupled NER (TC-NER) ¹⁰¹. NER relies on identification of damaged nucleotides (primarily due to structural deviations in the DNA double helix) by specific protein(s) (Rad4-Rad23 in yeast and XPC in humans for GG-NER and elongating RNA Polymerase II for TC-NER) ¹⁰¹. Subsequently, the damaged region is accessed by general transcription factor, TFIIH, and XPG followed by XPA and XPF, resulting in the removal of about 21-23 nucleotides from the damaged region ¹⁰¹. DNA polymerases and ligases fill in the

damaged region ¹⁰¹. If the nucleotide damage occurs in a transcribed region, the rate of repair for this kind of damage is significantly faster and relies on the identification of the damage by elongating RNAPII ¹⁰¹. An additional factor (Rad26 in yeast and CSB in humans) gets recruited to the damaged area of the transcribed genome and results in coupling the TC-NER with GG-NER ¹⁰¹.

iii) Replication mismatches: DNA replication is intrinsically a high-fidelity process, but it can introduce nucleotide mismatches ¹⁰². The mismatched nucleotides, if not repaired during the process of replication itself, recruit the mismatch repair process. Unrepaired mismatches increase the mutation rates in the genome, resulting sometimes in the death of the cells ¹⁰². In addition, mismatches serve a useful purpose of increasing the potential for genetic variability for cells, by increased mutagenic potential. It is not surprising then that disruption of mismatch repair appears to be a favored mechanism for cancer evolution such as for colon cancer (about 50% hereditary non-polyposis colon cancer is due to mutations in MSH2 and MLH1 genes, that perform critical functions in mismatch repair) ¹⁰². Briefly, mismatch repair relies on multiple proteins that recognize the mismatch and excise the mismatched regions as well as components of replication machinery. The fundamental mechanism for mismatch repair is conserved from *E.coli* to humans, with minor details and regulatory features being different ¹⁰².

iv) Double strand break: Double strand breaks (DSBs) in DNA are one of the most severe forms of DNA damage. DSBs can occur in a programmed or an un-programmed fashion ¹⁰³. An example of programmed DSB is the generation of antibody diversity in immune cells. Another example is during generation of male or female gametes through the process of meiosis ¹⁰³. In addition, cells face a wide variety of insults that can cause DSBs such as ionizing radiation and DSBs induced by reactive oxygen species. Generally speaking two, mutually exclusive,

pathways repair DSBs ¹⁰³: non-homologous end joining (NHEJ) and homologous recombination (HR). NHEJ relies on the recruitment of yKu70-80 complex to the DSB, with the help of the Mre11-Rad50-Xrs2 (Nbs1) (MRX/MRN) complex ¹⁰³. Recruitment of yKu70-80 results in the DSB ends being held together in physical proximity, in a relatively stable manner ¹⁰³. The DSB ends can then be re-ligated after limited end processing (if necessary) by the help of additional NHEJ factors such as Lig4 and repair-associated DNA polymerases ¹⁰³. Homologous recombination (HR), on the other hand, relies on the stable association of the MRX/MRN complex with the DSB ends ¹⁰³. Such a stable association is followed by the recruitment of end-processing factors such as Sae2 (CtIP in mammals), which promotes 5' → 3' exonuclease activity ¹⁰³. Such end-processing results in resected DNA ends, a particularly preferable substrate for the single strand DNA binding protein, RPA ¹⁰³. Subsequently, the RPA is exchanged for Rad51, in terms of coating ssDNA. This Rad51-DNA complex is then used for homology search, followed by recruitment of a vast array of other proteins that help in using the homologous DNA strand as a template to repair the DSB ¹⁰³. The decision to use one DSB repair pathway or another is one of the most crucial decisions that the cell makes in terms of repairing DNA damage ¹⁰³. This decision is based on the cell cycle stage of the cell, and availability of regulatory factors ^{103,104}. If a cell is in G1-phase, due to lack of CDK1 activity and absence of an additional homologous copy of DNA (for haploid genomes like budding yeast), cells use NHEJ to repair the DSB ^{103,104}. If the cell is in S-G2/M stage, there is ample activity of cyclin-dependent kinases (primarily CDK1, which activates the exonuclease activity of Sae2/CtIP), which tilts the balance in favor of HR ^{103,104}. In addition to the cell cycle stage, yKu70-80 acts as a repellent for recruitment of Sae2/CTIP to DSBs and hence inhibits HR ^{103,104}. In mammalian cells, additional levels of regulation exist which depends upon 53BP1 and BRCA1 ^{103,104}.

BRCA1 is associated with breast cancer and 53BP1 was discovered as a p53 binding protein¹⁰⁵. It was subsequently discovered that the major function of 53BP1 is to regulate pathway choice after DSB in mammalian cells¹⁰⁵. 53BP1 gets recruited to the chromatin, depending upon the status of histone methylation (specifically H4K20me2) and occludes the access of BRCA1 to the DSB¹⁰⁵. BRCA1 associates with resection enzymes and thus 53BP1 inhibits the first step required for diverting the DSB through HR pathway¹⁰⁵. Recently additional factors have been discovered that contribute to the decision-making process after DSB. One of them is Rif1 (Rap1-interacting factor 1), which functions through binding to 53BP1 and inhibiting the recruitment of BRCA1 to the DSB, thus predisposing the DSB to be repaired by NHEJ¹⁰⁶⁻¹⁰⁸. Inappropriate pathway choice can have disastrous consequences for the cell. For example, if a haploid cell decides to perform HR during G1 phase (like budding yeast, *S.cerevisiae*), it will likely end up using a region of the genome with poor homology and thus increase the genomic instability (due to strand exchange reactions that occur during HR)¹⁰³. To repair any kind of DNA damage, cells need to sense the DNA damage and then mount a response to repair it. This coordinated activation of signaling cascade is called DNA damage checkpoint, a focus of the following section.

1.7 DNA damage Checkpoint Activation:

Once a cell's DNA is damaged, the damage needs to be recognized by the cell and the appropriate signaling response needs to be activated so that the cell can repurpose the cellular machinery in repairing this DNA damage. Some aspects common to any kind of checkpoint activation involves sensing the DNA damage, recruiting signaling proteins to sites of DNA damage, activating a kinase cascade for effector functions and eventually regulating cell cycle progression and DNA repair^{103,109}. In eukaryotes and for double strand breaks (DSBs), the

process begins with the recruitment of the MRX (MRN in humans) complex to the ends of double strand breaks. MRX/MRN recruits the apical kinase, Tel1 (ATM in humans), in the vicinity of the DSB^{103,109}. This is followed by phosphorylation of Serine 129 (Serine 139 in humans) of histone H2A (H2A.X in humans) in the vicinity of the double strand break, resulting in what is commonly called γ -H2A.X^{103,109}. From yeast to humans, γ -H2A.X acts as a recruitment mechanism for a wide variety of proteins including adaptor proteins and chromatin remodelers to modulate various aspects of DNA damage signaling and repair^{103,109}. Subsequent to the early wave of γ -H2A.X formation, resection enzymes are activated which result in formation of ssDNA regions^{103,109}. These ssDNA regions are coated by RPA and recruit and activate Mec1 (ATR) kinase^{103,109}. The activation increases the domain size of γ -H2A.X in the vicinity of DSB^{103,109,110}. In yeast, γ -H2A.X formation is followed by recruitment of Rad9, an adaptor protein and the yeast ortholog of 53BP1^{103,109,110}. Rad9 binds in the vicinity of the DSB, and helps in the recruitment of the effector kinase, Rad53 (Chk2 in humans)^{103,109}. Rad53 gets hyper-phosphorylated and phosphorylates Rad9 to result in full activation of DNA damage checkpoint and the downstream activity of Rad53 results in cell cycle arrest, transcriptional modulation, and regulation of DNA repair *per se*^{103,109}. Chk1 kinase plays a minor role in this signal transduction pathway in yeast. In humans, there are additional proteins that function in this entire process, such as the MDC1 protein, which acts downstream of ATM/ATR to amplify the DSB signaling^{103,109}. In all eukaryotes, aspects of DSB signaling and DSB repair are intimately tied to chromatin components, which will be discussed in the following section.

1.8 Interplay of chromatin with DSB signaling and DSB repair:

Since all eukaryotes have their genetic material in the form of chromatin, all aspects of DSB repair and signaling are regulated and/or influenced by components of chromatin. This

includes DSB sensing, DSB processing, repair, tolerating the DSB and cell cycle progression. The aspects of chromatin that influence DSB signaling and repair include but are not limited to histone modifications, histone variants, ATP-dependent chromatin remodeling, and histone chaperones. The first signal of a DSB is the phosphorylation of Serine 129 of histone H2A (γ -H2A.X, Serine 139 in human H2A.X) ^{103,109,110}. This phosphorylation is catalyzed by a slew of kinases: Mec1/Tel1 in yeast and ATM/ATR and DNA-PK in human cells ^{103,109,110}. γ -H2A.X influences the recruitment kinetics of DNA repair proteins, activity of resection enzymes, recruitment of the cohesin complex for facilitating proximity between sister chromatid during HR, and amplification of DSB signaling cascade ^{103,109,110}. Given the myriad number of functions that γ -H2A.X is involved in during DSB response, γ -H2A.X deficient cells are sensitive to DSB causing agents and the γ -H2A.X-null mouse is immuno-deficient (γ -H2A.X also influences antibody re-arrangement) ^{109,110}. In addition to γ -H2A.X, there is phosphorylation of other histone residues, such as histone H4 serine1, and H2A serine 121 that play a critical role in DSB signaling and repair ^{109,110}. H4S1phos is catalyzed by casein kinase and is required for appropriate non-homologous end joining of DSBs while H2AS121ph is catalyzed by Sgo1 kinase. H2AS121ph is required for the recruitment of the chromosome passenger complex (CPC) during chromosome segregation ^{109,110}.

Acetylation of histones is a general signal for relaxed chromatin and it is quite well known that acetylated chromatin represents an ‘open chromatin’ stage. In terms of DSB signaling and repair, histone acetylation and deacetylation plays a critical role in pathway choice, activation of DSB signaling, repair of DSBs and restoration of chromatin structure after DSB repair. Immediately after a double strand break, deacetylation of histone H3/H4 occurs, and this is dependent upon the Rpd3/Sin3 deacetylase complex ^{109,110}. This deacetylation ensures a stable

chromatin structure, which is more amenable for NHEJ. Similar observations have also been made in human cells, where HDAC1 and HDAC2 are recruited immediately to the DSB to deacetylate H3K56 and H3K9 so as to make the chromatin more conducive for NHEJ^{111,112}. In contrast, H4K16Ac gets induced after DSB, probably as a means of disrupting higher order chromatin structure and allow the NHEJ repair machinery to access the DNA^{109,110}. In support of this idea, an H4K16A mutant in yeast is deficient in NHEJ^{109,110}. Interestingly, the level of histone acetylation increases when cells switch to homologous recombination (HR). This includes acetylation of multiple residues of histone H4 (K5, 8, 12 and 16) and other histones as well, such as H2A^{109,110}. It is thought that this acetylation correlates with a rather dynamic movement of DNA in the vicinity of the DSB for the purpose of strand exchange and other downstream processes in HR^{109,110}. Consistent with this thinking, a number of histone acetyltransferases (HATs; such as NuA4 in yeast and Tip60 in human cells) get recruited to the vicinity of DSBs^{109,110}. Furthermore, loss of NuA4 or Tip60 activity renders the cell sensitive to DSB-causing agents, further providing evidence that these HATs are critical for DSB repair^{109,110}.

Histone methylation has emerged as a major contributor to appropriate DSB signaling and repair in multiple eukaryotes. Histone methylation occurs on multiple lysine residues of histone H3 and H4. For the purposes of DSB signaling and repair, methylation of lysines 4, 9, 36 and 79 on histone H3 and lysine 20 on histone H4 are critical^{109,110}. Set1 catalyzes H3K4me in yeast (MLL family in humans). H3K4me was shown to be crucial for DSB repair in yeast, specifically through the NHEJ pathway, and H3K4me3 and Set1 was observed in the vicinity of a newly induced DSB^{109,110,113}. H3K9 methylation does not exist in budding yeast but is associated with heterochromatin structures in fission yeast and higher eukaryotes^{109,110,113}. H3K9me3 is typically

bound by HP1 protein and after DSB; HP1 is evicted from the chromatin (in a casein kinase dependent manner) allowing for the availability of H3K9me3 for other chromatin binding factors such as the Tip60 HAT^{109,110,113}. Tip60 contains an H3K9me3 binding domain and recruitment of Tip60 to the chromatin makes the chromatin more relaxed and allows for the appropriate DSB repair pathway to be recruited and repair to be accomplished^{109,110,113}. This coordinated mechanism allows for the repair of DSBs induced in heterochromatic areas. Methylation of histone H4 is critical for proper progression through cell cycle and regulation of DSB repair pathway choice. H4K20 is methylated by PR-Set7 and SUV420H1 (H4K20me1, and H4K20me2/3 respectively)^{109,110,113}. 53BP1 recognizes H4K20me2/3 and regulates DSB pathway repair choice. Methylation of H3K36 has emerged as a novel regulator of DSB response and DSB repair in yeast as well as human cells and is the focus of this dissertation (Chapter 2 deals with the discovery that H3K36me regulates DSB response and repair in budding yeast).

Another way chromatin structure can be dynamically altered is by regulated incorporation and eviction of histone variants and activity of histone chaperones. Histone variants are altered versions of canonical histones that have very different biophysical properties owing to subtle (and sometimes quite significant) differences in amino acid sequences. In humans, the major sensor of DSB is γ -H2A.X, which is a phosphorylation on the histone H2A variant, H2A.X^{109,110}. The incorporation of H2A.X in lieu of H2A is dependent upon the human FACT complex, which helps in the H2A-H2A.X exchange reaction around a DSB^{109,110}. Consistent with this phenomenon, loss of FACT complex member, SSRP in humans, result in loss of γ -H2A.X^{109,110}. In yeast however, the major H2A is H2A.X, therefore such a reaction may not exist. However, work from this dissertation reveals that a temperature sensitive mutation of yeast FACT complex, renders them exquisitely sensitive to DSB causing agents, thus establishing FACT-

dependent histone exchange as a critical regulator of cellular response to DSB. Another critical histone variant that functions after DSB is the H2A variant, Htz1 in yeast (H2A.Z in humans). Htz1 is typically associated with the +1 nucleosome around the TSS and in the sub-telomeric heterochromatin⁴⁶⁻⁴⁸. Htz1 containing nucleosomes are unstable and hence easy to disrupt⁹⁴. In accordance, Htz1 helps in positively regulating end-resection after DSB^{109,110}. Htz1 is transiently incorporated around a DSB and then evicted from around the DSB^{109,110}. This dynamic incorporation and eviction is critical for appropriate resection kinetics through the activity of both the Exo1 and Sgs1-Dna2^{109,110}. Consistently, *htz1Δ* results in diminished capacity for homologous recombination and reduced amplification of DSB signaling, as measured by hyperphosphorylation of Rad53¹¹⁴. Consistent with yeast studies, H2A.Z incorporation is critical for the activity of CtIP and hence loss of H2A.Z from human cells renders them radiosensitive and incompetent in performing homologous recombination¹¹⁵. Additionally, Htz1 gets modified (ubiquitylated and sumoylated), both of which allow an unrepaired DSB to be relocated to the periphery of nuclear membrane, eventually providing sufficient time for a slow DSB repair process to occur¹¹⁴. Moreover, the major H3-H4 histone chaperone, Asf1, is required for acetylation of newly synthesized histones (primarily at H3K56) and their deposition in the chromatin once DSB repair has been accomplished. In line with this, Asf1 is required for later stages of DSB repair and *asf1Δ* cells are sensitive to ionizing radiation and DSB-inducing chemicals¹⁰⁹.

Large scale chromatin structure modulation, as required by DSB repair and its signaling pathways, necessitates the recruitment and activity of ATP-dependent chromatin remodelers. Therefore, deletion of critical subunits of most of the ATP-dependent remodelers makes them sensitive to genotoxic agents, specifically to DSB inducing agents. ATP-dependent remodelers

are required at almost all stages of DSB signaling and repair. For example, RSC (Remodeler of Structure of Chromatin) remodelers are recruited to the DSB, along with the MRX complex¹⁰⁹. This recruitment allows for disruption of nucleosome structure to facilitate MRX binding to DSB and subsequent stable association of yKu70-80¹⁰⁹. RSC is also required for recruitment of the cohesin complex so that sister chromatids can be in physical proximity to facilitate HR. Additionally, RSC functions towards the end of the HR pathway so that the nucleosome structure can be restored¹⁰⁹. Similarly, SWI/SNF in humans allows for initial chromatin remodeling and facilitates the recruitment of MRN-ATM and other DSB repair proteins; therefore, loss of SWI/SNF renders human cells radiosensitive¹⁰⁹. Many of these chromatin remodelers require interaction with various histone modifications, some of which are found and enriched around a DSB. This allows for a temporal and spatial regulation of multiple aspects of DSB signaling and DSB repair.

Table 2: Chapter one summary

Regulation of chromatin structure and its influence on genome functions

- Chromatin is a dynamic structure, which compacts the eukaryotic genome, and regulates a wide variety of cellular functions and processes.
- Histones, non-histone proteins, ATP-dependent remodelers, histone variants and non-coding RNAs comprise chromatin and influence chromatin organization and function.
- Lysine 36 methylation of histone H3 (H3K36me) and histone H2A variant, Htz1, are major regulators of chromatin, which the dissertation will be focussed on.
- H3K36me regulates DSB signaling and repair (Chapter 2).
- Dynamic incorporation/eviction of Htz1 is dependent on Nap1 and Chz1 (Chapter 3).

CHAPTER 2: AN RNA POLYMERASE II-COUPLED FUNCTION FOR HISTONE H3K36 METHYLATION IN CHECKPOINT ACTIVATION AND DSB REPAIR¹

2.1 Overview

Histone modifications are major determinants of DNA double-strand break (DSB) response and repair. Here we elucidate a DSB repair function for transcription-coupled Set2 methylation at H3 lysine 36 (H3K36me). Cells devoid of Set2/H3K36me are hypersensitive to DNA-damaging agents and site-specific DSBs, fail to properly activate the DNA-damage checkpoint, and show genetic interactions with DSB-sensing and repair machinery. Set2/H3K36me₃ is enriched at DSBs, and loss of Set2 results in altered chromatin architecture and inappropriate resection during G1 near break sites. Surprisingly, Set2 and RNA polymerase II are programmed for destruction after DSBs in a temporal manner – resulting in H3K36me₃ to H3K36me₂ transition that may be linked to DSB repair. Finally, we show a requirement of Set2 in DSB repair in transcription units – thus underscoring the importance of transcription-dependent H3K36me in DSB repair.

2.2 Introduction

Eukaryotic genomes are constantly subjected to exogenous and endogenous forms of DNA damage¹¹⁶. Double strand breaks (DSBs) can lead to temporary loss of genetic information

¹ This chapter previously appeared as a shortened article in Nature Communications. The original citation is as follows: Jha, D. K. *et al.* An RNA Polymerase II-coupled function for histone H3K36 methylation in checkpoint activation and DSB repair. *Nat. Commun.* 5:3965 doi: 10.1038/ncomms4965 (2014).

and failure to repair DSBs can lead to severe genome instability and cell death. DSBs can be programmed (e.g., meiosis and immunoglobulin rearrangements) or caused by exogenous agents (e.g., ionizing radiation (IR), ultra-violet⁹³ and anti-cancer drugs)^{116,117}.

In eukaryotes, chromatin plays a fundamental role in regulating the cellular response to DNA damage¹¹⁷. Among the factors that contribute to the DNA damage response (DDR) are histones and their post-translational modifications (e.g., phosphorylated H2A serine 129; γ -H2A.X in metazoans), ATP-dependent chromatin remodelers (e.g., RSC, INO80, TIP60), and histone variants (e.g., Htz1)¹¹⁷. Transcription-associated histone modifications, including H3 lysine 4 methylation (H3K4me) and H3 lysine 79 methylation (H3K79me) also contribute to DNA damage response and repair¹¹⁷. Interestingly, a majority of stalled replication sites tend to occur in transcribed genes¹¹⁸, increasing the propensity for the collision of transcription and replication bubbles eventually resulting in DSBs¹¹⁹. Yet, how the transcription apparatus influences DSB repair is not well understood.

One major regulator of chromatin structure during transcription is H3 lysine 36 methylation (H3K36me). This mark is deposited by the Set2 methyltransferase and is highly conserved from yeast to humans^{81,120-124}. Set2 is recruited, at least in part, through binding to hyper-phosphorylated RNA Polymerase II (RNAPII) after RNAPII enters the productive elongation phase^{81,120-124}. Set2 recognizes the phosphorylated C-terminal domain (CTD) of RNAPII through the presence of a domain called the SRI domain (for Set2-RNAPII interaction domain)^{121,122}. In yeast, Set2/H3K36me regulates chromatin structure in the bodies of genes by activating the histone deacetylase complex Rpd3S^{81,83,125,126} and by regulating histone exchange through regulating the activity of Asf1, Chd1 and ISW1b complexes^{85,127}. Outside of a role for

Set2 in transcription elongation, much less is known regarding how this enzyme contributes to other DNA-templated functions.

2.3 Results:

2.3.1 Set2/H3K36me is required for resistance to DSB

To test whether Set2 and H3K36me function in DNA damage repair, we assessed the sensitivity of yeast cells lacking *SET2* to various genotoxic agents. Deletion of *SET2* caused sensitivity to the DSB-causing agent phleomycin (an IR-mimic), mild sensitivity to the alkylating agent methyl methane sulfonate (MMS), but no sensitivity to hydroxyurea (HU; replication stress) or UV (nucleotide damage) (**Fig. 2A**). The phleomycin sensitivity was rescued by transforming the *set2Δ* strain with full-length *SET2* (**Fig. 2B**). In contrast, sensitivity of the *set2Δ* strain could not be suppressed by transformation with a catalytically inactive *SET2* mutant (*SET2_{H199L}*); thus, methylation activity is required for survival after DSB (**Figs. 1B and 1F**). To further confirm the importance of Set2 in the DSB response, we utilized a strain (JKM179) in which a galactose-inducible, site-specific DSB in chromosome III can be repaired only by non-homologous end joining (NHEJ)¹²⁸ (**Fig. 1C**). Consistent with the phleomycin-sensitivity found with deletion of *SET2*, *set2Δ* was also sensitive to this galactose-induced DSB and was rescued by expressing wild-type (WT), but not catalytically inactive, Set2 (**Figs. 2C, 2D and 2F**). We ruled out the *MAT*-specific effect by using a strain with the *HO* cut site in *ADH4* gene and found that *set2Δ* was sensitive to a reparable Gal- inducible DSB as well (**Fig. 3A**). Recently, it was suggested that Set2 functions in DNA damage in a catalysis-independent manner¹²⁹, however examination of the levels of H3K36me in the presumed C201A catalytic mutant used by Winsor *et. al* revealed that it only abolished the tri-methyl form of H3K36 (**Fig. 3B**). Importantly, and

consistent with a role of Set2 methylation at H3K36 in this phenotype and DSB repair, we found that mutation of H3K36 (H3K36A) confers sensitivity to phleomycin (**Fig. 2E**).

Set2 functions through its association with the elongating (phosphorylated) form of RNAPII¹²¹. We therefore asked whether the DNA damage-induced phenotype we observed in the absence of Set2 and H3K36me is connected to its RNAPII function. We previously characterized a domain in the C-terminus of Set2, termed the SRI domain, which is essential for coupling Set2 with the transcribing polymerase¹²¹. Mutation of this domain uncouples Set2 from RNAPII and results in selective loss of H3K36me3 (**Fig. 2F** and¹³⁰). Significantly, mutation of the SRI domain of *SET2* (*SRIΔ*) could not rescue the sensitivity of *set2Δ* to persistent gal-induced DSB (**Fig. 2D**). Taken together, these data suggest that Set2 functions in DSB repair through its interaction with elongating RNAPII. They further suggest the possibility that transcribing polymerase itself may play an important role in DSB repair – a finding that would be consistent with studies showing RNAPII is present at DSBs¹³¹.

.2.3.2 *SET2* is functionally connected to DSB response and repair

To further establish that Set2 functions in cellular survival against genotoxic insults, we selected 30 genes representative of the pathways involved in DDR and repair and analyzed double mutant sensitivity to MMS. We performed our genetic interaction screen using MMS because of its ability to activate several DNA repair pathways as compared to phleomycin, thus allowing us to initially capture more possible genetic interactions between *SET2* and DDR genes. Our screen revealed that *SET2* genetically interacts (both positively and negatively) with a subset of DDR and repair genes, albeit to different extents (**Fig. 4H**).

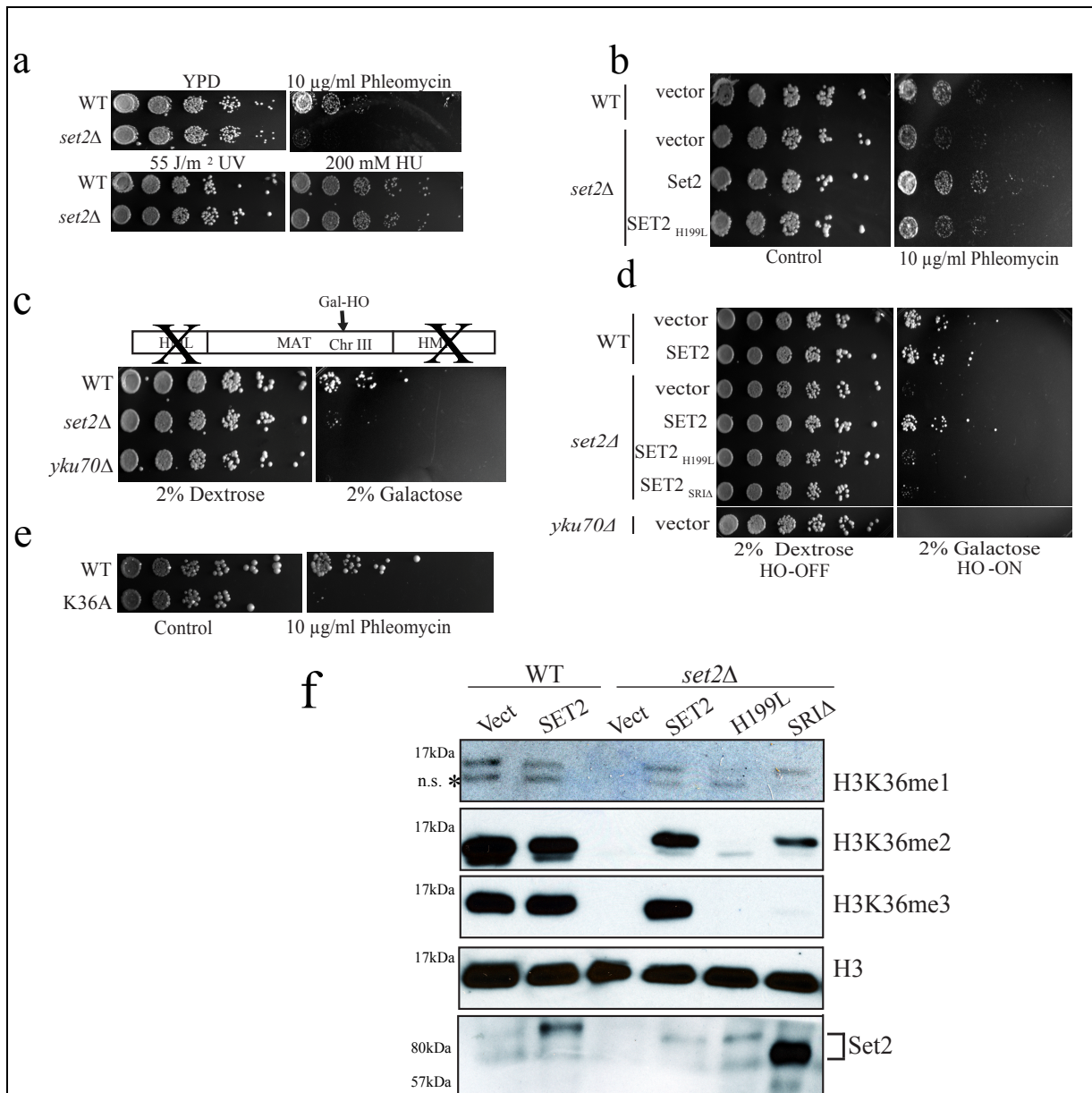


Figure 2. Methylation by Set2 at H3K36 and RNAPII-Set2 interaction is required for cellular resistance against double strand break (DSB). Five-fold serial dilutions of over-night cultures (grown either in YPD or appropriate selection medium for plasmids) were spotted on indicated plates and pictures were taken after 2-4 days. For immunoblots, log phase cultures were used for preparing whole cell lysates as described in Experimental Procedures. (A) A *set2Δ* strain is sensitive to phleomycin but not to hydroxyurea and UV. (B) Sensitivity of *set2Δ* to DSB can be rescued by wild-type *SET2* but not by a catalytically dead (*SET2_{H199L}*) mutant. (C) *set2Δ* is sensitive to persistent Homothallic (HO) endonuclease-mediated DSB in the “donorless” strain JKM179. A schematics of the “donorless” strain is shown where the Gal-induced DSB is in the MAT locus of chromosome III. This strain has the HML and the HMR deleted and hence the DSB can be repaired

only by NHEJ. (D) Rescue of *set2Δ* sensitivity to persistent DSB by wild-type *SET2* but not by a catalytically dead (*SET2_{H199L}*) or the *SRIΔ* mutant. (E) H3K36A phenocopies *set2Δ* on phleomycin. (F) Immunoblots showing the expression from the constructs used in Figs 1B and 1D.

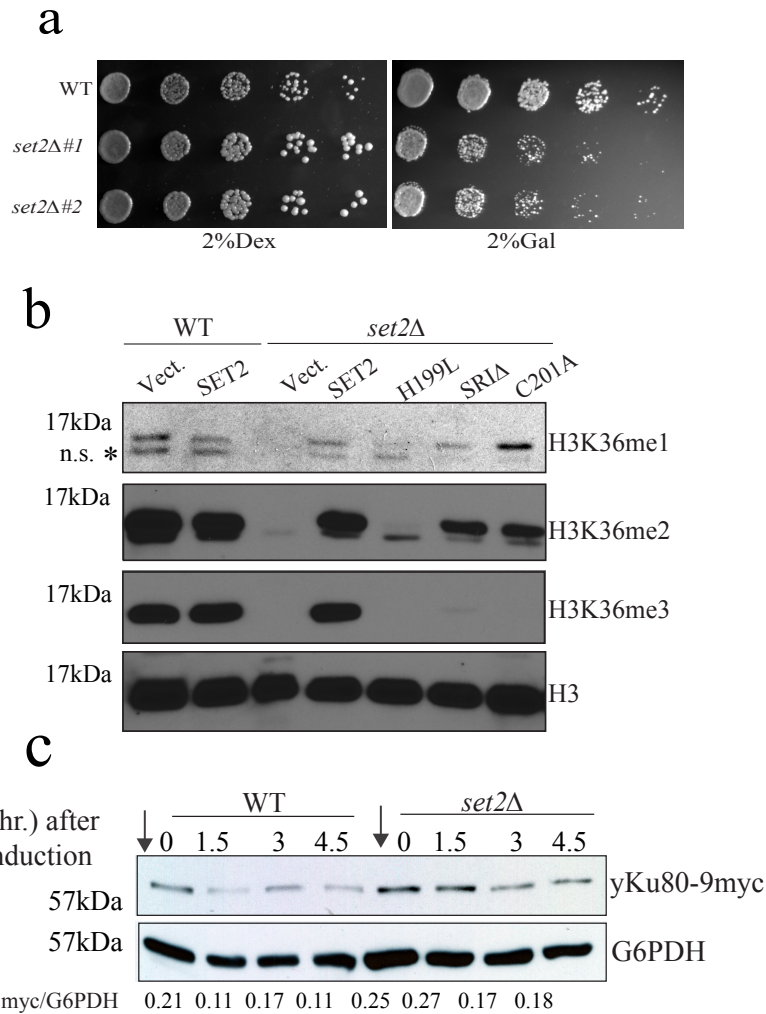


Figure 3. *set2Δ* is sensitive to persistent but reparable DSB at ADH4 locus and *set2Δ* does not alter yKu80 protein levels. (A) *set2Δ* are sensitive to persistent and reparable DSB at the ADH4 locus. (B) C201A has significantly higher amounts of H3K36me2 and H3K36me1 as compared to H199L. (C) Deletion of *SET2* does not alter yKu80 protein levels. The arrows indicate the time of galactose-induction. The numbers below are yKu80/G6PDH ratio.

In addition to recapitulating some prior genetic interactions (e.g., between *SET2* and *SLX5*) reported by the Idekker group¹³², we discovered several novel genetic interactions upon MMS treatment (e.g., *RAD9* and *RAD51*) (**Fig. 4H**). We focused on DSB-specific genes and repeated the genetic interactions using phleomycin (examples shown in **Fig. 4A, B, C and F**). Interestingly, the *set2Δrad9Δ* double mutant was more sensitive to MMS and phleomycin than either single mutant alone, suggesting that Set2 functions in parallel to Rad9, to provide resistance to DSB (**Fig. 4C**). Like the *set2Δ* single mutants, the *set2Δrad9Δ* synthetic sickness was rescued by WT *SET2*, but not by a catalytically- dead version of *SET2* (*SET2_{H199L}*) (**Fig. 4C**). These results agree with similar findings recently reported in a high-throughput genetic interaction map using multiple genotoxic agents¹³³.

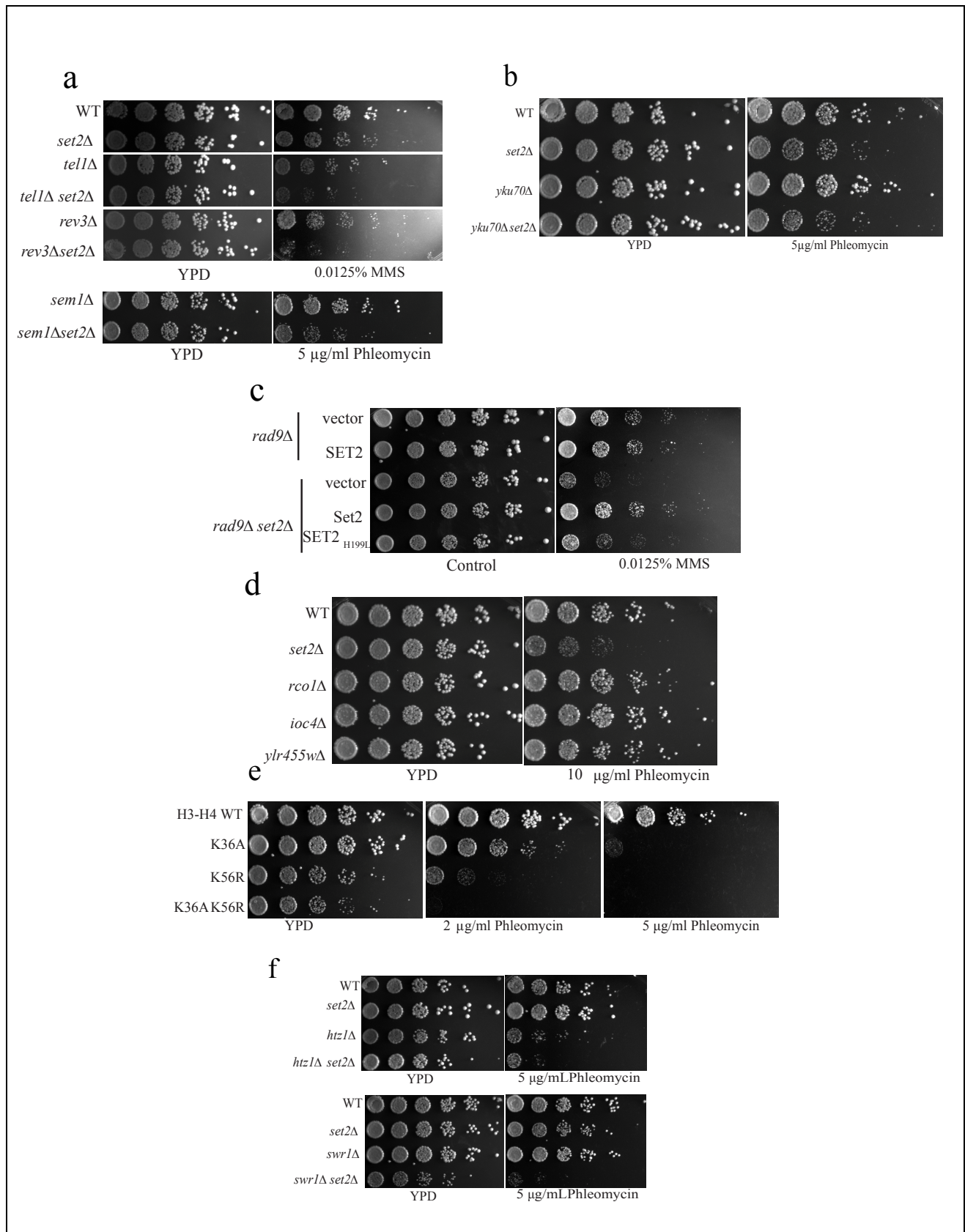
Because Set2 antagonizes the histone chaperone Asf1 to regulate histone exchange during transcription elongation⁸⁵, we also asked whether the sensitivity of *set2Δ* might be due to mis-regulated histone exchange after DSB. To test this, we analyzed the *asf1Δset2Δ* double mutant on phleomycin. However, the double mutant was synthetically sick on phleomycin (**Fig. 4G**), indicating that Set2 is required for survival in the absence of Asf1 after DSB. Our data show that in regards to DSB, Asf1 and Set2 have independent functions.

Since Set2/H3K36me is a histone modification associated with transcription elongation, we wondered whether any of the genetic interactions observed might be an indirect consequence of transcriptional alterations. However, transcription is only mildly affected in *set2Δ*^{134,135}, and most of the changes are relatively modest increases in gene expression¹³⁵. Notably, only a handful of genes are down-regulated in *set2Δ* and do not include any canonical DDR or repair genes. Consistent with this, the gene expression and pathway analysis performed by Lenstra *et al.* showed that *set2Δ* do not cluster with processes related to DDR and repair¹³⁵. Additionally,

we asked whether the protein levels of an early DSB response factor might be altered in *set2Δ*. We found no significant change in the proteins levels of γ Ku80, before or after DSB (**Fig. 3C**). Thus, the specific sensitivity of *set2Δ* to DSB-causing agents is not attributable to an indirect effect of gene expression changes.

2.3.3 Set2/H3K36me regulates checkpoint activation after DSB

To determine if the sensitivity of *set2Δ* was due to defective DNA-damage signaling, we exposed asynchronous cultures of WT and *set2Δ* strains to either MMS (M) or phleomycin (P) and monitored activation of γ -H2A.X (or H2AS129ph) and Rad53 (yeast homolog of mammalian Chk2). We observed reduced levels of Rad53 activation and γ -H2A.X in *set2Δ*, suggesting attenuated DSB damage response signaling (**Figs. 5A, 5B and 6B**). Deletion of *SET2* in the evolutionarily divergent yeast species *Schizosaccharomyces pombe* also resulted in reduced H2AS129ph when exposed to phleomycin (**Fig. 6A**).



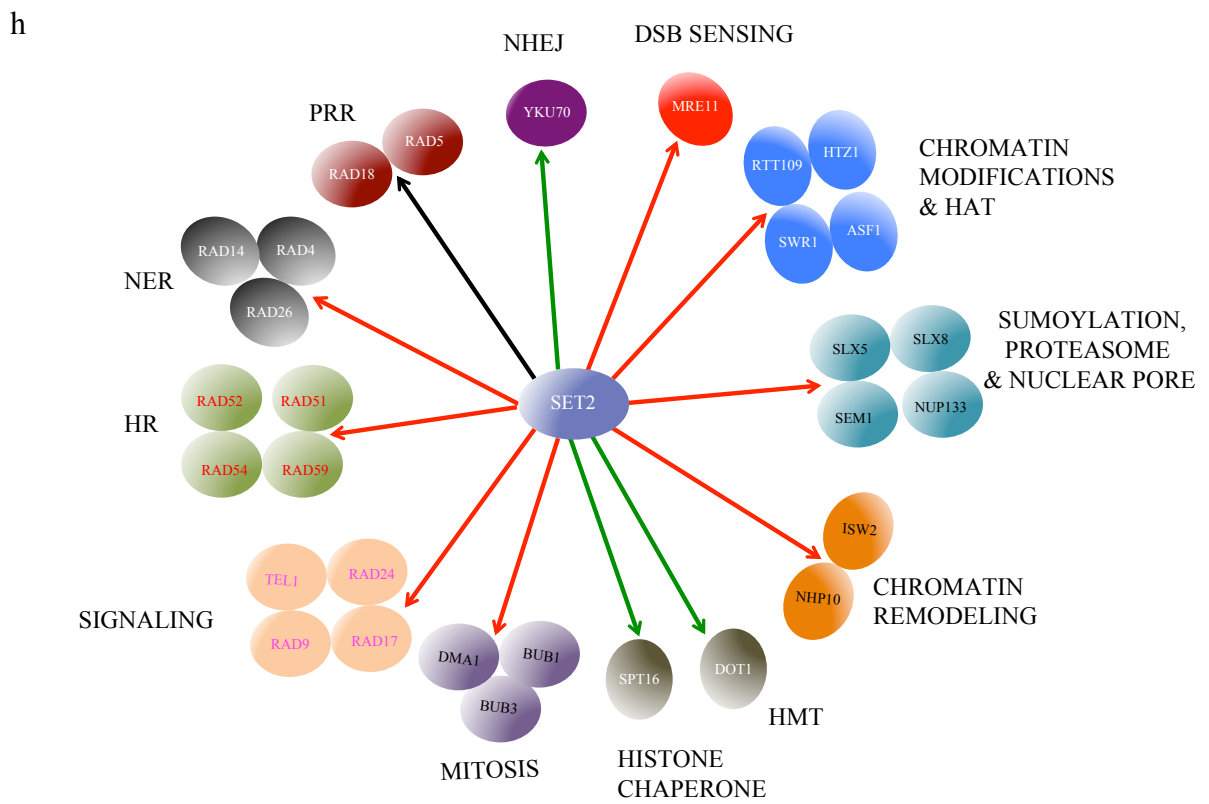
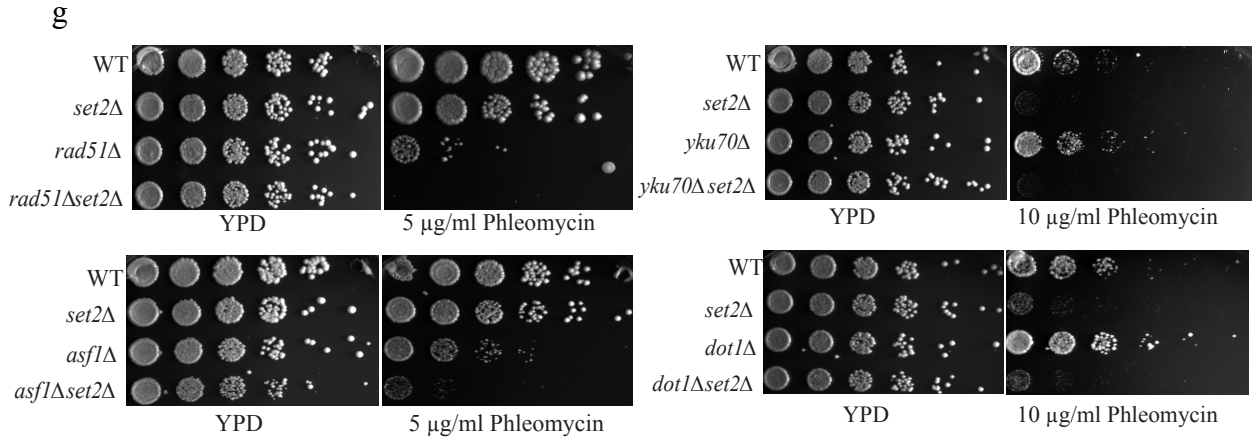


Figure 4. SET2 functionally interacts with DNA damage response and repair genes. (A) Representative serial dilution growth assays for some of the single mutants (*yfg1Δ*) and double mutants (*yfg1Δset2Δ*) on MMS and phleomycin. (B) *set2Δ* is epistatic to *yku70Δ* on phleomycin induced DNA damage. (C) Wild-type but not a catalytically dead (*SET2^{H199L}*) Set2 can rescue synthetic sickness of *rad9Δset2Δ* to MMS. (D) None of the known effector proteins, downstream of H3K36me, phenocopied the sensitivity of *set2Δ* on phleomycin. (E) H3K36me functions in a pathway parallel to H3K56R after phleomycin-induced DSB. (F) *set2Δ* is synthetic sick to *htz1Δ* and *swr1Δ* on phleomycin. (G) *set2Δ* is synthetic sick with deletions of HR machinery such as *rad51Δ* and histone chaperone *asf1Δ* while epistatic to *yku70Δ* and *dot1Δ* on phleomycin induced DNA damage. (H) Summary of the entire genetic screen, with functional processed the corresponding genes are involved in.

γ -H2A.X activation is one of the earliest steps after DSB-induction and occurs with extremely fast kinetics¹³⁶. To determine if this reduced level of γ -H2A.X was due to inefficient activation or faster de-phosphorylation (which normally occurs later in the DDR pathway)¹³⁷, we monitored the activation of γ -H2A.X after DSB-induction by phleomycin. We observed significantly lower levels of γ -H2A.X within the first hour of phleomycin treatment of *set2Δ* cells (**Fig. 5C**), implying a function for Set2 at an early step after DSB. Additionally, and in line with reduced activation of DNA damage checkpoint, Rad53 hyper-phosphorylation was severely reduced in a *set2Δ* strain in a similar time-scale (**Fig. 5D**). Importantly, we found Rad53 activation was also reduced in a H3K36A strain (**Fig. 5E**). Taken together, our data show that Set2-mediated H3K36me is essential for maximal activation of the DNA damage checkpoint after DSB induction.

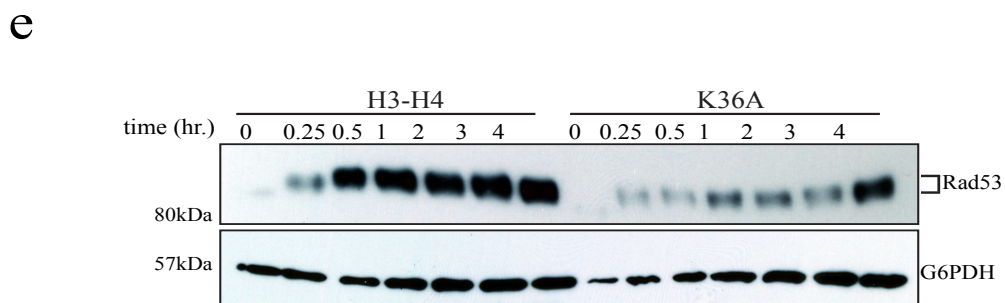
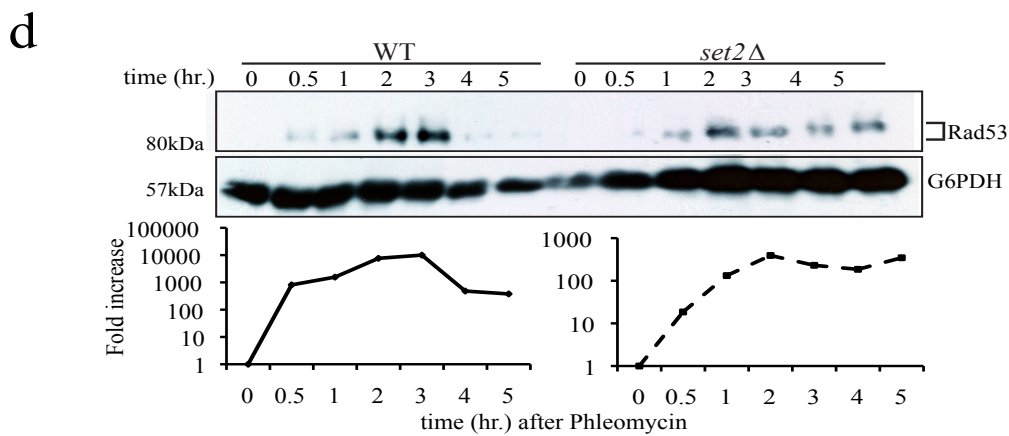
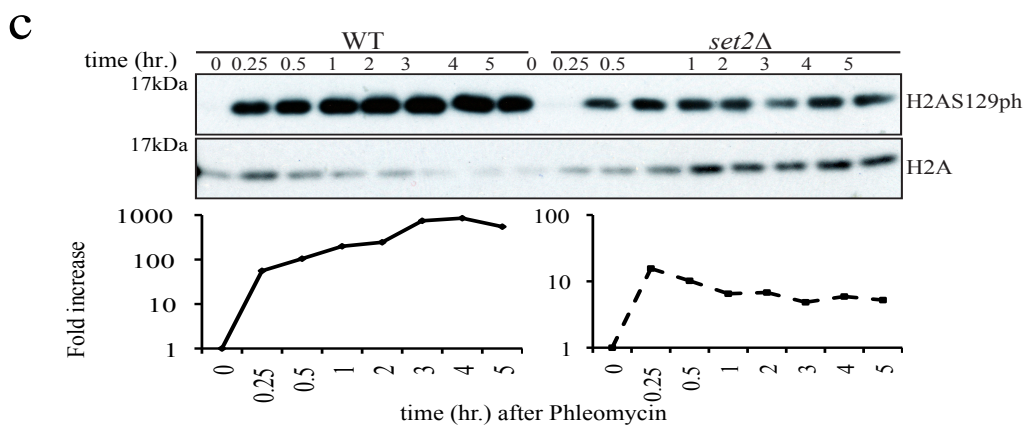
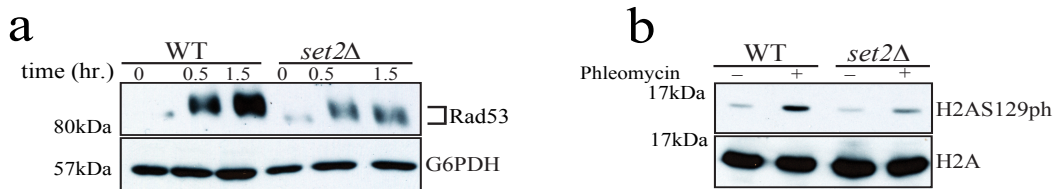
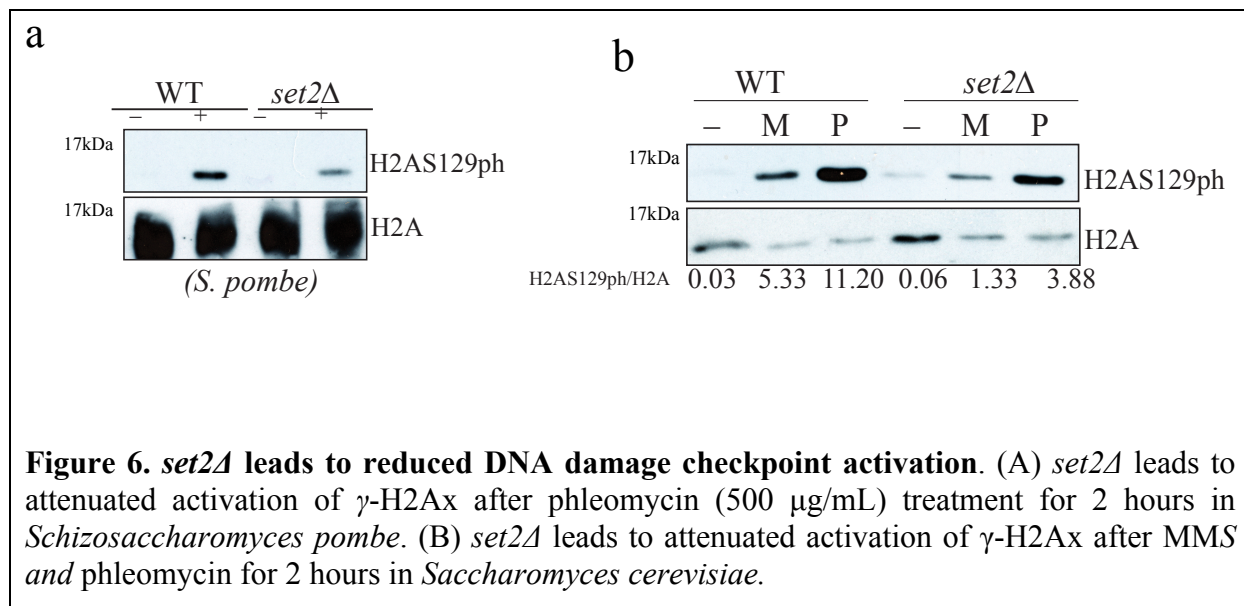


Figure 5. DNA damage signaling is attenuated in *set2Δ*. Log-phase cells were exposed to phleomycin for indicated times and whole cell extracts were prepared (see Methods). (A) Diminution in Rad53 hyper-phosphorylation at indicated time-periods in a *set2Δ* after phleomycin treatment. The antibody to Rad53 is against the protein and G6PDH is used as a loading control. (B) Abrogated γ -H2A.X activation in *set2Δ* after phleomycin (50 μ g/mL) treatment for two hours. (C) Time-course showing the activation of γ -H2A.X after phleomycin treatment. Quantification (H2AS129ph/H2A) of the western blot shown in Fig 3C. (D) Full activation of Rad53 was monitored after phleomycin treatment in WT and *set2Δ*. Quantification (Rad53/G6PDH) is plotted below the blot, which shows abrogated DNA damage checkpoint activation (semi-log plot). (E) H3K36A mutant cells also show abrogated DNA damage checkpoint activation as monitored by Rad53 activation kinetics.



2.3.4 H3K36me2 and me3 are DSB-inducible and present at DSBs

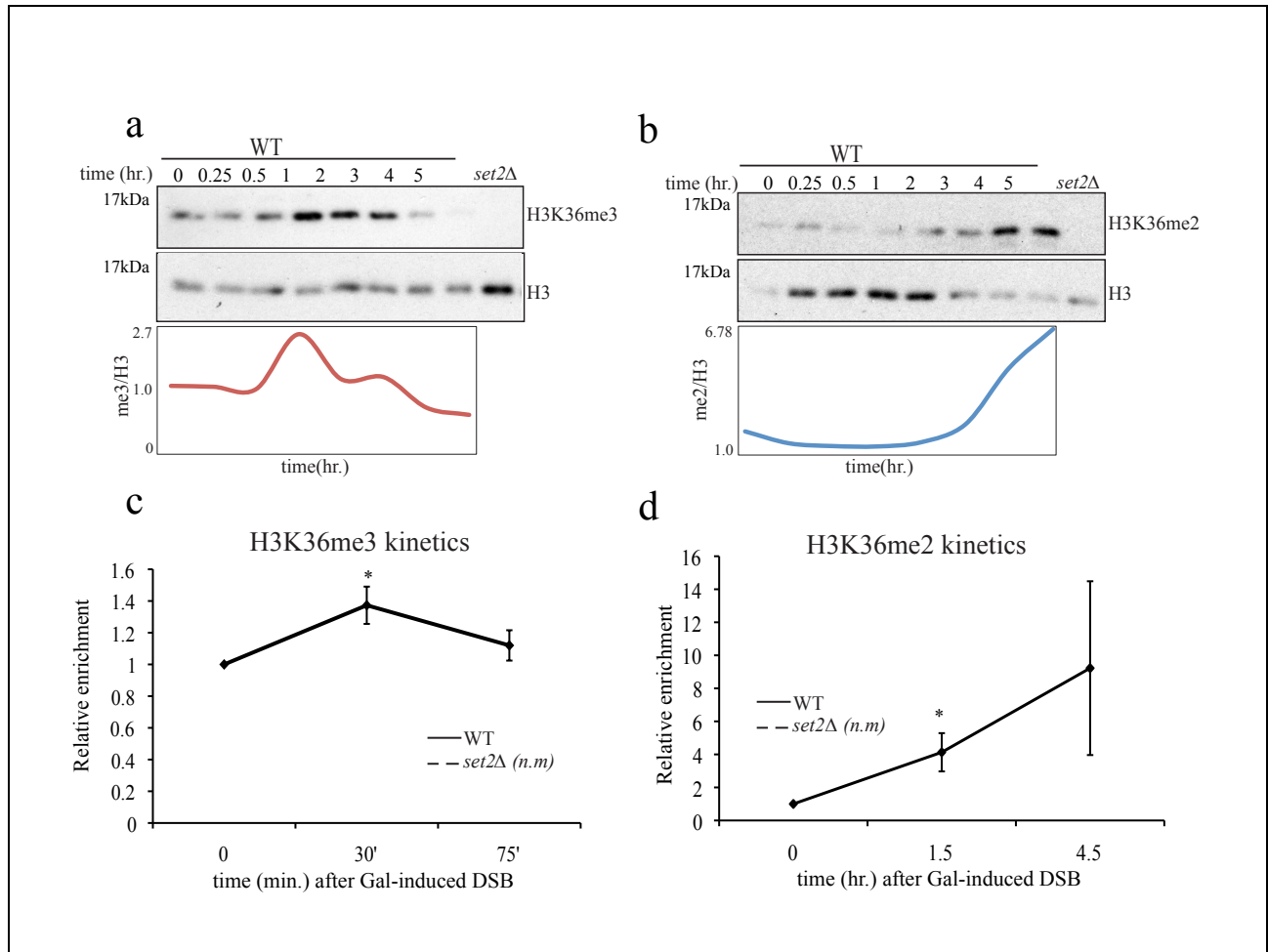
Because the catalytic function of Set2 is responsible for providing resistance to DSBs (Fig. 2) and full activation of DDR (Figs. 5 and 6), we next determined if the levels of H3K36me change after induction of DSB. We induced DSBs using phleomycin in an asynchronously growing culture and monitored H3K36me3 levels by Western blot analysis. Interestingly, H3K36me3 levels increased globally within an hour after exposure to phleomycin and then returned to basal levels (Fig. 7A). In contrast, H3K36me2 increased with much slower

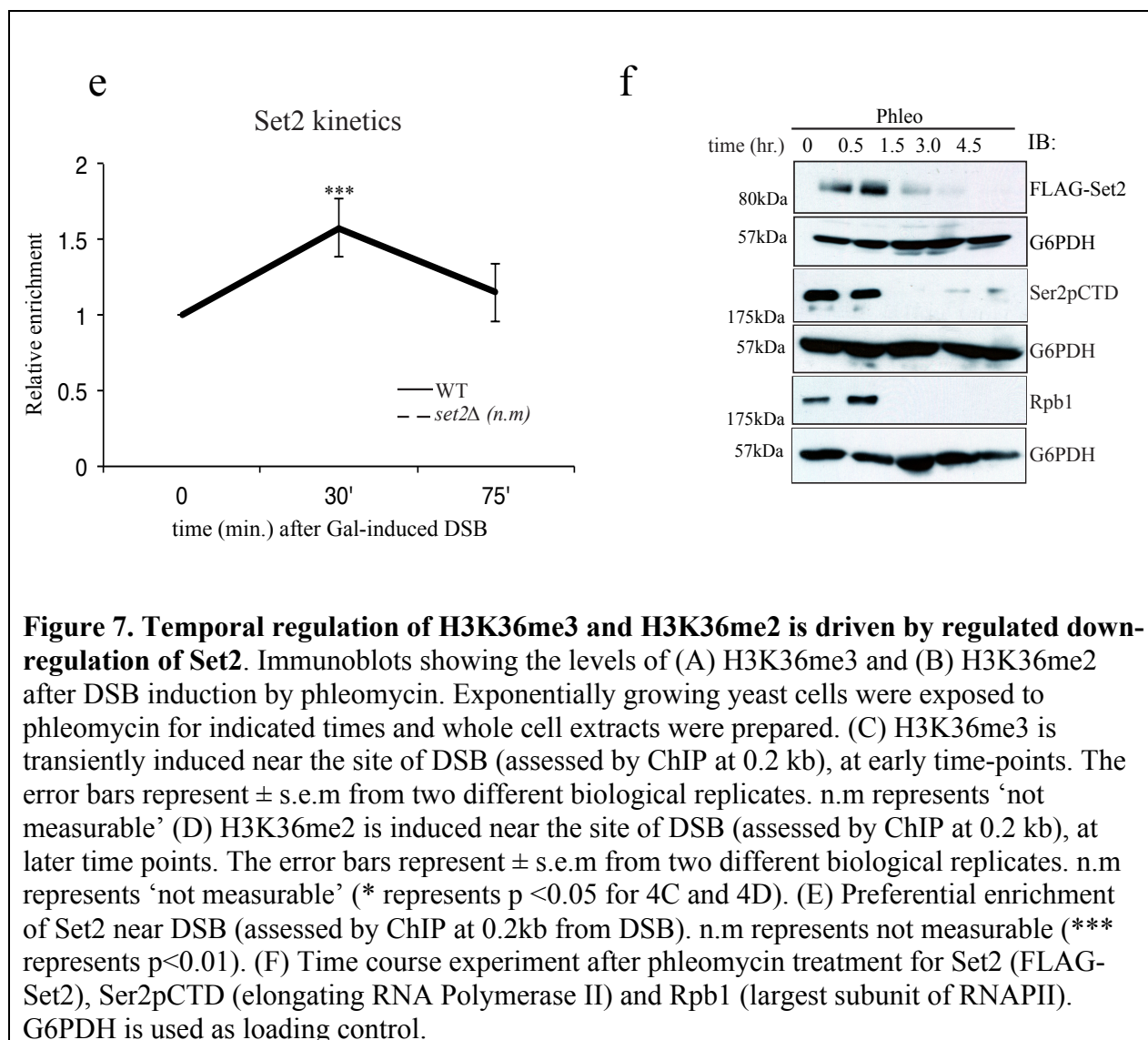
kinetics (**Fig. 7B**) and reached its highest levels at a later time-point (i.e., 4-5 hours after phleomycin treatment). Although it is possible that the increase in H3K36me2 at the later time-point was an active response to DSB, the increase coincided with the decrease in H3K36me3 – suggesting a specific loss of H3K36me3 to form more H3K36me2. To further verify that we were monitoring a DSB-inducible histone modification, we examined the levels of H3K36me3 near the site of DSB (0.2 kb distal to the DSB in the *MAT* locus) at early time-points to accurately capture a transient induction. H3K36me3 was increased, although modestly, within 30 minutes of galactose-induced DSB and tapered off approximately 75 minutes after DSB induction (**Fig. 7C**). This degree of increase is in line with the changes reported for H4 acetylation around the DSB^{138,139}. Consistent with global H3K36me2 levels measured by immunoblot (**Fig. 7B**), ChIP analysis indicated that H3K36me2 was induced at a later time point than H3K36me3 (**Fig. 7D**). Further, we detected an enrichment of Set2 at the DSB at an early time-point following DNA damage (**Fig. 7E**). The specificities of our H3K36me3, H3K36me2 and Set2 antibodies were confirmed by inclusion of a *set2Δ* sample (**Figs. 7A-E and Fig. 8**). Collectively, our data indicates H3K36me3 is DSB-inducible and transitions into H3K36me2 – a finding which coincides with transiently enriched Set2.

To further understand the molecular basis for the temporal regulation of H3K36me2 and H3K36me3, we monitored the global levels of Set2 following DNA damage. Upon MMS and phleomycin treatment, we found that Set2 protein levels were significantly decreased (**Fig. 7F**). Surprisingly, we also noticed that the levels of Rpb1 (the largest subunit of RNAPII), and consequently the Ser2 phosphorylated form of RNAPII CTD (Ser2p CTD), also degraded after DNA damage in a proteasome-dependent manner (**Fig. 7F and Figs. 8B, 8F**). Collectively, these

results reveal a programmed destruction of Set2 and RNAPII after DSB, which may be an important event in DSB sensing and repair.

To monitor if we see a similar reduction in the levels of RNAPII in the vicinity of a DSB, we did ChIP analysis for RNAPII around the *MAT* DSB. Consistent with the presence of Set2, we see RNAPII to be present at the same locus. Additionally, after 30 minutes of DSB induction, we can see significant reduction in the level of RNAPII (**Fig. 8G**), a result consistent with our global analysis. To our knowledge, this is the first demonstration of proteasome-dependent regulation of RNAPII after DSB in any model system.





To further understand how Set2 is regulated after DSB, we immunoprecipitated FLAG-tagged Set2 at several time-points following phleomycin treatment. We noticed an increase in pS/T-phosphorylation (a mark commonly associated with phosphorylation-dependent degradation¹⁴⁰) concomitant with reduced Set2 levels (**Fig. 8D**). While Set2 degradation is likely attributed to loss of RNAPII interaction, an alternate hypothesis could be that Set2 is targeted for phosphorylation-dependent degradation in a checkpoint-dependent manner after DSB. However, we found that Set2 levels were still decreased in a number of key checkpoint mutants

tested (**Fig. 8E**). These data show that in WT cells, Set2, RNAPII and H3K36me are regulated after DSB, consistent with a role for Set2/H3K36me in regulating cellular resistance to DSB.

2.3.5 Interplay between Set2 and chromatin regulators after DSB

Our genetic and biochemical evidence suggests that Set2 has a methylation- and RNAPII-dependent function after DSB. Set2-catalyzed H3K36me modulates chromatin structure via activation of the Rpd3S histone deacetylase complex^{81,83,125,126}, antagonizing the function of Asf1⁸⁵ and regulating ISW1b function¹²⁷. Thus, we investigated whether any of these pathways contribute to the function of Set2 after DSB. As mentioned above, the *asf1Δset2Δ* double mutant is synthetically sick on phleomycin, suggesting that Set2 and Asf1 function in parallel after DSB (**Fig. 4G**). Consistent with this finding, we also noticed synthetic sickness of H3K36A with H3K56R (H3K56Ac being a marker of histone exchange) on phleomycin (**Fig. 4E**). To test the other possible H3K36me effector proteins, we deleted *RCO1* (Rpd3S-specific subunit), *IOC4* (Isw1b-specific H3K36me effector protein) and *YLR455w* (a PWWP-containing putative H3K36me binder) and determined if any of these strains phenocopied *set2Δ*. None of these known or putative H3K36me effector proteins showed similar phleomycin sensitivity as *set2Δ* in isolation (**Fig. 4D**). Whether specific combinations of these effectors are required or if a novel effector protein is reading H3K36me remains to be determined.

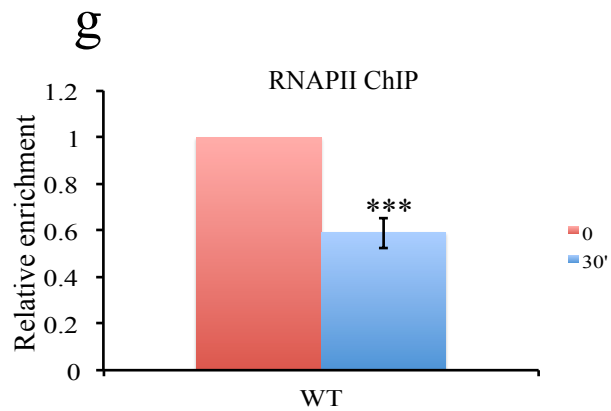
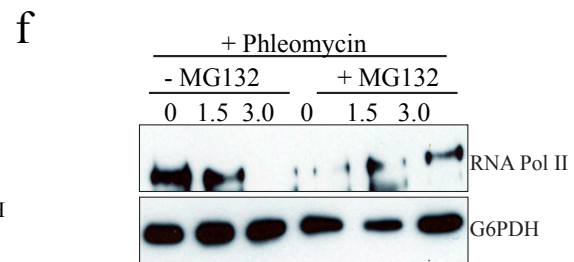
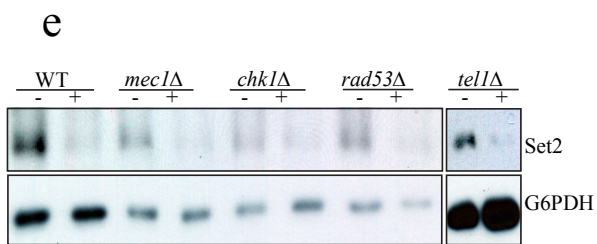
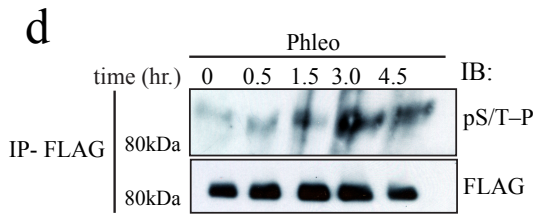
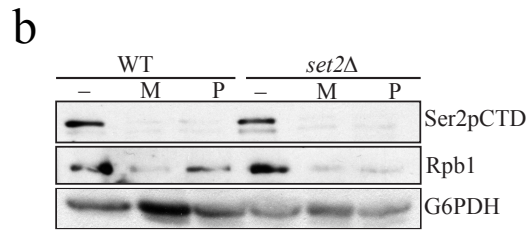
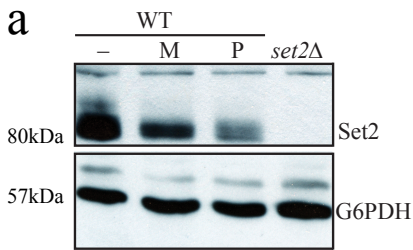


Figure 8. Regulation of Set2 and Rpb1 after DSB. (A) Set2 is regulated after MMS and Phleomycin induced DNA damage. (B) Ser2 pCTD and Rpb1 are down-regulated after MMS and Phleomycin induced DNA damage. (C) FLAG-M2 or HA-7 (beads against the HA tag) beads were used to immunoprecipitate Set2-FLAG from an untagged (BY4742) and Set2-3XFLAG strains and immunoblotting was performed with indicated antibodies. IP's with untagged BY4741 strain, HA-7 beads (beads with monoclonal antibody against HA tag) were performed to confirm the specificities to FLAG tag and the FLAG- M2 beads respectively. Additionally, G6PDH immunoblot was done on the IP samples to confirm the specificity of the pull-down. (D) FLAG-Set2 was immunoprecipitated at indicated time-points after phleomycin treatment and blotted for either FLAG or pS/T-P antibody. The input western blot for the IP is shown in Fig. 4F. (E) RNA Polymerase II gets degraded after DSB in a proteasome-dependent manner. MG-132 addition to the phleomycin-treated samples prevents Rpb1 degradation. (F) 4H8 antibody to RNA Polymerase II was used to chip Rpb1 at 0.2kb after DSB induction. Within 30' after DSB induction, Rpb1 IP signal is reduced. (***) represents $p < 0.01$ from at least 2 independent biological experiments).

We next investigated other histone modifiers known to play a role in the DDR, Dot1 and the histone variant Htz1. Dot1-dependent H3K79 methylation (H3K79me) and Htz1 are two chromatin components that are crucial for DSB response and repair¹⁴¹⁻¹⁴⁶. H3K79me modulates the DSB checkpoint response by recruiting or stabilizing the Rad9 adaptor protein on chromatin^{146,147} and inhibits DSB end-resection in a Rad9-dependent fashion^{148,149}. Htz1 has been implicated in a multitude of events occurring after DSB. We investigated the genetic interactions between *SET2* with *DOT1* and *HTZ1* to determine whether Set2 is part of any of the known pathways (or processes) in which these proteins function after DSB. We observed that *set2Δ* was synthetically sick with *htz1Δ* and *swr1Δ* (**Fig. 4F**), but *set2Δ* suppressed the mild resistance of *dot1Δ* to phleomycin (**Fig. 4G**). These data reveal that Set2/H3K36me is required for cell survival in the absence of Swr1/Htz1 function. They also suggest that Set2 and Dot1 might function in antagonistic manner to regulate cellular response to DSB.

2.3.6 Set2 regulates chromatin dynamics around a DSB

Based upon synthetic sickness of *set2Δ* with genes involved in homologous recombination, early abrogation of DNA damage checkpoint and sensitivity to ‘error-prone NHEJ’ (as revealed by persistent DSB in JKM179 ‘donor-less’ strain) (**Fig. 2C**), we investigated if the early steps of chromatin remodeling might be defective in cells deleted for *SET2*. Thus, we induced DSB (in asynchronous cultures) by galactose treatment in the JKM179 donor-less strain and performed a time-course-based ChIP experiment for histones, their post-translational modifications and histone variants, at regions near the DSB and at an unrelated locus (ARS315) as a control. We monitored the DSB induction kinetics, using primers across the induced DSB, in WT and *set2Δ* and found that to be identical (**Fig. 9A**). We also confirmed the reduced DNA damage checkpoint activation in *set2Δ* by monitoring γ -H2A.X around a DSB. Consistent with previously published results for γ -H2A.X around a DSB, we observed a rapid accumulation of γ -H2A.X within an hour of DSB induction. In contrast, *set2Δ* showed no significant γ -H2A.X activation (**Fig. 9C**).

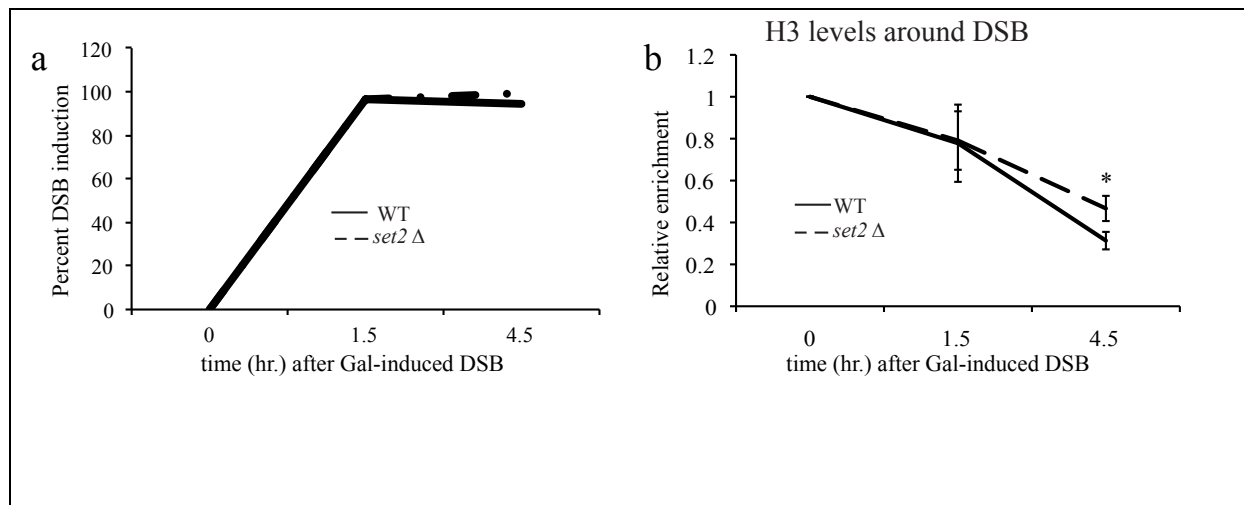
After a DSB, an early response of WT cells is to ensure a de-acetylated chromatin state, thereby enabling NHEJ in yKu70-80-dependent fashion¹⁵⁰⁻¹⁵³. Removal of yKu70-80, due to activation of Sae2 (and other resection enzymes) results in DSB being processed for homologous recombination¹⁵³, which correlates with increased acetylation of histones^{138,139}. Consistent with previously published results for H4 acetylation¹⁵⁰, in WT cells, H4 acetylation decreased early, followed by an increase in H4 acetylation (**Fig. 9D, solid line**, at 0.2kb away from DSB). In contrast, H4 acetylation was significantly higher in *set2Δ* cells compared to WT cells around 1.5 hour after gal-induced DSB (**Fig. 9D, dashed line**). Notably, the subsequent increase in H4 acetylation seen in WT cells did not occur in *set2Δ* cells (**Fig. 9D, dashed line**), indicating that

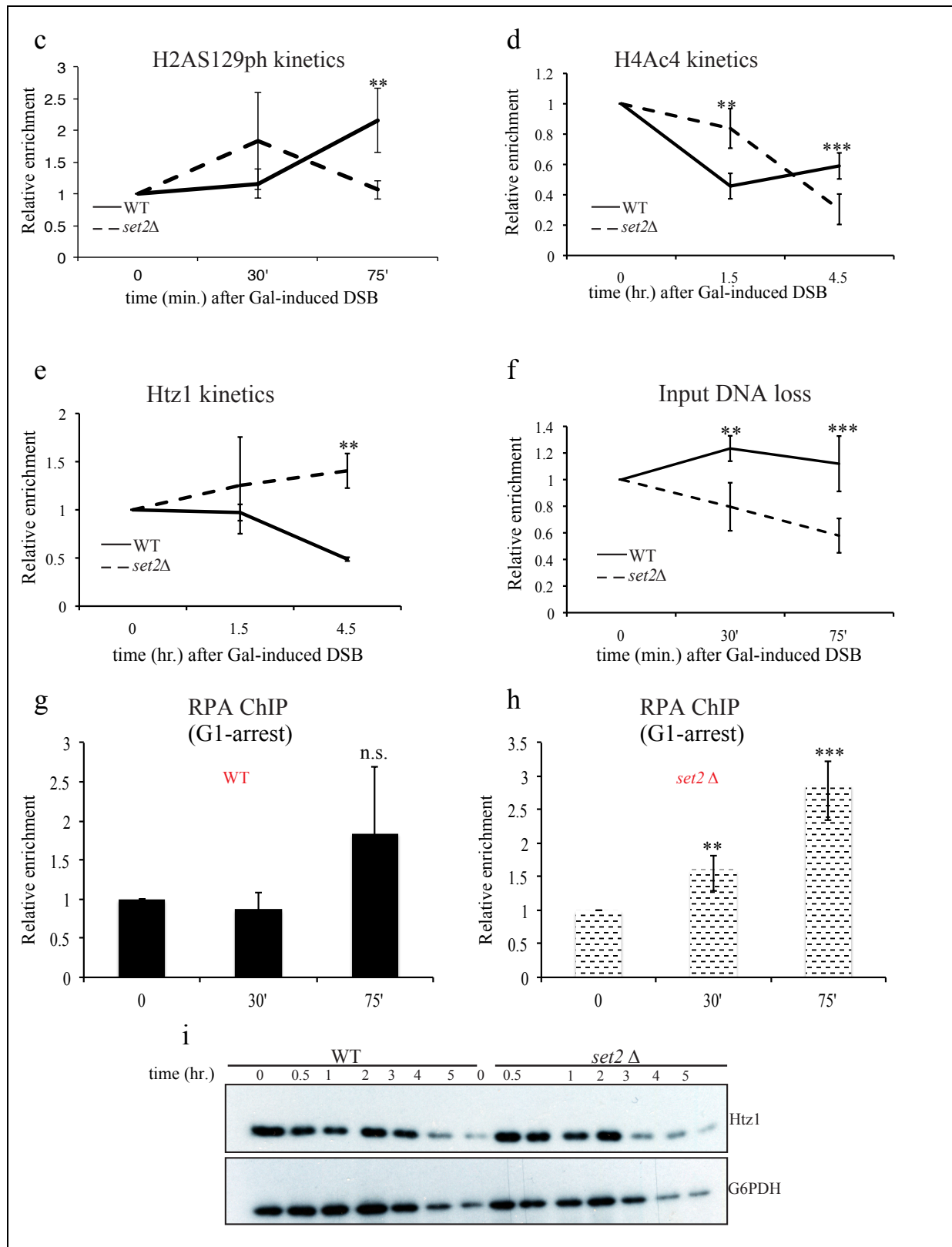
the dynamic changes in H4 acetylation that normally occur after a DSB were altered in the absence of Set2 – a result consistent with the idea that chromatin structure at DSBs is influenced by Set2 and H3K36me. Because NuA4 drives, in large part, H4 acetylation at DSBs, the altered H4 acetylation seen in *set2Δ* cells may have been due to altered NuA4 activity (a result also consistent with the finding that NuA4 function is partially dependent on H3K36me¹⁵⁴).

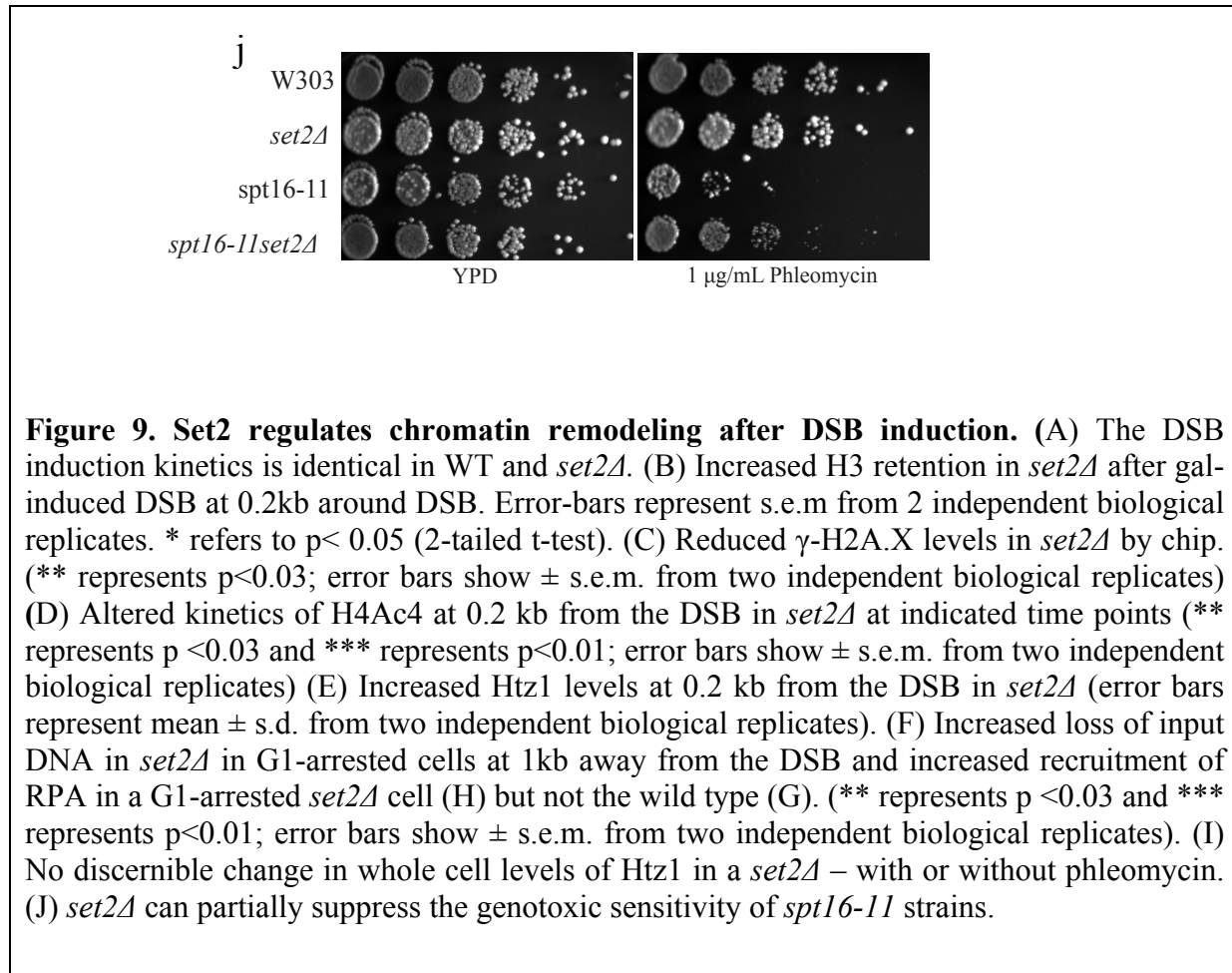
Given the observed changes in H4 acetylation, we next looked at Htz1, an H2A histone variant that is deposited at DSBs by the SWR1 complex, which recognizes acetylated histones^{47,48,155}. Consistent with published literature, Htz1 levels decreased in the vicinity of the DSB in WT cells (**Fig. 9E**)¹¹⁷. In contrast, there was more retention of both Htz1 and H3 around the same DSB in *set2Δ* cells (**Figs. 9E and 9B**). The level of Htz1 was not altered globally (**Fig. 9I**). Aberrant retention of Htz1-containing nucleosomes around the DSB reduces the available biochemical pool of substrate for Tel1 (i.e., H2A) and this may provide a molecular basis for the defects in the DNA damage checkpoint that is observed in the absence of Set2 (i.e., reduced γ -H2A.X), although we formally do not rule out an abrogated activation of Tel1 as a molecular explanation. However, a similar antagonistic relationship has been observed in the case of *ino80Δ* (chromatin remodeling complex required for removing Htz1 from chromatin), where increased retention of Htz1 reduces γ -H2A.X¹⁴³.

Given the critical role nucleosomal architecture plays in DSB response and the known role of FACT, a major regulator of nucleosome structure, in cellular resistance to DSBs in mammalian cells¹⁵⁶, we next investigated if *SET2* functionally interacts with the FACT complex. Interestingly, the Spt16 subunit of FACT regulates H2A.X exchange at DSBs in human cells, indicating that FACT regulates nucleosome dynamics at DSBs. In yeast, mutants of Spt16 (e.g., *spt16-11*) are sensitive to replication stress and high temperature and significantly, are

suppressed by deletion of *SET2*^{157,158}. We therefore reasoned that FACT mutants may be sensitive to genotoxic agents and this genotoxic sensitivity would be suppressed by *set2Δ*. As shown in **Fig. 9J**, we found that the *spt16-11* allele was extremely sensitive to phleomycin at permissive temperature. Consistent with the idea that Set2 opposes the action of FACT function¹⁵⁸, deletion of *SET2* suppressed, albeit partially, the DSB sensitivity of the *spt16-11* strain. These data suggest the intriguing possibility that Set2 and FACT have opposing effects on nucleosomal dynamics at DSBs.







2.3.7 Set2 regulates DSB repair in the context of transcription

We next asked what the functional consequence of losing Set2 and H3K36me would be on DNA repair and repair pathway choice. Our data show that loss of Set2/H3K36me results in aberrant retention of Htz1-containing nucleosomes at DSBs, suggesting an unstable nucleosome architecture around these regions since Htz1-containing nucleosomes result in less stable nucleosomes¹⁵⁹. Importantly, a recent study showed that Htz1-containing nucleosomes aid in Exo1-dependent end-resection¹⁶⁰.

We therefore used the input DNA from our cycling cells and monitored the loss of input DNA (as a surrogate readout of end resection). We did not detect any difference in the rate of

input DNA loss compared to that of *set2Δ* cells (**data not shown**). However, end-resection is heavily influenced by the cell cycle (G1 vs. G2/M), and smaller differences in resection kinetics may not become apparent in cycling cells. Therefore, we arrested cells in G1 by α -factor and monitored the loss of input DNA. In WT cells, we did not see any significant loss in input DNA, but, in *set2Δ* cells, the input DNA was rapidly lost, suggesting that *set2Δ* cells show faster end-processing in G1-arrested cells – a time when resection is normally suppressed (**Fig. 9F**). We confirmed this by monitoring the enrichment of single-strand DNA binding protein, RPA, in G1-arrested cells. We observed that even within 30 minutes after DSB induction, there is more RPA around a DSB in a *set2Δ* as compared to WT (**Fig. 9G and 9H**). This effect is likely a direct consequence of having more Htz1-containing nucleosomes in a *set2Δ* as well as reduced γ -H2A.X, which is known to be inhibitory to resection¹⁴⁹.

One prediction from this observation would be that Set2 should regulate non-homologous end-joining (NHEJ), and in the absence of Set2, one should see lower end-joining efficiency. A canonical assay used to monitor the efficiency of end-joining is the calculation of the ratio of colony numbers obtained after transformation of linearized plasmids to that obtained from transforming a circular plasmid (i.e., re-ligation efficiency). Using a plasmid where we generated a blunt-end cut in the plasmid multiple cloning site, we observed that there was no difference in the re-ligation efficiency between WT and *set2Δ* strains (**Fig. 10A**). However, since Set2 functions in the context of transcription units, we hypothesized that the function of Set2 in DNA repair would be more evident if our cut site was in the context of a gene body. We therefore carried out the plasmid re-ligation assay again, but in this case, with the cut site within the LacZ gene body. Strikingly, we observed a significant increase in plasmid re-ligation efficiency in *set2Δ* strains (**Fig. 10B**). We take these results to mean that although Set2 regulates pathway

choice with a likely preference towards promoting NHEJ, the loss of Set2 does not completely ablate this function – hence, some plasmid would be re-ligated that would then serve as a template for ensuing HR as the balance has been tilted to this pathway. Importantly, HR is a canonical mechanism of repair in transcription units^{161,162}, which would further exacerbate the *set2Δ* phenotype resulting in more re-ligation.

We next asked if this increased re-ligation efficiency is indeed a consequence of more recombination events, presumably due to transcription¹⁶¹. To answer that question, we deleted *RAD51* in *set2Δ* and monitored the re-ligation efficiency. Consistent with the idea proposed above, we observed that the increase in plasmid re-ligation efficiency in a *set2Δ* was suppressed by deletion of *RAD51* (**Fig. 10B**), indicating that *set2Δ* cells exhibit increased HR. To investigate if this effect was specific for the type of DSB induced, we used another restriction enzyme (SacI) that creates staggered ends, again in the context of transcription. Even in this context, we observed higher plasmid re-ligation efficiency in *set2Δ* strains (**Supplementary Fig. 10C**). This phenotype of *set2Δ* is reminiscent of *rsc* and *sth1* mutants, where linearization of the plasmid by digestion in a transcription unit resulted in higher re-ligation efficiency than wild-type cells¹⁶³. Although the precise mechanism of increased re-ligation efficiency is not yet understood, these results reinforce the idea that Set2/H3K36me plays an important role in DSB repair, especially in the context of transcription.

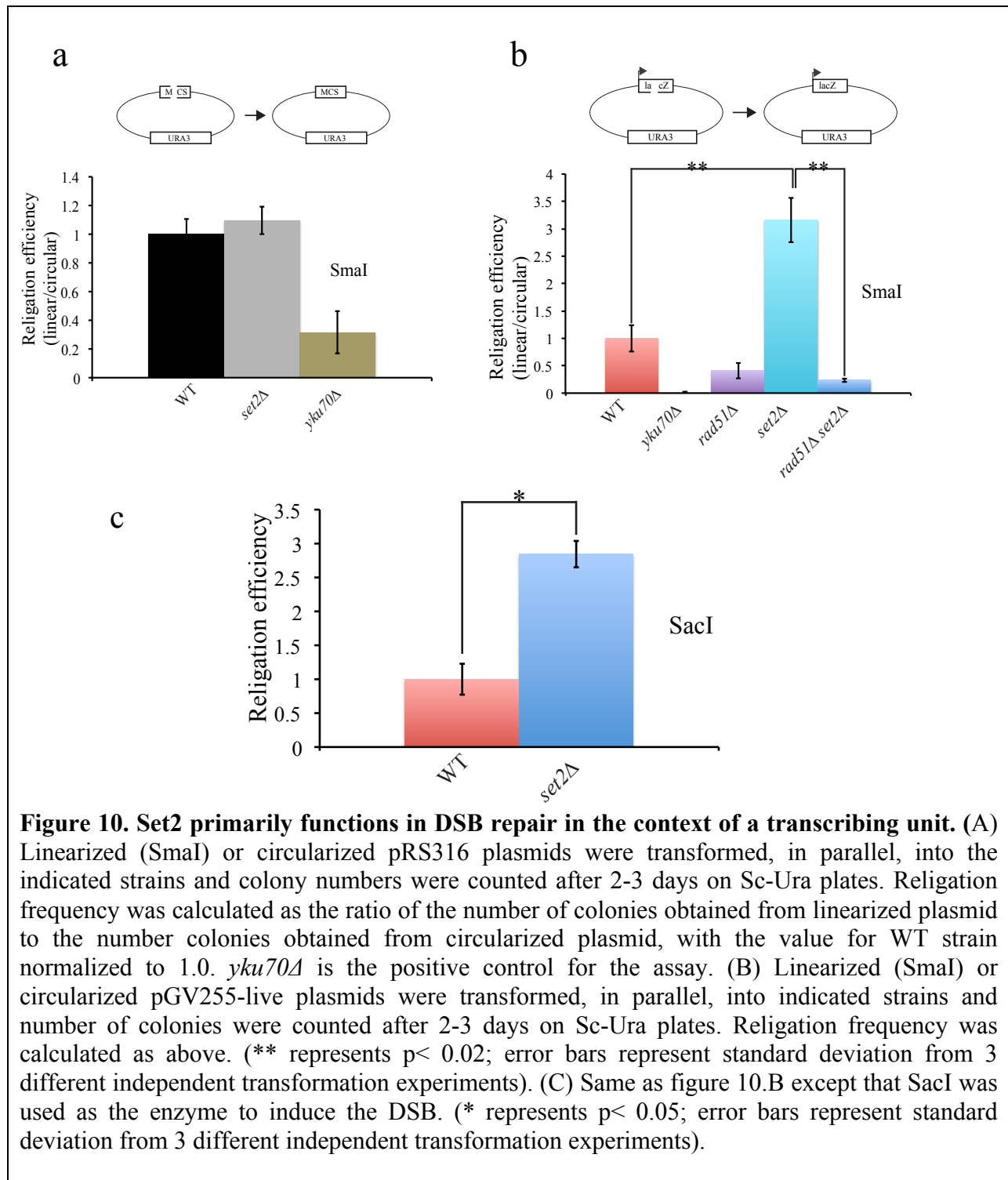
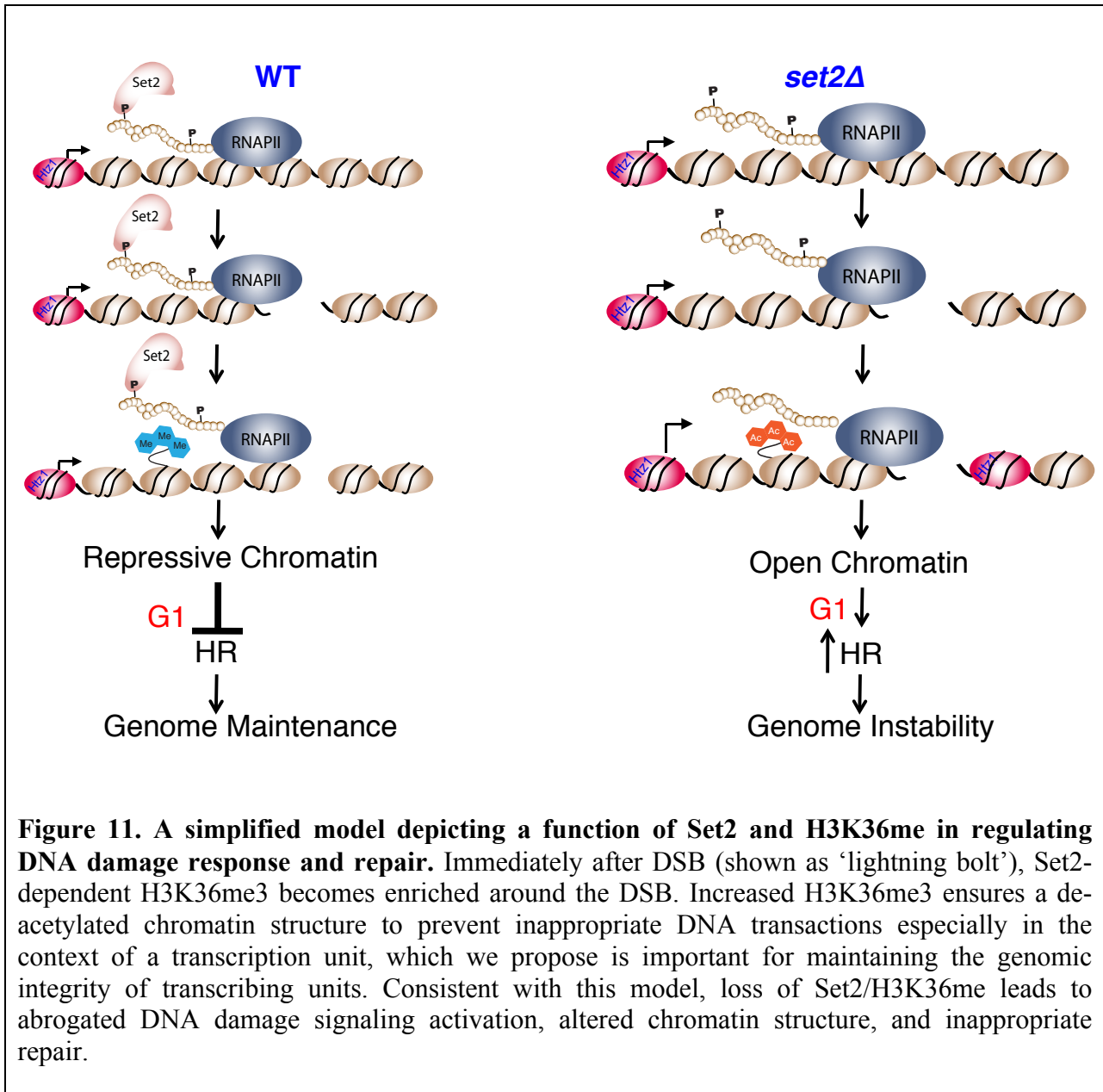


Figure 10. Set2 primarily functions in DSB repair in the context of a transcribing unit. (A) Linearized (SmaI) or circularized pRS316 plasmids were transformed, in parallel, into the indicated strains and colony numbers were counted after 2-3 days on Sc-Ura plates. Religation frequency was calculated as the ratio of the number of colonies obtained from linearized plasmid to the number colonies obtained from circularized plasmid, with the value for WT strain normalized to 1.0. *yku70Δ* is the positive control for the assay. (B) Linearized (SmaI) or circularized pGV255-live plasmids were transformed, in parallel, into indicated strains and number of colonies were counted after 2-3 days on Sc-Ura plates. Religation frequency was calculated as above. (** represents $p < 0.02$; error bars represent standard deviation from 3 different independent transformation experiments). (C) Same as figure 10.B except that SacI was used as the enzyme to induce the DSB. (* represents $p < 0.05$; error bars represent standard deviation from 3 different independent transformation experiments).



2.4 Discussion

In this article, we provide genetic and biochemical evidence that Set2, and its methylation at H3K36, functions at an early step after DSB and plays a role in DSB repair. Specifically, we find Set2/H3K36me is critical for proper DSB checkpoint activation and impinges on pathway choice—results that can be linked to its function with elongating RNAPII. The role of Set2/H3K36me in DDR and repair is likely to maintain appropriate chromatin structure at break sites, which impinges on the molecular events that occur during DNA repair.

Our data provide a temporal picture of how Set2 and H3K36me might modulate chromatin structure after a DSB. Using time-course immunoblotting and ChIP, we found that loss of Set2 leads to reduced γ -H2A.X, increased acetylation of H4 and aberrant retention of H3 and Htz1 at break sites. We propose that this altered chromatin architecture underlies the increased end-resection observed in G1-arrested cells, suggesting that HR is activated sooner in *set2 Δ* at G1. Additionally, we found that loss of Set2 leads to increased HR, when a DSB is in the gene body. Future experiments will be required to determine whether H3K36me3 or H3K36me2 plays an important role in recruiting any DSB repair factors to control repair pathway choice, in a cell-cycle and/or transcription-dependent manner. Although H3K36me2 affects Ku70-80 recruitment to DSB in human cells⁵⁴, such recruitment appears not to occur in cycling yeast cells as we did not see any significant alterations in Ku80 recruitment in *set2 Δ* (data not shown). We found that Set2 and RNAPII are programmed for destruction after DSBs in a proteasome-dependent manner, which correlates with a transition of H3K36me3 to H3K36me2 (Fig. 7 and 8). Although the function of this transition in DSB repair is not yet known, we hypothesize that this methyl-state transition after DSB functions to ensure a chromatin structure that is temporally ‘tunable’ for DSB repair. We speculate that the fine-tuning of chromatin

structure via H3K36me states would come from the ability of these different methyl states to activate/regulate functions of HATs and HDACs⁵⁵.

With regards to Htz1, the dynamic level of Htz1 around a DSB is critical for multiple steps in the response to DSB. Intriguingly, both *in vivo* and *in vitro*, H3K36me3 and Htz1 are mutually exclusive^{56, 57}; hence, one function of an early increase in H3K36me3 at sites of DSBs could be to prevent Htz1 deposition, thereby allowing more H2A (H2A and Htz1 being mutually exclusive in chromatin) to be phosphorylated to form γ -H2A.X domains. Consistent with this idea, we observed increases in Htz1 and lower γ -H2A.X in a *set2 Δ* (Figs 5 and 9).

Our study found that Set2's function in DDR and repair is dependent on its association with elongating RNAPII (Fig. 2). Consistent with this, we observed that when a DSB is in the context of transcription, deletion of *SET2* leads to an increase in HR events (Fig. 10). This result might be explained by the fact that Set2 loss tips the balance away from NHEJ to HR, which can be a preferred mechanism for break site repair in transcription units. We speculate that Set2-dependent chromatin compaction in G1 aids in preventing HR events, which would further prevent inappropriate recombination events that would arise in genes at this point in the cell cycle. It is also interesting to note that Set2/H3K36me is correlated with transcription rates and gene lengths¹⁵, which might fine-tune the appropriate type of repair that would occur in genes undergoing distinct rates of transcription.

The dependence of Set2/H3K36me for proper repair in gene bodies provides further evidence for an RNAPII-dependent DNA damage-sensing mechanism. Lindsey-Boltz and Sancar⁵⁸ postulated the existence of such a DNA damage 'sensor' due to the extremely slow off-rate of RNAPII on DNA. Consistent with this idea, studies (including these herein) have found RNAPII at sites of DSB in yeast (and mammals)¹⁹ and NuA4 and other chromatin modifiers that

associate and function at DSBs are also associated with RNAPII². In mammalian cells, DSB induces local chromatin silencing if the DSB is in a gene body. We surmise that the transcription machinery can be ‘co-opted’ by the DNA repair and signalling machinery to sense DNA damage and then use the already available chromatin modifiers (ATP-dependent remodellers/histone variants) to access and repair the damage, followed by restoration of the chromatin structure. This scenario would be especially useful during gene transcription induced R-loop formation, which can result in single or double-strand breaks⁵⁹. Interestingly, both transcription and DSBs result in fairly identical mitotic recombination events⁵², making the possibility of RNAPII as a ‘constitutive DSB sensor’ even more plausible⁵⁸. Given the stochastic nature of transcription⁶⁰, using the transcription apparatus as a sensor for DNA damage can be a useful strategy for cells to rapidly respond to exogenous or endogenous genomic insults. Consistent with this model, a recent paper by the Legube group⁶¹ shows that transcription units preferentially shunt the DSB to HR-dependent pathways. This phenomenon also was dependent upon the presence of the mammalian Set2 homologue, SETD2, and the presence of H3K36me3. We speculate that the DSB repair machinery can utilize the context-dependent chromatin environment to access and repair the DSB and maintain genome integrity.

Finally, the conservation of H3K36me across different species lends credibility to the idea that H3K36me is also important for DSB repair and damage response in other organisms. Indeed, Tim Humphrey’s group⁶² has discovered that the *S. pombe* Set2 also regulates pathway choice, because deletion of *SET2* alters the balance between NHEJ and HR. Interestingly, they find that Gcn5 acetylates H3K36 (ref. [63](#)) when Set2 is absent, and this activity leads to increased HR by presumably making the chromatin more accessible to the HR pathway. Additionally, Fnu *et al.*⁵⁴ showed that H3K36me2 catalysed by SETMAR/Metnase, which is not

a canonical H3K36 methyltransferase, is critical for NHEJ in human cells. Taken together, we propose Set2 as a key player in the DNA repair pathway that likely impinges on genome stability. As human SETD2⁶⁴ is mutated in a variety of cancers⁶⁵, we speculate that SETD2 has a conserved role in DNA repair that would explain its connection to human disease.

2.5 Methods

Yeast strains and plasmids

All strains, unless otherwise stated, were in the BY4741 background. The strain for *GAL*-inducible *HO* endonuclease (JKM179) was obtained from James Haber, Brandeis University and subsequent gene deletions (*SET2* and *YKU70*) were performed by gene replacement using the PCR tool kit. The strains are listed in Table 6.

Plasmids expressing *SET2* from its own promoter were obtained from Scott Briggs (Purdue University) and the H199L mutation was made in full-length *SET2* by site-directed mutagenesis (Quikchange, Stratagene).

DNA damage sensitivity assays

Cultures grown overnight were diluted to an OD₆₀₀ of 0.25, fivefold serially diluted and spotted on plates with or without relevant drugs. For UV experiments, cells were spotted on control plates and exposed to a range of UV dosage (from 20–60 J m⁻² in Stratagene crosslinker P1800, *rad4Δ* served as a positive control for sensitivity to UV). For *GAL*-inducible DSB, overnight grown cells were serially diluted (starting ODs of between 2 and 5) as indicated above and spotted on Sc-Ura plates containing either 2% dextrose or 2% galactose. Pictures were taken after 2–4 days. For liquid culture experiments, log phase cultures were exposed to phleomycin (250 μg ml⁻¹ except for Fig. 4b, wherein 50 μg ml⁻¹ was used to test whether the phenotype was due to a high concentration of phleomycin) for indicated times, and then extracts were prepared by SUMEB method. About 5 O.D equivalent of cells were taken and lysed by bead beating using the lysis buffer containing (1% SDS, 8 M urea, 10 mM MOPS, pH 6.8, 10 mM EDTA, 0.01% bromophenol blue). In all, 200 μl of buffer with 200 μl equivalent of glass beads were used to

lyse the cells. Bead beating was done for 6–8 min, intermittently, and the extracts were centrifuged, to clarify, and boiled at 95 °C for 5 min before loading the SDS–PAGE gel.

Whole-cell protein extract and immunoblots

Asynchronously grown mid-log (0.6–0.8 OD) phase cultures were lysed by SUMEB using glass beads, as mentioned above. For histones, 15% SDS–PAGE gels were run using Laemmli buffer. For Set2, RNA Polymerase II and Rad53 blots, 8% SDS–PAGE gels were run. Gels were transferred using a semi-dry Hoeffler apparatus at 45 mA per gel (constant current setting), 50 V for 1.5 h. For RNA Polymerase II, the Hoeffler setting was 55 mA per gel (constant current setting), 50 V for 1.5 h. Primary antibodies were incubated in 5% milk overnight and secondary antibodies were incubated in 5% milk for an hour. The immunoblots were developed using ECL-Prime from Amersham. Antibodies: H3K36me1 (ab9048; 1:1,000); H3K36me2 (active motif 39255; 1:1,000 and 4 µl for ChIP), H3K36me3 (ab9050; 1:10,000 and 3 µl for ChIP), C-terminal H3 (EpiCypher 13-0001; 1:2,500 and 2 µl for ChIP), Set2 (raised in lab; 1:5,000 or 1:10,000 and 5 µl for ChIP), Rad53 (obtained from Daniel Durocher, Canada; 1:2,000 (for Fig. 4a; ref. [66](#)) and Abcam 104232; 1:2,000 (for all other Rad53 blots), H2AS129ph (Active Motif 39271; 1:1,000 and 2 µl for ChIP), H2A (Active Motif 39235; 1:25,000 and 2 µl for ChIP), G6PDH (Sigma; 1:100,000), Ser2pCTD (1:100, gift from Dirk Eick, LMU, Munich, Germany), Rpb1 (Santa Cruz, yN-18, 1:1,000), anti-Myc (9E10, 1:2,500), 4H8 against RNA Polymerase II (Active Motif; 1:10,000 and 4 µl for ChIP). Rabbit (Amersham, Donkey anti-Rabbit), goat and rat (both Jackson ImmunoResearch Laboratories) secondary antibodies was used at 1:10,000. RPA antibody (2 µl for ~1 mg of chromatin) from Valerie Borde (Insitut Pasteur, Paris, France) was used for ChIP in Fig. 9.

ChIP

JKM179 and derivatives thereof were grown overnight in YPD and the saturated culture was used to start a fresh culture in YEP lactate, pH 5.5 (SC-Ura plus 2% Sucrose for Fig. 9F) at an OD₆₀₀ of 0.1 and grown at 30°C till the OD₆₀₀ reached 0.8–1.0. Galactose was added to a final concentration of 2% to induce the expression of *HO* endonuclease (at $t=0$ h). Samples were collected at required time-points and fixed with 1% (final concentration) formaldehyde. Cells were lysed using 300 mM FA lysis buffer (containing protease inhibitor cocktail). The lysed cells were sonicated (30% output, 6 pulses 6 times; 90% duty cycle) and clarified by centrifuging at full speed for 15 min. Immuno-precipitations were set up, overnight, with desired amount of proteins and antibodies (antibody amounts have been listed above). Protein G-sepharose beads (100 μ l 1:10 diluted beads per 400 μ l immunoprecipitation reaction) were added to the immunoprecipitation reactions and the reactions were allowed to incubate for 1 hour. Subsequent washes were done in 1.4 ml of 300 mM FA Lysis buffer, 500 mM FA-lysis buffer and LiCl solution (250 mM LiCl, 10 mM Tris, 0.5% each of NP-40 and sodium deoxycholate and 1 mM EDTA). The immunoprecipitates were resuspended in TE (pH 8.0) and treated with RNase for 30 min. The immunoprecipitates were then washed with TE (pH 8.0) and elution buffer was used to elute the DNA (15 min incubation in elution buffer followed by centrifugation at 3,000 r.p.m. for 2 minutes). The eluates were kept at 65°C overnight to carry out the de-crosslinking step and PCR purification kit (Qiagen) was used to extract the DNA. Details of PCR conditions, primer locations and analysis methodologies can be requested.

Immunoprecipitation

Immunoprecipitation for Set2-FLAG was performed in accordance with the manufacturer's protocol (SIGMA, catalogue no. A2220), using the 300 mM FA-lysis buffer used for ChIP experiments.

MG-132 experiment

Cells were grown in media containing proline as a nitrogen source overnight. The following morning, a fresh culture was started at OD 0.5 with 0.003% SDS and grown for 3 h before treatment with MG-132 (75 μ M) for another 30 min. Subsequently, phleomycin (250 μ g ml⁻¹) was added and samples were obtained at indicated times, and western blotting was performed as described above.

Plasmid re-ligation assay

About 3–5 μ g of circular plasmids were digested by indicated restriction enzymes. Running the digested plasmids on gels and performing routine gel extraction confirmed their linearization. Subsequently, 100 ng of linearized or circularized plasmids were transformed into indicated strains (LiAc/PEG method), in parallel. The colonies were counted on Sc-Ura plates after 2–3 days. Three independent transformation reactions were carried out.

Statistical analysis

For arriving at the *P* values in all the relevant experiments (ChIP assays and the plasmid re-ligation assay), we carried out unpaired Student's *t*-test in Microsoft Excel. The explanations for the error bars are mentioned in the corresponding figure legends with relevant *n* values. *P* < 0.05 was considered statistically significant.

Table 3. Chapter two summary

An RNA Polymerase II-coupled function for histone H3K36 methylation in checkpoint activation and DSB repair

- Set2 regulates DSB signaling activation and DSB repair.
- Set2-dependent H3K36me is dynamic after DSB and is regulated, at least in part through proteolytic destruction of Set2.
- RNA Polymerase II is also degraded after DSB.
- Set2's function after DSB repair is dependent upon transcription and loss of Set2 function from cells predispose them to perform homologous recombination.

CHAPTER 3: RATIONAL DESIGN OF H2A.Z MUTANTS UNCOVER DIFFERENTIAL CHAPERONE INTERACTIONS AND FUNCTION

3.1 Overview

H2A.Z (Htz1) is a histone variant that replaces canonical histone H2A in nucleosomes. It is involved in transcriptional regulation, DNA damage response, and heterochromatin silencing. H2A.Z deposition and eviction in chromatin is under the control of a number of ATP-dependent remodelers and histone chaperones. However, the underlying mechanisms for how these histone chaperones cooperate to deposit and evict H2A.Z in chromatin is lacking. Here, we uncover a role for the Chz1 chaperone, along with Nap1, in evicting H2A.Z from chromatin. Using molecular simulations, we refine a previously generated Chz1-H2A.Z-H2B structure to identify a series of H2A.Z residues that constitute part of a chaperone-specific binding surface. Mutation of these residues revealed differential requirements for Chz1 and Nap1 interaction. We also found that several of these H2A.Z mutants resulted in modest to severe growth defects that could be restored upon deletion of the H2A.Z deposition machinery. Furthermore, we show that these mutations show aggravated phenotypes when the functionally redundant chaperone is deleted. Based on our findings we propose a mechanism of H2A.Z maintenance in chromatin through a functional interplay of the SWR1C complex that deposits H2A.Z and the Nap1/Chz1 chaperones that, at least partly, function to evict H2A.Z from chromatin.

3.2 Introduction

Eukaryotic chromatin is regulated by multiple mechanisms that include, but are not limited to, post-translational histone modifications, ATP-dependent chromatin remodeling, and replacement of canonical histones with variants¹⁶⁴. While the canonical histone proteins are mainly deposited in the S-phase of the cell cycle, histone variants are synthesized independent of replication and their deposition and eviction at specific genomic loci are associated with distinct chromatin states^{164,165}. Variants of histone H2A are the most common and are found in most organisms from yeast to humans. H2A.Z (Htz1 in yeast) is a histone H2A variant that is highly conserved across species¹⁶⁵⁻¹⁶⁷. H2A.Z has been shown to be crucial for a variety of DNA processes involving regulation of chromatin structure during transcription¹⁶⁸⁻¹⁷⁰, maintenance of heterochromatin⁴⁶ and DNA damage response^{171,172}.

The function of H2A.Z is, in part, modulated by regulated deposition and eviction from chromatin^{167,171}. The major factor for regulated deposition of H2A.Z in chromatin is the SWR1 complex (SWR1C)¹⁷³. SWR1C is an ATP-dependent chromatin-remodeling complex that recognizes the acidic surface on the H2A.Z-H2B dimer¹⁷⁴ to deposit it into chromatin. Additionally, histone chaperones Nap1 and Chz1 have been implicated in appropriate deposition of H2A.Z into chromatin¹⁶⁷. Nap1 is thought to import H2A.Z into the nucleus and deliver it to Swr1-deposition machinery¹⁷⁵. A novel H2A.Z-specific chaperone, Chz1, has also been shown to deliver H2A.Z to Swr1 depositing machinery⁹⁹. However, removal of Chz1 and/or Nap1 does not severely impact H2A.Z function or deposition of H2A.Z into specific chromatin loci⁹⁹. To date, no clear mechanistic understanding exists regarding the differential functions of Nap1 and Chz1 in depositing H2A.Z to chromatin. In this study, we have attempted to understand the

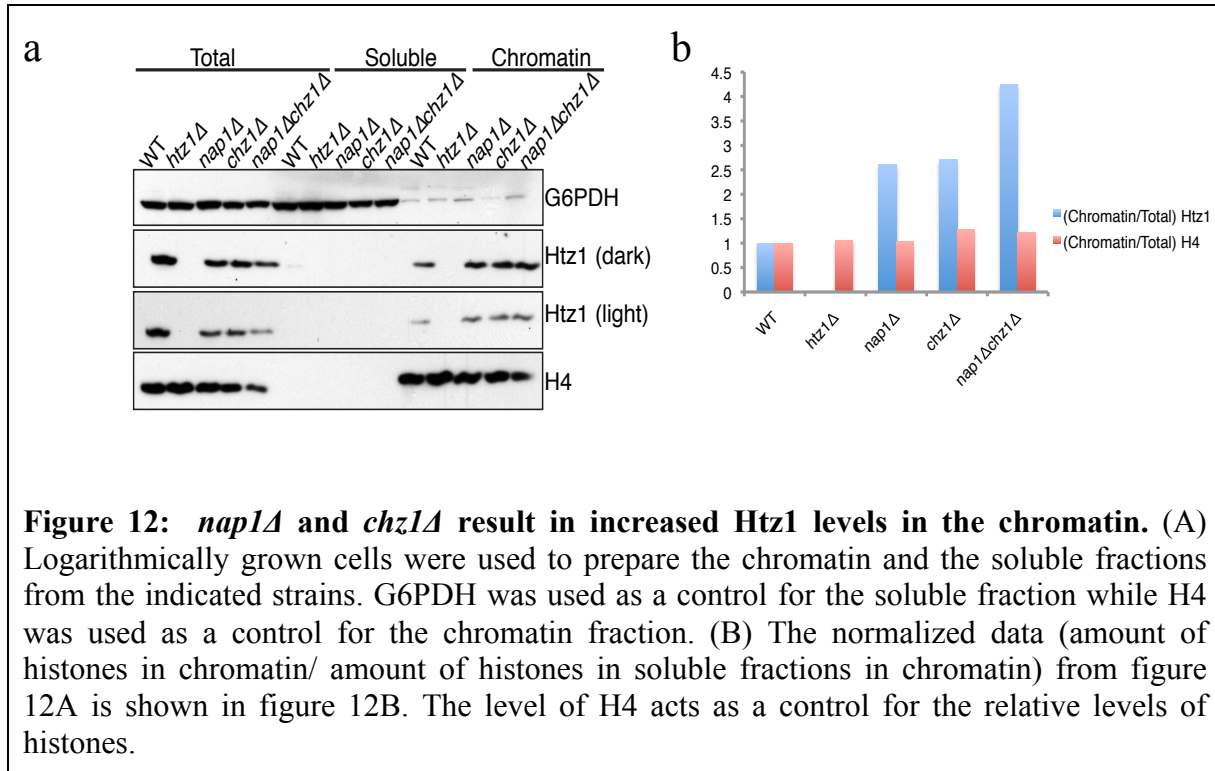
differential interactions between H2A.Z and its cognate chaperones – Nap1 and Chz1. Using structural modeling and discrete molecular dynamic (DMD) simulations, we have discovered specific residues on H2A.Z that are critical for interactions with either Chz1 or Nap1. Mutations in these residues lead to severe biological consequences, in terms of survival, with or without stressors (genotoxic or transcriptional). Using chromatin fractionation and genetic interactions between mutant H2A.Z residues and histone chaperones; we provide evidence that a major function of Nap1 and Chz1 is removal of H2A.Z from chromatin.

3.3 Results

3.3.1 Chz1 and Nap1 function in H2A.Z eviction

Given the importance of H2A.Z incorporation at specific locations across the genome, we sought to understand the role of H2A.Z binding proteins Chz1, Nap1, Swc2 and Swr1 (the remodeler involved in H2A.Z deposition) in modulating H2A.Z levels in chromatin. We utilized strains in which the genes encoding these proteins were deleted, and then determined both the cellular and chromatin-bound levels of H2A.Z in these strains. Deletion of *nap1Δ*, *chz1Δ*, *swc2Δ* and *swr1Δ* did not have any significant effect on overall H2A.Z protein levels in these strains (**Fig. 12 & data not shown**). However, chromatin-bound H2A.Z levels were significantly decreased in *swc2Δ* and *swr1Δ*, confirming Swc2 and Swr1 to be essential for H2A.Z deposition (data not shown). In contrast, we observed an increase in chromatin-bound H2A.Z levels in the absence of either Nap1, Chz1 or both indicating that their loss results in impaired eviction of H2A.Z from chromatin (**Figs. 12A and B**). To further understand the balance of H2A.Z deposition and eviction, we analyzed structural interactions of H2A.Z with Chz1 using the already available structural information for the Chz1-H2A.Z-H2B (CZB) complex¹⁷⁶. We

structurally defined important residues in H2A.Z that might be important in binding chaperones and H2A.Z depositing proteins.



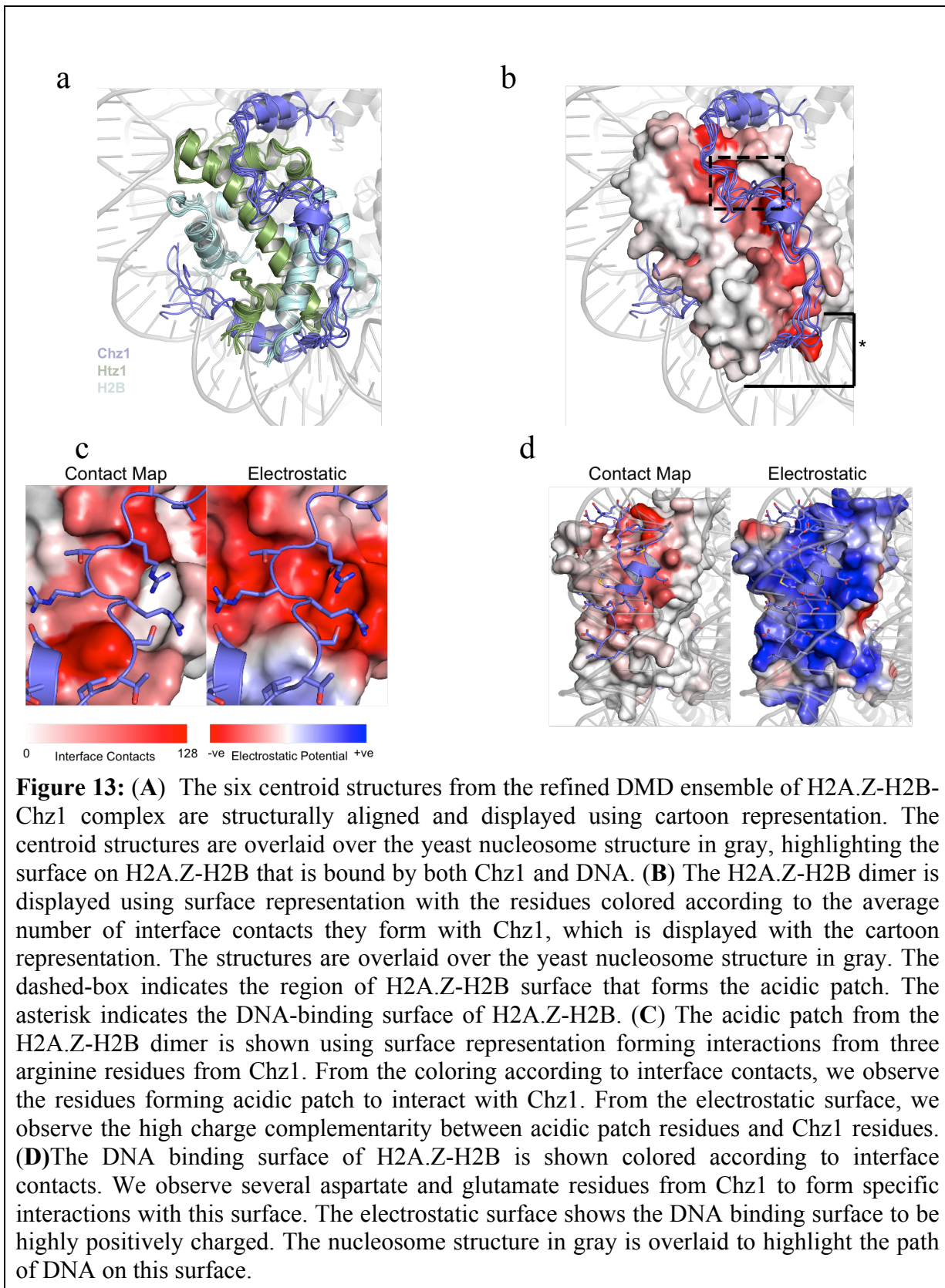
3.3.2 Constraint-driven CZB structural ensemble generated by DMD simulations

The NMR and biochemical data suggest Chz1 to be an intrinsically unstructured protein that does not adopt a compact globular fold or significant secondary structure even upon binding to H2A.Z-H2B dimer¹⁷⁶. Hence, to better understand the molecular recognition of H2A.Z-H2B by Chz1, we performed replica-exchange DMD simulations to sample multiple conformations of the CZB complex¹⁷⁶. To ensure that the set of conformations (ensemble) of CZB we used for structural analysis reflected native conformations, we used a set of filters to select a subset of structures from all the snapshots obtained from the DMD simulations. Using filters that included potential energy, electrostatics and violations of published Nuclear Overhauser Effect (NOE)

spectra of the CZB complex¹⁷⁶ we arrived at an ensemble of structures for the CZB complex (the DMD ensemble). In our DMD ensemble, the average violation of interface NOE constraints is 0.04 Å, lower than the average violation of interface NOE constraints in the published NMR ensemble (0.07 Å), thus indicating that the DMD ensemble of the CZB complex has excellent agreement with experimental distance restraints.

3.3.3 Diverse interactions drive specific recognition of H2A.Z-H2B by Chz1

Chz1 is unique compared to other histone chaperones of known structure; most of the histone recognition domain of Chz1 displays no secondary structure compared to globular, well-folded histone-recognition domains of histone chaperones whose structures are known (such as Asf1^{177, 178}, Nap1¹⁷⁹, Rtt106¹⁸⁰ and DAXX^{181, 182}). However, the extended coil structure of Chz1 enables an extensive and specific interface with H2A.Z-H2B. The histone recognition motif forms a lasso-like structure, covering two thirds of the circumference of H2A.Z-H2B (**Fig. 13A**) and the chaperone-histone interface buries 2462.2 ± 151.5 Å² solvent accessible surface area on average. To determine the binding interface of Chz1, we calculated average number of heavy-atom contacts formed by each residue of H2A.Z-H2B with residues of Chz1 in the ensemble. When we represent this binding interface as a heat map on the H2A.Z-H2B surface (**Fig. 13B**), we observe specific regions on the surface of H2A.Z-H2B that form interactions with Chz1. The highly negatively charged “acidic patch” of H2A.Z-H2B is specifically bound by a series of three arginine residues in Chz1 (R105, R106, R108, **Fig. 13C**). The DNA-binding surface of H2A.Z-H2B, which is highly positively charged, is bound by a negatively charged, highly complementary surface of Chz1 (**Fig. 13D**).



3.3.4 Interrogating the H2A.Z-H2B binding surface of Chz1

To understand the cellular role of residues in H2A.Z surface that are specifically recognized by Chz1 (and possibly Nap1 that also interacts with this histone variant), we performed a computational screen (see materials and methods) of the effect of point mutations on H2A.Z that lie in the H2A.Z-Chz1 binding surface. From this analysis, we selected three mutations in H2A.Z that were predicted to decrease its affinity towards Chz1 (**data not shown**). These mutations were present in three different regions of the Chz1-H2A.Z interface. R39 is present on the DNA binding interface of H2A.Z and the mutation R39D is predicted to destabilize Chz1 binding. As a control, we also selected R48D, in the DNA binding interface of H2A.Z, which is chemically similar mutation to R39D but which is predicted to have no major effect on Chz1 binding. Y65 is part of the acidic patch and forms specific interactions with Chz1, with Y65K mutation predicted to severely impair Chz1 binding. As a control, we selected D98K in the acidic patch, which is predicted to have modest effect on Chz1 binding. L93, part of the helix $\alpha 3$, forms hydrophobic interactions with Chz1 and the L93T mutation is predicted to severely destabilize H2A.Z-Chz1 interactions. S53 is part of loop1 and N76 is part of the long helix $\alpha 2$ and N76M and S53L are control mutations that are predicted to result in no significant change in H2A.Z-Chz1 interactions.

3.3.5 H2A.Z-Chz1 destabilizing mutants result in impairment of H2A.Z levels in chromatin

With our predicted set of mutations that result in either destabilization or no effect on Chz1-H2A.Z binding (**Table 5**), we next determined if these mutants would affect H2A.Z function and/or incorporation into chromatin. Point mutations were generated in a wild-type (WT) H2A.Z expression plasmid and then transformed in *H2A.Z* deleted cells. We first examined the

expression of these *h2a.z* mutants, and found that all of them expressed to a similar extent at the mRNA level (**Fig. 14B**). In contrast, immunoblot analysis of whole cell extracts (**Fig. 14A, upper panels**) and isolated chromatin fractions (**Fig. 14A, lower panels**) revealed that the total and chromatin-bound levels of several H2A.Z mutants were significantly different compared to WT. The most dramatic decrease in H2A.Z protein levels was observed for the Y65K and D98K mutants, followed by the R39D mutant (**Fig. 14A**). It is noteworthy that while H2A.Z protein levels are significantly diminished globally and in chromatin, we are still able to detect trace amounts in chromatin (data not shown).

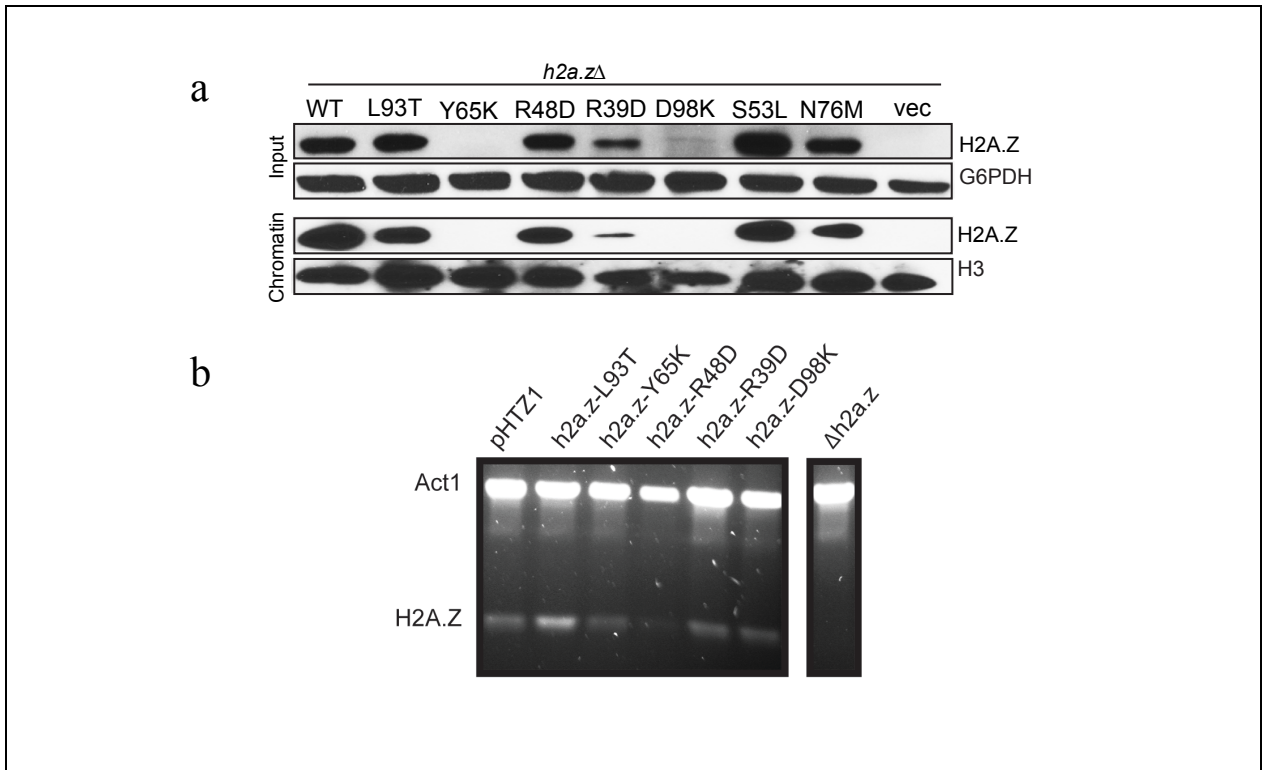


Figure 14: Protein (A) and RNA (B) levels of Htz1 mutants and their ability to get incorporated into the chromatin. (A) Whole cell extract (Input) and chromatin levels of designated mutants. As seen from the immunoblot, some Htz1 mutants are expressed at low levels in the whole cell extracts (e.g. Y65K and R39D) while others are differentially incorporated in the chromatin (N76M). (B) The RNA levels of these mutants are equivalent in cells, thereby ruling out a problem with transcription of the constructs. Figure courtesy, Michael Parra (Heritage University, Washington State).

3.3.6 H2A.Z mutations disrupt specific chaperone interactions

The altered cellular and chromatin-bound levels of our H2A.Z mutants led us to hypothesize that the decreases observed in H2A.Z might be due to altered binding of these mutants to one or more histone chaperones. To test this idea, we utilized TAP-tagged Nap1 and Chz1 strains in which *H2A.Z* was deleted and transformed with our H2A.Z mutants. We then probed the extent to which our H2A.Z mutants could co-immunoprecipitate (coIP) with either Nap1 or Chz1. The extremely reduced levels of the Y65K and D98K mutants precluded their assessment in these assays (**Fig. 14A**). In examination of Nap1-H2A.Z interactions, we found that the L93T mutant could immunoprecipitate with Nap1 at levels comparable to WT H2A.Z (Figure 2B). Significantly, however, Nap1-H2A.Z interaction was abrogated by mutations of R48D, R39D and S53L (**Fig. 15**). In examination of Chz1-H2A.Z interactions, the extent of immunoprecipitation of R39D, R48D, S53L and N76M H2A.Z mutants with Chz1 were not significantly different from H2A.Z WT (data not shown). However, significantly lower interaction was observed between the L93T mutant and Chz1, which is consistent with our computational predictions that L93T would have the most severe effect on Chz1 binding (**Table 5**). Thus, with rationally designed mutants of H2A.Z, we have uncovered two distinct classes of residues in H2A.Z that are critical for its interaction with different chaperones; R39D, R48D and S53L, part of the DNA binding interface of H2A.Z that is important for Nap1 interaction, while L93T on the α 3 helix is essential for Chz1 interaction. We also note that the striking decreases found in H2A.Z protein levels observed in the Y65K, D98K and R39D mutants in **Fig. 14A** are unlikely due to simple destabilization of Chz1 and/or Nap1 binding, as mutants that uncouple

these interactions do not result in lower H2A.Z levels. These observations suggest that the lower protein levels are due to another molecular mechanism rather than destabilization of H2A.Z-chaperone interactions.

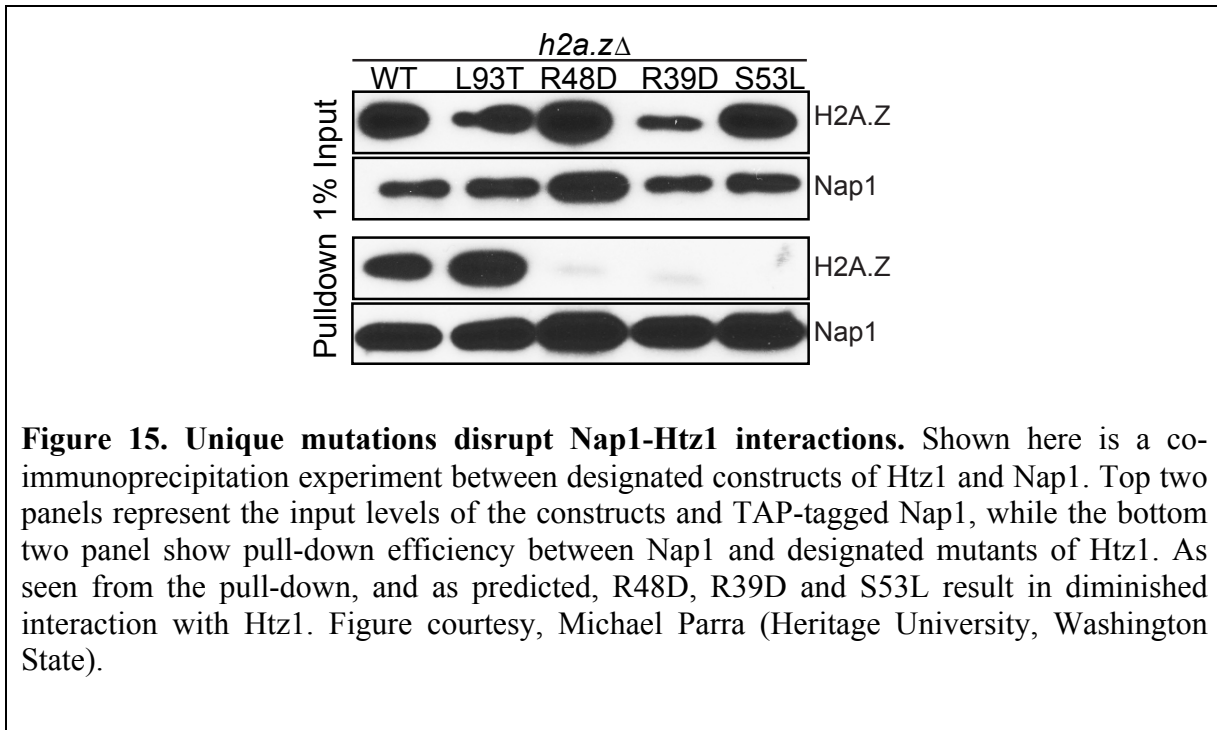


Figure 15. Unique mutations disrupt Nap1-Htz1 interactions. Shown here is a co-immunoprecipitation experiment between designated constructs of Htz1 and Nap1. Top two panels represent the input levels of the constructs and TAP-tagged Nap1, while the bottom two panel show pull-down efficiency between Nap1 and designated mutants of Htz1. As seen from the pull-down, and as predicted, R48D, R39D and S53L result in diminished interaction with Htz1. Figure courtesy, Michael Parra (Heritage University, Washington State).

3.3.7 Mutations predicted to affect H2A.Z-chaperone interactions disrupt H2A.Z function

Given the altered cellular and chromatin levels of our *h2a.z* mutants, along with the impaired H2A.Z-chaperone interactions we detected, we next asked if our *h2a.z* mutants would have any significant biological consequences in cells. Strikingly, the Y65K and D98K *h2a.z* mutants revealed severe growth defects, and in the case of the D98K mutant, sensitivity to all of the genotoxic stress agents tested (**Fig. 14A**) similar to previous studies¹⁷⁴. To our knowledge, our finding that the Y65K mutant confers severe growth defects even in the absence of genotoxic stressors is the first example of any mutations in H2A.Z resulting in significant defects in cell

viability. Of the mutations that we found to specifically affect either H2A.Z-Chz1 interaction (L93T) or H2A.Z-Nap1 interaction (R48D, R39D, and S53L), only the R39D mutation revealed a significant phenotype (i.e., sensitivity to caffeine and HU, similar to an *h2a.z* deletion (**Fig. 16A**). The R39D sensitivity is likely explained through the fact that the chromatin levels of this mutant are significantly down (**Fig. 14A**), rather than a specific disruption of chaperone interaction, as the R48D and S53L mutants that also disrupt Nap1-H2A.Z interaction show no phenotypes. The lack of observable phenotypes in the absence of preventing either Chz1- or Nap1-H2A.Z interaction is not surprising, as there is functional redundancy between these two chaperones⁹⁹. To test this, we combined our point mutations with deletion of either *NAPI* or *CHZI* and observed if we saw any growth defects after cellular stress. In line with our expectation, we observed that for mutations that disrupted Nap1-H2A.Z interaction (R48D), deletion of *CHZI* resulted in increased sensitivity to caffeine- a pleiotropic inducer of cellular stress (**Fig. 16B, upper panel**). Furthermore, when we deleted *NAPI* in mutants with disrupted Chz1-H2A.Z interaction (L93T), we increased the caffeine sensitivity of such cells (**Fig. 16B, lower panel**). In sum, we provide biochemical and biological evidence to suggest that Nap1 and Chz1 have non-overlapping binding surfaces on the H2A.Z-H2B nucleosomes and due to this, they can partially make support each other's function in dynamic incorporation/eviction of H2A.Z.

3.3.8 Characterization of a novel and toxic H2A.Z form that is dependent on chromatin deposition

The severe growth defects and extremely low levels of H2A.Z observed with the Y65K and D98K mutants led us to next address what might be the molecular basis behind this phenotype. We first asked whether these mutant forms of H2A.Z were toxic due to the fact they were being

incorporated into chromatin, albeit at extremely low levels (**Fig. 14**). If this were the case, we would predict that loss of the H2A.Z deposition machinery would suppress the slow growth phenotype. As shown in **Fig. 15A**, we found as expected that the Y65K *h2a.z* mutant was extremely sick under normal growth conditions. Surprisingly, deletion of *SWRI* in this context completely reversed the slow growth phenotype of the Y65K mutant (**Fig. 17A**), indicating that the Y65K growth defect is most likely caused by a defect of H2A.Z once deposited into chromatin. In contrast, deletion of *NAPI* did not reverse the slow growth defect of the Y65K mutant – a result consistent with our findings and others⁹⁹ revealing that Nap1 is required for H2A.Z eviction, and thus, is not preventing this variant from being deposited into chromatin. In addition to our growth assays under normal conditions, we also observed that the strong 6-AU (but not HU) sensitivity of the Y65K mutant was also reversed by deletion of *SWRI* and not *NAPI* (**Fig. 17A**). Taken together, these data imply that the toxicity of Y65K mutant is likely due to its deposition within chromatin, and that this mutant form is rapidly degraded.

The finding that the toxic phenotype of the Y65K *h2a.z* mutant could be reversed by deletion of *SWRI* led us to ask if *swr1Δ* would have any effect on the cellular levels of the Y65K H2A.Z protein. We examined the levels of WT or Y65K mutant H2A.Z levels in *h2a.zΔ*, *h2a.zΔ/swr1Δ* or *h2a.zΔ/nap1Δ* deleted cells. As expected, little to no Y65K H2A.Z levels were detected in the *h2a.zΔ* cells (**Fig. 17B**). In contrast, we found that deletion of *SWRI*, but not *NAPI*, restored Y65K H2A.Z levels to near WT levels (**Fig. 17B**). These data indicate that the incorporation of the Y65K mutant H2A.Z form is the basis for both the toxic phenotype as well as the rapid turnover.

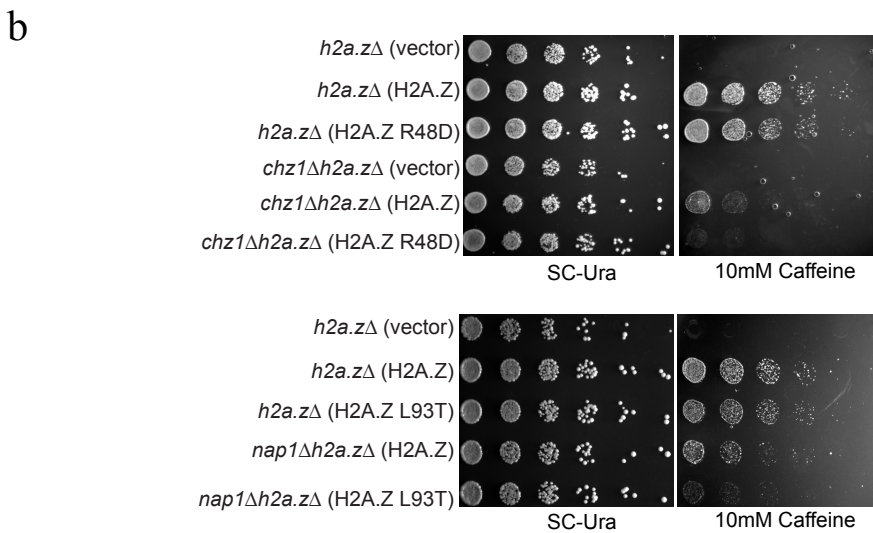
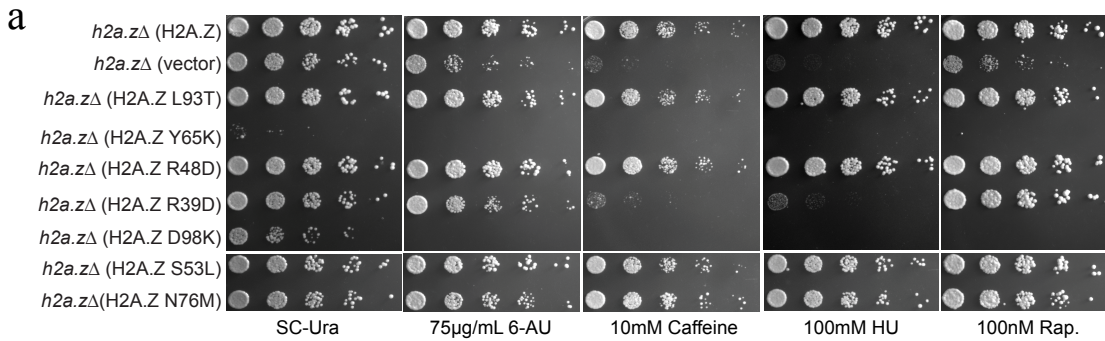


Figure 16. Biological consequences of the point mutants of Htz1. (A) Five-fold serial dilutions of indicated strains were spotted on either control (Sc-Ura) or drug-containing plates. The Y65K and D98K mutants of H2A.Z are slow growing. Mutants show varying degree of sensitivities to HU, Rapamycin, Caffeine and 6-AU. (B) Mutants of Htz1 combined with chaperone deletion increases the sensitivity to stress such as Caffeine. Shown in the upper panel is the combination of Htz1 mutant R48D, which disrupts Nap1-Htz1 interaction, and *CHZ1* deletion while the lower panel is the combination of Htz1 (L93T) mutant and *NAPI* deletion. The figure elucidates that loss of a chaperone, when combined with mutations of Htz1 that disrupt Htz1-chaperone interactions result in grave consequences for the cell.

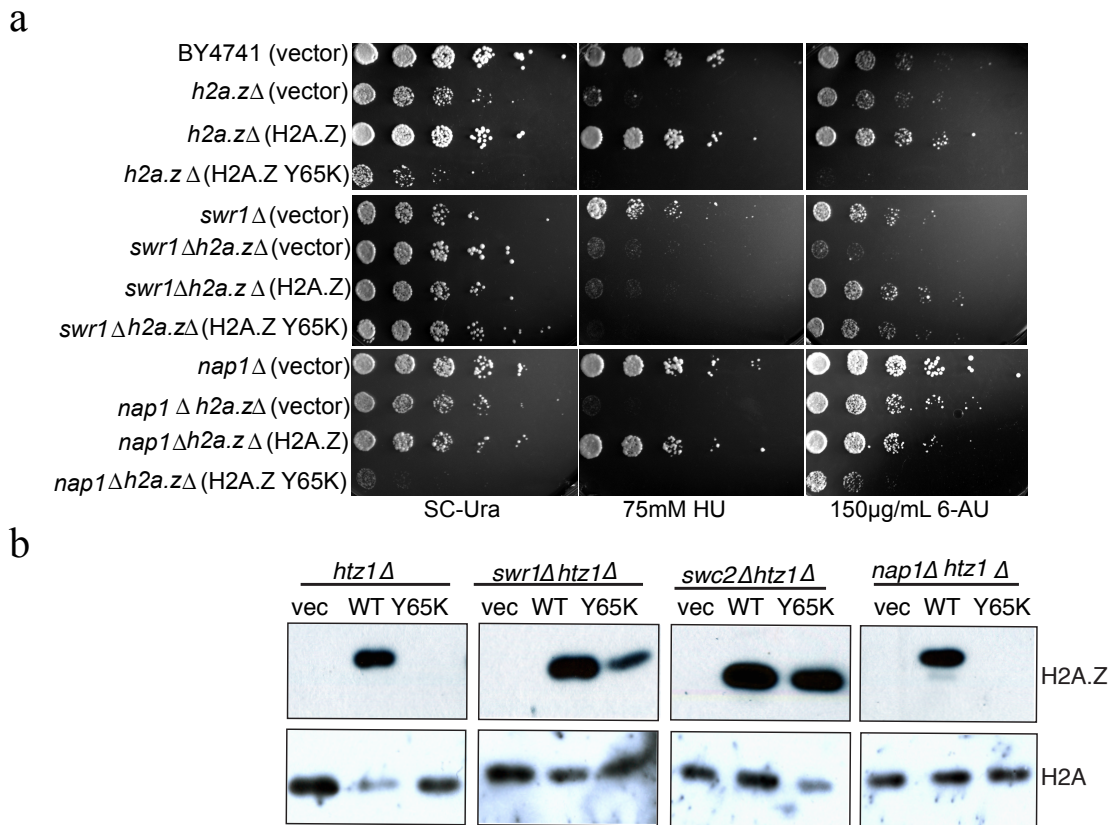


Figure 17. Chaperone deletions differentially effects H2A.Z mutations. (A) Deletion of *SWR1* can restore the slow-growth phenotype of the Y65K mutant while *nap1*Δ cannot. **(B)** Immunoblots showing the expression levels of H2A.Z off of plasmids in various strains. Y65K has lower H2A.Z protein levels, which can be at least partially rescued by *swr1*Δ and *swc2*Δ.

Discussion

An essential mechanism that underlies epigenetic regulation is the incorporation of histone variants, including H2A.Z, at specific genomic loci. Yet, how variant proteins are deposited and removed, in addition to what affect they have on chromatin structure and function remains a fundamental question in chromatin biology. Here, we provide new evidence that the Chz1 and Nap1 chaperones function, parallelly, to evict H2A.Z from chromatin (Fig. 12 and data not shown). These findings suggest a mechanism that precisely maintains H2A.Z levels in chromatin: deposition by SWR1C and eviction by Chz1/Nap1. How these two chaperones coordinate their activities, both temporarily and spatially, remain to be determined in future studies.

To uncover structural underpinning of chaperone-H2A.Z interaction, we generated a refined model of H2A.Z-bound to Chz1. Structure and conformational dynamics of the Chz1-H2A.Z-H2B (CZB) complex revealed a unique mode of histone recognition by Chz1 compared to other chaperones of known structure. Importantly, the binding interface of Chz1 encompasses the DNA-binding surface of H2A.Z and the acidic patch, in addition to H2A.Z-H2B surface distal to these regions. Swc2 (VSP72) binds to the acidic patch of H2A.Z^{99,174} and mutations in this region lead to diminished but not total abrogation of H2A.Z incorporation into chromatin¹⁷⁴, implying that multiple interactions of H2A.Z (including Swc2 and Chz1) would be affected by mutations in the acidic patch. Although two acid patch mutations were generated to interrogate Chz1-H2A.Z and Swc2-H2A.Z interaction in this study (Figures 13 and 14), we found unexpectedly that they were slow growing and had extremely low levels of H2A.Z – thus precluding further binding studies (see below and Figure 16).

Interestingly, all the mutants designed in the DNA-binding interface (Figure 18) showed abrogated interaction with Nap1 but not Chz1 (Figure 14 and data not shown). These data allow us to define multiple surfaces that are employed to engage specific chaperones for H2A.Z function. Such distinct binding surfaces for Chz1 and Nap1 may explain the synthetic sick genetic interaction between the two chaperones¹⁷⁵.

Two of the H2A.Z mutations identified in our simulations (Y65K and D98K) resulted in severely reduced H2A.Z protein levels and defective growth that was worse than *h2a.zΔ*. To test our hypothesis that the severe effects of these mutations are due to specific incorporation of mutant H2A.Z into chromatin, we performed chaperone deletions in the background of Y65K. We were able to rescue the slow growth phenotype of Y65K by deleting either *SWR1* or *SWC2* but not *NAP1*, suggesting that it is not the low level of H2A.Z *per se* in cells, which is harmful but rather the deposition of a form of H2A.Z that can't be evicted (i.e. Y65K). In line with this idea, we observe an increase in H2A.Z protein levels in the Y65K mutant in the background of *swr1Δ* and *swc2Δ*, where the mutant H2A.Z can't be deposited into the chromatin (Figure 17). Although an understanding of how these two mutants cause severe growth defects is not understood, it may be that these mutants alter nucleosome structure and/or dynamics at gene promoters to inappropriately affect gene transcription. It is interesting to speculate that the acidic patch might have multiple functions in chromatin by making functionally important intra- and/or inter-nucleosomal interactions that then are disrupted by Chz1 during the removal of H2A.Z, but used by Swc2 during its deposition.

Here we present a model of H2A.Z regulation by showing that Chz1 and Nap1 function to evict H2A.Z from chromatin. Together with the fact that Swr1 functions to deposit H2A.Z into chromatin, the collective data suggest that H2A.Z is tightly regulated by the actions of

chaperones that function to deposit and evict in order to maintain precise levels of H2A.Z in cells. It is the equilibrium of this deposition vs. removal that ultimately dictates the H2A.Z levels in chromatin, and hence genome function. Outside of H2A.Z, a similar mode of regulation has been made for the centromeric histone H3 variant, Cse4⁹⁸. Deletion of Snf2, a chaperone for the centromere specific histone Cse4, leads to marked mis-localization of this histone variant leading to aneuploidy. In light of similar results with respect to H2A.Z in recent studies¹⁸³, we surmise that mutant H2A.Z incorporation leads to mislocalization of H2A.Z in the genome that can lead to genome instability and hence defective growth.

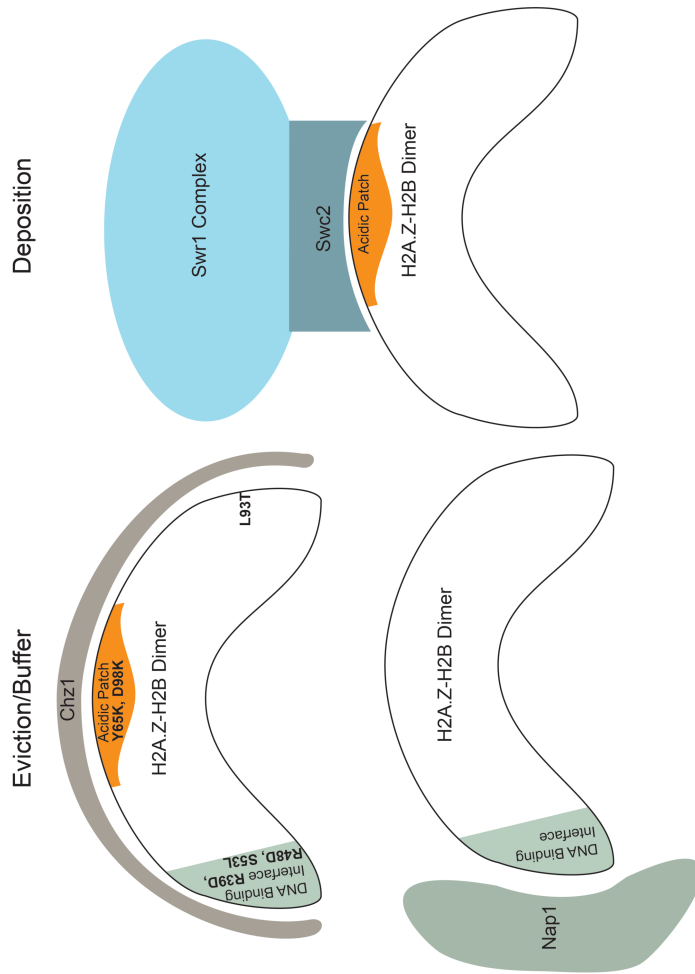


Figure 18. Hypothetical model for the basis of “separation-of-function” between different H2A.Z-specific chaperones. Chz1 forms a lasso-like structure around the dimer, forming interactions at multiple regions. Nap1 mainly interacts through the DNA-binding region of H2A.Z-H2B and Swc2 interacts with the acidic patch. This model explains our and others’ observations that Nap1 and Chz1 have non-overlapping functions in buffering the H2A.Z levels in the chromatin while the Swr1 complex regulates its deposition.

3.5 Materials and methods

CZB constructs used in structural studies. We used the NMR structure of CZB (PDB ID: 2JSS) as a starting structure for our simulations. This construct consists of H2A.Z (residues 22-118, UniProt ID: Q12692), H2B (residues 36-130, UniProt ID: P02294) and Chz1 (63-124). The NMR sample was constructed by connecting the C-terminus of H2B and N-terminus of H2A.Z to form a single peptide chain. In the construct used in our simulations, we treated H2A.Z and H2B as separate chains.

CZB DMD simulations. We employed replica exchange, parallelized discrete molecular dynamics to sample ensemble of conformations of the CZB complex. The DMD simulation methodology is described in detail elsewhere¹⁸⁴⁻¹⁸⁶. Briefly, we use Medusa force field¹⁸⁷ that is based on CHARMM19 non-bonded potentials¹⁸⁸, EEF1 implicit solvation parameters¹⁸⁹, geometry-based hydrogen bond potential and long-range electrostatic potential¹⁹⁰ to model various macromolecular interactions. The time unit of the all-atom DMD simulations is ~50 femtosecond¹⁸⁸ and the temperature is maintained using Anderson's thermostat¹⁹¹. We performed ten sets of DMD simulations for $\sim 1 \times 10^6$ time units with a total of 16 replicas, resulting in total sampling of $\sim 160 \times 10^6$ time units, or $\sim 8 \mu\text{s}$. The 16 replicas were set at following temperatures: 0.480, 0.495, 0.512, 0.528, 0.546, 0.563, 0.581, 0.600, 0.619, 0.638, 0.658, 0.679, 0.700, 0.722, 0.744 and 0.767 ϵ (reduced units¹⁸⁶; roughly corresponds to 240-383K). To increase sampling of Chz1, so as to optimize the Chz1-histone interface, while biasing the simulations towards known experimental data, we utilized two sets of constraints: (i) the backbone atoms of H2A.Z (Residues: 26-113) and H2B (40-129) were harmonically constrained to their starting coordinates with a spring constant of $0.4 \text{ kcal.mol}^{-1}.\text{atom}^{-1}$ ⁵⁰ the distance between a subset of atoms of Chz1 and the histones (determined using Nuclear Overhauser

Effect (NOE) – NMR spectroscopy), were restrained with a two-well potential (Supplementary Figure 3). The list of NOE restraints were utilized from earlier study with minor modifications¹⁷⁶: (i) Since our force field does not consider aliphatic hydrogens, the constraints containing aliphatic hydrogens were modified to contain the carbon atom to which the hydrogens were bonded, and the constraint length was increased by 1 Å to reflect the additional bond-length;⁵⁰ all restraints were increased by 1 Å to account for the standard deviation of the NOE signal.

Simulations analysis – identifying a refined CZB ensemble. We calculated several parameters of the simulation snapshots to identify a subset of snapshots (the refined ensemble) that features an optimized protein-protein interface and also agrees well with experimental distance restraints. We used our published electrostatic potential¹⁸⁵, Medusa potential¹⁸⁷ and the mean NMR violations as criteria to identify the refined ensemble. If the distance between two atoms is higher than the experimental distance, the difference between the observed distance and the experimental distance gives the violation value for that distance restraint. The average of such values over all distance restraints gives the mean NMR violation. After filtering out high energy structures and structures with high NMR violations, we identified a refined ensemble of 1454 structures. We determined the mean NMR violation of this refined ensemble as follows. Since the NOE signal is proportional to the ensemble-averaged $1/r^6$ between two atoms, we determined the average $1/r^6$ from our filtered ensemble and then calculated r from that average. This distance r for each distance restraint was used to calculate the mean NMR violation of the ensemble. We observe the mean NMR violation of this ensemble to be lower than observed for the published NMR ensemble, indicating excellent agreement with experimental structural data for the CZB complex.

Interface analysis. We define a contact as a pair of atoms (one from H2A.Z-H2B and the other from Chz1) that are not hydrogen and are within a distance of 6 Å of each other. For the refined ensemble from DMD, we calculated the average number of contacts formed by each residue of H2A.Z-H2B with Chz1. We colored each residue in the H2A.Z-H2B interface with Chz1 (on structural figures) based on the average number of contacts formed by the residue.

Estimation of change in binding affinity upon mutation. We calculated the change in binding energy of H2A.Z-H2B to Chz1 upon mutation using Medusa¹⁹²⁻¹⁹⁴. We performed 17 possible point mutations (all residues except proline, cysteine and the native amino acid) at all residues of H2A.Z that were part of the interface with Chz1 (Figure 1C) to determine a list of mutations that destabilize the CZB complex. Medusa calculations involve a Monte Carlo based simulated annealing procedure that uses rotamer libraries of amino acids for fast minimization of its energy function while leaving the backbone fixed. Medusa uses a combination physics-based terms (van der Waals, hydrogen bond, solvation) and knowledge-based terms (backbone and side chain torsions). We averaged the free energy obtained from at least 500 Medusa calculations for each of the six centroid structures (from the refined ensemble) to obtain $\Delta\Delta G$ for each mutation. We define $\Delta\Delta G$ as:

$$\Delta\Delta G = (DG_{\text{Complex-Mut}} - DG_{\text{H2A.Z-H2B-Mut}}) - (DG_{\text{Complex-WT}} - DG_{\text{H2A.Z-H2B-WT}}),$$

where $DG_{\text{Complex-Mut}}$ is the stability of the mutant H2A.Z-H2B-Chz1 complex, $DG_{\text{H2A.Z-H2B-Mut}}$ is the stability of the mutant H2A.Z-H2B dimer, $DG_{\text{Complex-WT}}$ is the stability of the wild type H2A.Z-H2B-Chz1 complex and $DG_{\text{H2A.Z-H2B-WT}}$ is the stability of the wild type H2A.Z-H2B dimer. Thus, a destabilizing mutation would result in a positive $\Delta\Delta G$.

Yeast strains and plasmids. The chromosomal copy of the histone H2A.Z (*HTZI*) gene was deleted in the following yeast strains: 1) a strain bearing TAP-tagged Chz1 (Open Biosystems),

2) a strain bearing TAP-tagged Nap1 (Open Biosystems), 3) a strain bearing *nap1D* (Open Biosystems), 4) a strain bearing *swr1D* (Open Biosystems), and 5) a strain bearing *swc2D* (Open Biosystems). H2A.Z was replaced with the NatMX gene deletion cassette in these strains using PCR mediated gene disruption¹⁹⁵. The resulting yeast strains were screened on media containing cloNAT (Werner Bioagents) at 100 mg/mL. Strains were confirmed by PCR amplification and Western blot analysis. Plasmids containing either a WT or mutant H2A.Z allele (see below) were transformed into the resulting deletion strains. Yeast strains used in this study are listed in Table 7.

Plasmid construction. The pRS416-based Htz1-2Flag vector (a gift from Dr. C. Wu) was used as a template to generate all subsequent plasmids bearing mutations to H2A.Z. All mutations were made by site directed mutagenesis (QuikChange kit, Stratagene) and confirmed by sequencing.

Whole cell extract, Chromatin fractionation and Immunoblotting. For analysis of total protein levels, whole cell extracts were made using established protocols¹⁹⁶. Chromatin was isolated from strains using established protocols¹³⁷. Electrophoresis and immunoblot analysis were performed as described elsewhere¹⁹⁷.

Co-immunoprecipitation. *H2A.Z* was deleted in the TAP-*CHZ1* and TAP-*NAPI* (from Open Biosystems) and co-immunoprecipitation was performed as before¹⁷².

Table 4: Chapter 3 Summary

Rational Design of H2A.Z Mutants Uncover Differential Chaperone Interactions and Function

- Nap1 and Chz1 are involved in evicting Htz1 from chromatin.
- Nap1 and Chz1 have non-overlapping surfaces of interaction on H2A.Z-H2B nucleosomes
- Rationally designed mutations in Htz1 disrupt the interaction between Nap1/Chz1 and H2A.Z-H2B and they have biological consequences on cellular response to stress.
- Inappropriately deposited mutants of H2A.Z result in massive defects in cellular growth and the phenotype can be suppressed by deleting the H2A.Z deposition machinery.

CHAPTER 4: CONCLUSIONS, UNANSWERED QUESTIONS AND DISEASE RELEVANCE

4.1 Conclusion for Chapter 2

Eukaryotic cells experience a plethora of DNA lesions; the most severe form being a DNA double-strand break (DSB), which can result in chromosomal rearrangements or cell death. DSBs can be caused by endogenous events (e.g., meiotic DSBs or replication through single-stranded nicks) and exogenous agents (e.g., exposure to gamma-radiation). Cells respond to DSBs by activating the DNA damage response (DDR), which performs a number of functions including delaying the cell cycle to facilitate DNA repair. In mammalian cells, induction of DSBs activates the ATM and ATR (Tel1 and Mec1 in budding yeast) kinase-signaling cascades, which results in phosphorylation of downstream substrates such as histone H2A.X (H2A in yeast) and 53BP1 (Rad9 in yeast). Two major pathways, non-homologous end joining (NHEJ) and homologous recombination (HR), repair the majority of DSBs, and pathway choice is contingent on whether DSB ends are resected or not. This is dependent on the balance between factors promoting NHEJ (Ku, 53BP1, RIF1) and resection (CtIP, MRN, EXO1, BLM and DNA2), which is in turn influenced by chromatin structure and the phase of the cell cycle in which DNA damage occurs.

An emerging theme is the critical role that chromatin plays in multiple aspects of the cellular response to DSBs¹⁰⁹¹⁰⁹¹⁰⁹. Lysine 36 methylation of histone H3 (H3K36me) is a post-translational modification conserved from yeast to human cells. In yeast, Set2 is the sole

methyltransferase that catalyzes H3K36 mono-, di- and tri-methylation (H3K36me1, H3K36me2, and H3K36me3), whereas its human ortholog, SETD2, catalyzes only H3K36me3. Through an association with the hyper-phosphorylated, elongating form of RNA Polymerase II (RNAPII), Set2/SETD2 is recruited to the bodies of actively transcribed genes where it catalyzes H3K36 methylation. One major function for Set2-mediated H3K36me2/me3 in budding yeast is the recruitment and activation of a histone deacetylase complex (Rpd3S) as well as an ATP-dependent chromatin-remodeling complex (Isw1b). These complexes function in the wake of elongating RNAPII to maintain chromatin integrity by creating a compact chromatin environment restrictive to intragenic or ‘cryptic’ transcription. In human cells, H3K36me2 catalyzed by SETMAR/Metnase has been implicated in non-homologous end joining (NHEJ). H3K36me3 catalyzed by SETD2 also prevents cryptic transcription and regulates alternative splicing⁸⁸⁸⁸⁸⁸ and mismatch repair. Five new papers from the de’Almeida, Humphrey, Legube and Strahl labs^{1,91,198-200} further expand the function of Set2/SETD2 and H3K36 methylation by demonstrating their involvement in DDR and DSB repair. Here, we draw evidence from these five recent publications to compare and contrast the emerging roles of yeast Set2 and human SETD2 in three main aspects of DSB repair: DDR, NHEJ/HR pathway choice and the link between transcription and DNA repair.

Two of the aforementioned studies support roles for yeast Set2 and human SETD2 in DNA damage checkpoint activation. Using budding yeast as a model system, Jha and Strahl show that loss of H3K36me resulting from Set2 deletion (*set2Δ*) leads to reduced phosphorylation of histone H2A Ser129 and Rad53, signifying attenuated DNA damage checkpoint activation. Similarly, using human clear cell renal cell carcinoma (ccRCC) cell lines, Carvalho *et al.*, show that activation of DDR is defective in SETD2-deficient or -depleted cells,

as measured by reduced ATM activation, γ H2AX, delayed 53BP1 recruitment to DNA damage sites, p53 stabilization and downstream activation of p21, the major cyclin-dependent kinase inhibitor that is required for DNA damage dependent cell-cycle arrest. These findings are consistent with a reported role for Set2 in checkpoint activation in fission yeast, and indicate that Set2/SETD2 impacts a very early aspect of DNA damage sensing, an unexpected finding for a histone modification.

In two yeast model systems, both Jha and Strahl (budding yeast) and Pai *et al.* (fission yeast) show that Set2 promotes NHEJ (**Fig.19a**)^{1,198}. Jha and Strahl show that deletion of *SET2* or mutation of H3K36 is sensitive to DSBs induced by phleomycin, radiation, or a Homothalic (HO)- endonuclease. In the case of fission yeast, Pai *et al.* show that Set2 promotes Ku recruitment and/or retention at a DSB. Using a mini-chromosome based DSB repair assay, they show that loss of Set2 substantially increases the frequency of gene conversion, suggesting that Set2 inhibits HR. Similarly, Jha and Strahl observed that when a linearized plasmid was transformed into *set2Δ* cells, re-ligation efficiency was significantly increased and was almost entirely dependent on Rad51 – an HR component. This suggests that loss of Set2 favors repair via HR. Consistent with these observations, studies in both fission and budding yeast indicate that loss of Set2 results in a relatively open chromatin structure, as measured by chromatin immunoprecipitation (ChIP) of acetylated histone H4, Htz1 (yeast homolog of the mammalian H2A variant, H2A.Z) and micrococcal nuclease (MNase) digestion. This, in turn, increases resection kinetics (as measured by loss of input DNA signal, increased recruitment of RPA by ChIP in G1-arrested cells and increased RPA recruitment by immunofluorescence), indicating that loss of Set2 promotes recruitment of the HR repair machinery.

These yeast studies also revealed that H3K36 modification influences repair pathway choice. Pai *et al.* demonstrate an antagonistic relationship between H3K36me3 and H3K36 acetylation (H3K36ac) by showing that deletion of the H3K36 methyltransferase, Set2, increases the level of H3K36ac and reduces NHEJ. Conversely, deletion of the H3K36 acetyltransferase, Gcn5, increases the level of H3K36me3 and reduces HR. Collectively, these results suggest that Set2 and Gcn5 compete to modify H3K36, creating a ‘chromatin switch’ between NHEJ and HR. Furthermore, they show that H3K36me levels are high in G1 and H3K36ac levels are high in S/G2, and that the cell cycle distribution of these histone modifications conform to the preferred repair pathway in each cell cycle phase: NHEJ in G1 and HR in S/G2.

In contrast to the above findings, human SETD2 is required for HR (**Fig. 19b**)^{91,199,200}. Using a well-established GFP reporter system in which repair of an I-SceI endonuclease-induced DSB by HR generates an intact GFP gene, Aymard *et al.*, Carvalho *et al.*, and Pfister *et al.* show that siRNA-mediated depletion of SETD2 resulted in reduced HR. Loss of SETD2 also reduced formation of RPA foci⁹¹, RAD51 foci^{91,199} and recruitment of RAD51 to DSBs, as measured by ChIP^{91,200}. Moreover, SETD2 depletion reduces DSB end-resection, as shown by an *in vivo* assay that measures single-stranded DNA generated by the resection machinery in the vicinity of a DSB⁹¹. Together, the Aymard *et al.* and Pfister *et al.* studies support a model in which SETD2-dependent H3K36me3 anchors Lens Epithelium-derived Growth Factor p75 (LEDGF) to chromatin through its PWWP domain. Following DSB induction, chromatin-bound LEDGF recruits the resection enzyme CtIP, which promotes resection and recruitment of RAD51. However, Carvalho *et al.* showed that RAD51 recruitment was reduced without defects in resection.

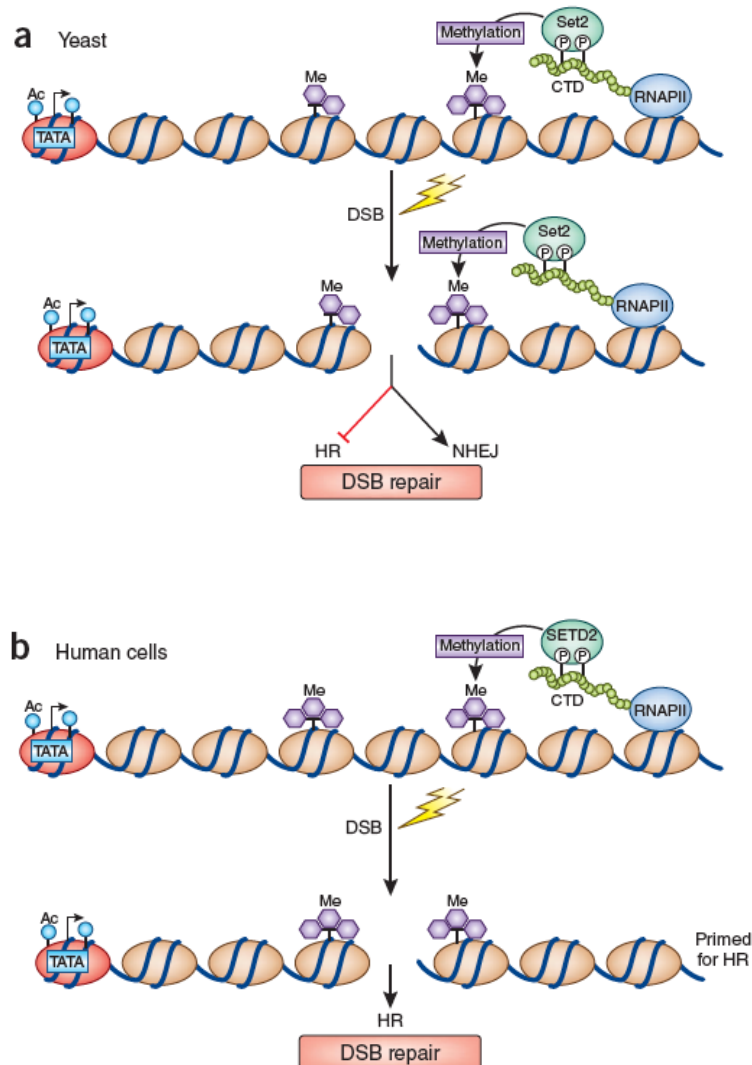


Figure 19. H3K36 methylation functions in DSB sensing and repair. (A) In the context of transcribing RNAPII, yeast Set2 catalyzes all forms of H3K36 methylation (mono-, di- and trimethylation). Set2 methylation contributes to transcription elongation by recruiting deacetylases and ATP-dependent remodeling complexes to maintain chromatin integrity. Five recent reports^{9–13} identify a new role for Set2 in DSB repair. In budding and fission yeast, Set2 is recruited to sites of DSBs in an RNAPII-dependent manner. H3K36 methylation regulates DNA-integrity-checkpoint activation, chromatin architecture at DSBs and repair-pathway choice (preference for NHEJ). P denotes phosphorylation. (B) In human cells, preexisting H3K36me₃ marks generated by SETD2 during transcription are used to anchor LEDGF, which in turn recruits CtIP after DSB induction to promote DNA end resection and repair of the DSB via HR. The lightning bolt indicates a DNA-damage event generating a DSB, and red nucleosomes indicate the +1 nucleosome at the 5' end of genes, which typically contains the H2A variant H2A.Z (Htz1) and is marked by histone acetylation. CTD, C-terminal domain.

As opposed to what was observed in human cells, both yeast papers show that Set2/H3K36me negatively regulates DNA end resection. One reason for the apparent discrepancy could arise from the possibility that in the absence of SETD2, reduced damage-induced γ H2AX phosphorylation may lead to reduced 53BP1 recruitment, thereby permitting resection, a result alluded to in Carvalho *et.al*. However, resection in mammalian cells is compromised by the additional requirement for SETD2 to recruit CtIP, in a LEDGF-dependent manner. In yeast, loss of Set2 may similarly reduce Rad9 (53BP1) recruitment through reduced H2A phosphorylation or other checkpoint-dependent events, thus permitting resection. Nevertheless, LEDGF is not evolutionarily conserved in budding and fission yeast. Thus, in contrast to mammalian cells, Sae2 (CtIP) may be recruited to DSB sites independently of Set2, thereby promoting efficient resection and HR in yeast. In addition, Set2 in yeast catalyzes all three forms of H3K36 methylation (me1, me2 and me3), while human SETD2 catalyzes only H3K36me3. Therefore, the differences between yeast and human cells could also be a result of different methylation states having different, perhaps even opposing, functions after DSBs are formed. Indeed, human H3K36me2 promotes NHEJ while H3K36me3 promotes HR. Moreover, SETD2 is significantly larger than the yeast Set2 proteins, with an extended uncharacterized N-terminus which may harbor unique functions in the repair process.

The demonstrated role of Set2/SETD2 in DNA repair raises the question of whether H3K36me3 levels increase in response to DNA damage. In the two yeast systems, H3K36me3 rapidly accumulates at the site of DSBs, but in human cells, no increase in SETD2 or H3K36me3 was observed at DSB sites^{91,199,200}, suggesting that H3K36me3 levels are pre-set, presumably by prior transcription, and may be sufficient for downstream functions in DSB repair. Indeed, Aymard *et al.* show that, in human cells, HR preferentially repairs transcriptionally active

regions. A rare-cutting endonuclease (AsiSI) was used to generate around 150 DSBs across the genome, which were then sub-divided into RAD51- or XRCC4-enriched DSBs by chromatin immunoprecipitation-sequencing (ChIP-seq). RAD51 enrichment implied the use of HR while XRCC4 enrichment suggested that the DSB was being repaired by NHEJ. Surprisingly, RAD51-enriched DSBs tended to occur in transcriptionally active regions and this preference was lost when transcription was abolished by addition of the transcriptional inhibitor DRB. Conversely, reactivating a repressed gene directed DSB repair towards HR. These findings indicate that HR preferentially repairs DSBs in transcriptionally active regions of the genome. Given that H3K36me3 is correlated with transcription frequency and gene length in yeast, it will be interesting to investigate how DSBs are repaired in genes of varying lengths and transcription rates in human cells.

Additional support for a transcription-coupled function for Set2/H3K36me was provided by Jha *et.al*¹. By using a truncated form of Set2 that inhibits its interaction with RNAPII, these authors demonstrated that Set2 association with RNAPII is critical for its DNA repair function. Furthermore, Jha and Strahl observed a substantial reduction in the protein levels of Set2 and RNAPII after DSB, which they found to be reduced in a proteasome-dependent manner. Why RNAPII and Set2 are degraded after DSB induction remains unclear, but the requirement to prevent transcription around a DSB to allow for DNA repair events might offer a plausible explanation. The interaction of Set2 with RNAPII is conserved in human cells as well, thereby raising the intriguing possibility that the role defined for H3K36 methylation in DSB signaling and repair in all organisms is intertwined with transcription elongation. Further studies will be needed to elucidate how transcription-dependent H3K36me regulates DSB repair.

The identification of a role for H3K36me3 in HR in human cells contrasts with a previous report, which showed that SETMAR/Metnase-mediated H3K36me2 promotes DSB repair through NHEJ. The distinct repair pathways associated with H3K36 di-methylation (NHEJ) and trimethylation (HR) suggests the tantalizing prospect that, in mammalian cells as in yeast, H3K36 modification contributes to DSB repair pathway choice, albeit via different histone marks. However, studies by Pfister *et al.* showed that depleting SETD2-dependent H3K36me3 results in reduced HR while NHEJ was unchanged. The authors inferred the pathways taken by the induced DSB by using an I-SceI inducible DSB in the *HPRT* gene and sequencing the repair products. Surprisingly, depleting either SETD2 or RAD51 resulted in a significant increase in microdeletions, with break junctions being associated with regions of micro-homology (2-4bp) on either side of the break site. These findings suggest that HR genes may suppress micro-homology mediated end-joining (MMEJ), in which end-joining is dependent on short stretches of micro-homology. Microdeletions also frequently occur in various cancer cells and the observation that loss of SETD2 increases the incidence of micro-deletions has repercussions for tumorigenesis in cancers in which SETD2 is frequently mutated (e.g., clear cell renal carcinoma (ccRCC)).

If H3K36me functions in DSB repair, one would expect that this histone mark would help to maintain genome integrity. In agreement with this hypothesis, Kolodner and colleagues used bioinformatic analysis to show that the budding yeast *SET2* gene shows genetic interaction with genes that suppress gross chromosomal rearrangement (such as *MRE11*, *RAD9*) – thereby reinforcing the idea that loss of Set2 might contribute to chromosomal abnormalities. Furthermore, and outside of DSB repair, Li *et al.*⁹⁰ showed that SETD2/H3K36me3 also contributes to DNA mismatch repair in an MSH6-dependent manner. The authors showed that

MSH6 is recruited to chromatin through an interaction of MSH6 (its PWWP domain) with H3K36me3, which aids in repairing nucleotide mismatches. Consistent with an important role for SETD2 in maintaining overall genome stability, SETD2 was identified as a tumor suppressor, and is frequently mutated in a number of cancer types. The identification of roles for SETD2/H3K36me3 in DDR, DSB repair, along with mismatch repair provide new mechanistic insights into how SETD2 may function as a tumor suppressor.

4.2 Outstanding Questions

Some important outstanding issues relating to set2/SETD2 and genome stability raised by these studies include: (1) What is the mechanism by which SETD2 promotes DNA damage checkpoint activation? Although, two studies have shown that there is attenuation of DNA damage checkpoint activation in yeast and human cells, both these studies did not elaborate on the mechanism of this attenuation. Our study raises the possibility that this can be achieved in two non-exclusive ways: a) Since we show that there is more Htz1 containing nucleosomes around the DSB, there is not enough substrate for Tel1 in yeast cells to subsequently phosphorylate around a DSB. b) We have also shown that loss of SET2 results in an open chromatin environment surrounding the DSB- as evidenced by more Htz1 and more H4 acetylation. This open chromatin structure resulted in increased resection kinetics, as seen by faster loss in input DNA and increased RPA recruitment. As a result of faster resection, Tel1 may get removed from the chromatin, reducing the overall level of Tel1 around the DSB and thus reduced DNA damage checkpoint activation.

Another interesting possibility can come from abrogated acetylation-dependent activation of ATM kinase. In human cell, ATM gets acetylated by Tip60 HAT, which is recruited to the

chromatin through its interaction with H3K9me3. The domain that recognizes H3K9me3 (chromo-domain in a Tip60 subunit), also recognizes H3K36me and therefore loss of H3K36me from the chromatin may reduce the recruitment or stability of Tip60 on the chromatin.

(2) Is there any correlation between transcription rate or gene length and the repair proficiency of DSBs induced in gene bodies? Transcription of genes involves major disruption of chromatin structure and generation of free DNA stretches. These free DNA stretches can be temporarily bound by nascently transcribed RNAs to form what is called R-loops. These R-loops are inherently recombinogenic, and can induce DSB. In line with this idea, R-loops tend to induce Serine 10 phosphorylation of histone H3 (H3S10ph), which tends to repress the chromatin. It would be intriguing to monitor the DSB frequency in various regions of the genome and correlate them with transcription frequencies enrichment of particular histone modifications and repair pathway choices for those DNA breaks. Using the Asi-inducible DSB system generated in the Legube lab, followed by RNA-seq of the transcriptome and chip-seq for XRCC1 and Rad51, we can perform these experiments.

(3) What is the mechanistic basis and significance of RNAPII degradation after DSB induction? In our study, we clearly showed that just like what happens after UV exposure, RNAPII gets degraded after DSB. This degradation was clearly dependent upon the proteasome function. Besides the degradation of RNAPII, we showed that Set2 was also degraded after DSB, in a fashion that does not solely depend on the presence of checkpoint kinases. One interesting possibility is that other kinases such as stress-activated kinases (e.g. Hog1) or kinases activated due to nutritional stress (e.g. PKA/PKC) can phosphorylate and help in regulating Set2 levels after DSB. For RNAPII, the degradation can be triggered by the same Def1-Rsp5 system, which targets it for degradation after UV-damage. To get at these questions, we can use the MultiDsk

protein, which is an affinity tag consisting of multiple ubiquitin-binding domains from the Dsk1 protein in yeast. We can pull immuno-affinity precipitate the ubiquitinated proteome with the multi-dsk tag and then immunoblot for RNAPII. This experiment can be performed in wt and mutant strains (such as Def1delete, Rsp5 temperature sensitive and other candidate E3 ubiquitin ligases). (4) What is the contribution of SETD2/H3K36me3 loss-dependent MMEJ to chromosomal aberrations in tumorigenesis? While many mechanistic questions remain, it is clear that these findings define H3K36me as a critically important and evolutionarily conserved chromatin mark in maintaining genome stability. Our studies have significantly enhanced the knowledge about the biological functions of Set2/H3K36me, raised interesting new questions relevant to genomic integrity and their connections to human health.

4.3 Disease Relevance

The Cancer Genome Atlas (TCGA) has made significant efforts to molecularly characterize cancer genomes, in order to understand the genetic basis for tumorigenesis and develop new therapeutic regimens. This massive effort has resulted in the realization that chromatin components are one of the most frequently mutated genes, with significant correlations to patient prognosis. Loss of function mutations, loss of heterozygosity and over-expression of several chromatin modifiers have come to define the epigenetic landscape of the cancer genome. Effects on mis-regulated transcriptional landscape drive some of the phenotypes seen after mis-regulation of chromatin factors, but that is not the complete story. A large number of these chromatin modifiers are major regulators of genomic integrity and inappropriate chromatin modification/ regulation will impinge on the mutational potential, landscape and the downstream adaptability of cancer cells. One such chromatin modifier is the human homolog of Set2, SETD2, which is responsible for H3K36me3 in human cells.

SETD2 is significantly mutated in clear cell renal carcinoma (ccRCC), a type of kidney cancer, glioblastoma multiformae (GBMs) and bladder cancer. Curiously, another important driver mutation in GBM is the mutation of lysine 9 and 36 of histone H3 variant, H3F3A, to Methionine, which results in loss of H3K9me3 and H3K36me3 in these cells. Some of the functions in SETD2 lacking ccRCC cells as well as H3K36M mutant cells arise from the effect of SETD2 on alternative splicing. However, work from Guo Min-Li and Tim Humphrey clearly shows that loss of H3K36me3 increases the mutational landscape of ccRCC cells- through mis-regulated mismatch repair and double strand break repair. In terms of mismatch repair, H3K36me3 was shown to recruit MSH6, through a PWWP domain, and stabilize and facilitate its activity on S-phase chromatin. Thus, presence of SETD2 resulted in more proficient mismatch repair in S-phase in human cells. Work from the Humphrey lab shows that H3K36me3 recruits PSIP1/p75/LEDGEF protein, which facilitates the recruitment of human CTIP protein. CTIP is required for resection after DSB and hence mis-regulated CTIP recruitment increases the cell's ability to shunt the DSB from HR to MMEJ and thereby increases genomic abnormalities. Interestingly, even the over-expression of the demethylase that removes H3K36me3, JMJD2A, is tumorigenic. Seminal work from the Whetstine laboratory reveals that over-expression of JMJD2A results in H3K36me3, along with H3K9me3, and hence results in open chromatin structure. Such an open chromatin structure is conducive for recruitment of MCM complex to certain areas of the genome, resulting in re- replication of the genome. In addition, even H3K36me2 has emerged as a major regulator of genome integrity and transcription regulation in human cells. H3K36me2 catalyzed by the non-SET domain containing H3K36me2 transferase, SETMAR, helps in recruitment of human Ku70-80 and thus promote NHEJ-dependent repair of DSBs. In human cells, NSD2 also regulates H3K36me2 and over expression of NSD2 correlated

with more aggressive tumors in mouse models and over-all mis-regulated transcription of NF- κ B regulated transcripts. In sum, over the past years, our work and others' have established Set2 and H3K36 methylation as a major regulator of genome function- both in transcription and DNA repair and paved the way for appropriate targeting of this critical chromatin modifier in human disease, most critically in cancer.

4.4. Conclusion for chapter 3:

A canonical nucleosome consists of two copies each of histones- H2A, H2B, H3 and H4 ⁴. They form what are called core histones and are synthesized in a replication-dependent manner ⁴⁵. On the contrary, different versions of these core histones exist in all eukaryotes, which gets incorporated in a time and genomic location dependent manner. Histone H⁴⁴⁴⁴⁴²²2A has the most number of variants, among all and Htz1 (mammalian H2A.Z) is one of the most conserved variant from yeast to human ⁴¹. It is ~60% identical to the canonical histone H2A but the difference between H2A and Htz1 results in very profound changes in the biophysical characters of the Htz1-containing nucleosomes ⁴¹. For these regions, histone variants, in general, and Htz1, in particular, acts as a bookmark for the genome. Htz1 is present at the -1 and +1 nucleosomes and sub-telomeric heterochromatin. Htz1 is typically depleted in the gene bodies ⁴⁶⁻⁴⁸. The idea behind the presence of Htz1 at -1 and +1 nucleosome is to allow for a more easily dissociable nucleosome, such that transcription activation can be facilitated. In addition, Htz1 deposition is also regulated around a double-strand break and centromeres ^{94,114}.

The machinery for the deposition of Htz1 in budding yeast involves a myriad number of histone acetyltransferases, histone chaperones and ATP-dependent chromatin remodeling ⁹⁴. Deposition of Htz1 in the chromatin is driven by a sequential set of events involving the import of Htz1-H2B dimer into the nucleus with the help of Nap1 histone chaperone ⁹⁴. Subsequently,

Nap1 is supposed to deliver Htz1-H2B to SWR1 chromatin remodeling complex⁹⁴. SWR1 is a multi-protein complex containing the actual ability to deposit histones into the chromatin, using the energy of ATP. SWR1 relies on a hierarchical binding to the linker DNA around the NFR region at the promoter and the hyperacetylated H3/H4 around the promoter^{95,96}. SWR1 complex has subunits that can physically bind to the DNS (RuvB family members). In addition, SWR1 has a facultative subunit, Bdf1, which contains bromo-domains, which bind to acetylated histones^{48,95}. Bdf1 has been shown to be interacting with acetylated histone H3/H4, one primary reason why Htz1 is restricted to the promoter region^{48,95}. In addition to the Nap1-dependent delivery of Htz1-H2B dimer to SWR1, Chz1 is another chaperone, which is specific for Htz1-H2B dimer and delivers this dimer to SWR1 for eventual deposition⁹⁹. However, the fraction of Htz1 deposition being dependent upon Nap1 or Chz1 is currently unknown. Additionally, contrary to the notion that Nap1 and Chz1 are redundantly functioning, *nap1Δ* and *chz1Δ* do not phenocopy each other on caffeine or benomyl⁹⁴.

Although a lot of stress is typically put on the deposition of histone variants, equally important is their eviction from the chromatin. This is evidenced by the observation that inappropriate deposition of the centromeric histone H3 variant, Cse4, in the chromatin results in genomic instability and there are elaborate SWI/SNF and FACT dependent mechanisms to evict the inappropriately deposited the Cse4⁹⁴. In chapter 3 of this study, we show that Htz1 is aberrantly deposited around the DSB, and which eventually results in a permissive chromatin structure and inappropriate DSB processing. In chapter 3, we provided biochemical evidence for a novel function of Nap1 and Chz1 in removing the Htz1. We showed that loss of Nap1 or Chz1 or both, increases the levels of Htz1 in the chromatin. Using molecular modeling and docking (onto a Chz1- Htz1 nucleosome), we predicted critical residues for interactions with both Chz1

and Nap1. We showed that the interaction surfaces for Chz1 and Nap1 are only partially overlapping, and therefore the two chaperones are only partially redundant in terms of their Htz1-related functions. We showed the biological significance of these residues (caffeine and 6-azauracil sensitivity). Finally, our unbiased analysis revealed a mutation in Htz1 (Y65K), which when expressed in cells, result in extremely low levels of htz1 and has slow growth phenotypes both with drugs and without drugs. Interestingly, we can show that Y65K is present in chromatin, albeit at extremely low levels and deletion of the Htz1 deposition almost completely restores the Htz1 levels and viability to different stressors.

In addition, INO80 complex has been also shown to function in the eviction of Htz1 containing nucleosomes and replacing it with H2A-nucleosomes^{37,171}. After the activation of DNA damage checkpoint, INO80 complex removes Htz1 containing nucleosomes from around the DSB in favor of H2A nucleosomes³⁷. This, in turn, increases the amount of likely substrates for Mec1/Tel1 i.e. phosphorylation of H2A Serine 129 phosphorylation (Y-H2A.X). Later on the Peterson group also showed that INO80 is not only required for removal of Htz1 from chromatin around a DSB, but it is also required for removing Htz1 from non-specific places in the genome¹⁷¹. Furthermore, it was recently shown that loss of Arp5 subunit of INO80 complex, increases the amount of Htz1 present in +1 nucleosomes, genome-wide, providing another evidence that removal of histone variants from chromatin is as per much important, if not more, as their deposition⁹⁵.

4.5 Unanswered Questions and Perspective:

Studies in chapter 3 have opened up a lot of interesting questions regarding Htz1 biology and the functions of these Htz1 chaperones in cellular functions. Some of these questions, with potential experimental strategies will be discussed subsequently:

1. What areas of the genome show increased deposition of Htz1 in *nap1del* and *chz1 del*?

Given that we show that, by immunoblot, that Htz1 levels in the chromatin in the *nap1del* and *chz1 del* is significantly more than the wild type cells. However, we do not provide any further evidence regarding the genomic locations that are most affected. One possibility is that, INO80 is primarily responsible for removing Htz1 from +1 nucleosomes near the promoter, while Nap1 and Chz1 (in conjunction with a chaperone, INO80 or something else) helps in removing Htz1 from within gene bodies. Another attractive possibility can come from the possibility that in *nap1Δ* and *chz1Δ*, the Htz1 enrichment is coming from centromere, telomere and other heterochromatic environment. The second possibility is supported by the observation that *nap1Δ* and *chz1Δ* have sensitivities to microtubule depolymerizing agent, Benomy, arresting yeast cells in G2/M. To get at either possibility, we can isolate the MNase-digested chromatin (producing only mono-nucleosome fractions) and then perform a ChIP followed by high-throughput sequencing experiment (ChIP-seq) for Htz1. We have already standardized the procedures for MNase-ChIP for Htz1 in wild type, *htz1Δ*, *nap1Δ*, *chz1Δ* and *nap1Δchz1Δ* and we hope to address this question in the near future.

2. Neither Nap1 nor Chz1 have an enzymatic activity that can allow them to dismantle an Htz1-containing nucleosome and exchange it out of the chromatin. This raises the possibility that Nap1 and Chz1 are working in conjunction with another chaperone. One

way to address this possibility is to observe functional interactions (genetic and physical) between *NAPI*, *CHZI* and canonical chaperones Htz1 such as *SWR1*, *INO80* and *FUN30*. If Nap1 and Chz1 functions through any of these canonical chaperones, we would be able to identify a complex with Nap1-Htz1- and one of these (or other candidate chaperones) by using co-immunoprecipitation experiments.

3. We have shown that Y65K is expressed, at the protein level, at extremely low levels, but it is still deposited in the chromatin. We have not yet shown the ability of this mutant version of Htz1 to bind to SWR1 or other Htz1-depositing chaperones. This can be tested by co-immunoprecipitation experiments between Y65K and components of SWR1 complex. We can follow this up with a ChIP-seq experiment for Htz1 (Y65K) to identify the regions where Y65K can get deposited in the chromatin. This will reveal the fundamental reason why the Y65K mutant is slow growing and is sick in response to multiple stressors, typically to a greater extent than an *htz1 del*.

Histone variants have emerged as a critical regulator of transcription, heterochromatin structure, genome maintenance and cell cycle regulation. In line with these findings, mutations in the H3.3 variant of histone H3, H3.3K9M and H3.3K36M, are driver mutations for pediatric glioblastoma multiformae (GBMs)^{42,52-54}. Additionally, H2A.Z deletion is embryonically lethal in mammals thereby revealing the major role H2A.Z plays in organismal development⁹⁴ and emphasizing the multi-faceted function of H2A.Z in cellular processes.

Table 5. LIST OF YEAST STRAINS USED IN CHAPTER 2

Strains	Relevant Genotype	Source
BY4741	MATa <i>his3Δ0 leu2Δ0 met15Δ0 ura3Δ0</i>	Open Biosystems
<i>set2Δ</i>	MATa <i>his3Δ0 leu2Δ0 met15Δ0 ura3Δ0 set2Δ::NATMX</i>	This study
<i>yku70Δset2Δ</i>	MATa <i>his3Δ0 leu2Δ0 met15Δ0 ura3Δ0 yku70Δ::HPHset2Δ::NATMX</i>	This study
<i>asf1Δset2Δ</i>	MATa <i>his3Δ0 leu2Δ0 met15Δ0 ura3Δ0 asf1Δ::KANMXset2Δ::NATMX</i>	This study
<i>rad51Δset2Δ</i>	MATa <i>his3Δ0 leu2Δ0 met15Δ0 ura3Δ0 rad51Δ::KANMXset2Δ::NATMX</i>	this study
JKM179	<i>HOΔ, hmlΔ::ADE1, MATalpha, hmrΔ::ADE1, ade1-100, leu2,3-112, lys5, trp::hisG, ura3-52, ade3::GAL::HO</i>	James Haber, Brandeis University
JKM179 <i>set2Δ</i>	<i>HOΔ, hmlΔ::ADE1, MATalpha, hmrΔ::ADE1, ade1-100, leu2,3-112, lys5, trp::hisG, ura3-52, ade3::GAL::HO set2Δ::KANMX</i>	This study
JKM179 <i>yku70Δ</i>	<i>HOΔ, hmlΔ::ADE1, MATalpha, hmrΔ::ADE1, ade1-100, leu2,3-112, lys5, trp::hisG, ura3-52, ade3::GAL::HO yku70Δ::KANMX</i>	This study

JKM179yKu80-9Myc	<i>HOΔ, hmlΔ::ADE1, MATalpha, hmrΔ::ADE1, ade1-100, leu2,3-112, lys5, trp::hisG, ura3-52, ade3::GAL::HO YKU80::YKU80-9MYC::KAN</i>	This study
JKM179yKu80-9Myc	<i>HOΔ, hmlΔ::ADE1, MATalpha, hmrΔ::ADE1, ade1-100, leu2,3-112, lys5, trp::hisG, ura3-52, ade3::GAL::HO YKU80::YKU80-9MYC::KANset2Δ::HPH</i>	This study
WT (H3-H4 shuffle; WZY42)	<i>MATa, ura3-52, lys2-801, ade2-101, trp1Δ63, his3Δ200, leu2Δ1, hht1- hhf1::pWZ405-F2F9-LEU2, hht2- hhf2::pWZ403-F4F10-HIS3, Ycp50-copyII (HHT2-HHF2, URA3+)</i>	Zhang <i>et.al</i> ; EMBO Journal; 17-11; 3155-3167, 1998
H3K36A	same as above, except <i>Ycp50-copyII (HHT2K36A-HHF2, TRP+)</i>	Zhang <i>et.al</i> ; EMBO Journal; 17-11; 3155-3167, 1998
WT (H3-H4 shuffle)	<i>MATa his3Δ200 leu2Δ1 ura3-52 trp1Δ63 lys2-128δ (hht1-hhf1)Δ::LEU2 (hht2- hhf2)Δ::HIS3 Ty912Δ35-lacZ::his4 <pDM9></i>	Duina And Winston; MCB; 24; 2; 561-572
K36A	<i>MATa his3Δ200 leu2Δ1 ura3-52 trp1Δ63 lys2-128δ (hht1-hhf1)Δ::LEU2 (hht2- hhf2)Δ::HIS3 Ty912Δ35-lacZ::his4 <pK36A></i>	Jerry L. Workman, Stowers Institute,
K56R	<i>MATa his3Δ200 leu2Δ1 ura3-52 trp1Δ63 lys2-128δ (hht1-hhf1)Δ::LEU2 (hht2- hhf2)Δ::HIS3 Ty912Δ35-lacZ::his4 <pK56R></i>	Jerry L. Workman, Stowers Institute,
K36AK56R	<i>MATa his3Δ200 leu2Δ1 ura3-52 trp1Δ63 lys2-128δ (hht1-hhf1)Δ::LEU2 (hht2- hhf2)Δ::HIS3</i>	Jerry L. Workman, Stowers Institute,

	<i>Ty912Δ35-lacZ::his4 <pK36AK56R></i>	
DY150	<i>MATa ade2 can1 his3 leu2 trp1 ura3</i> (W303)	David Stillman, University of Utah
<i>htz1Δ</i>	as above except <i>htz1Δ::KanMX</i>	David Stillman, University of Utah
<i>set2Δ</i>	DY150 <i>set2Δ::Hph</i>	This study
<i>htz1Δset2Δ</i>	DY150 <i>set2Δ::Hph htz1Δ::KanMX</i>	this study
YMS196 <i>set2Δ</i>	YMS196 except <i>set2Δ::NATMX</i>	YMS196 obtained from Nevan Krogan, UCSF
SP1173 WT (<i>S.pombe</i>)	<i>h- leu1-32 his2 ura4 ade6-216</i>	Shiv Grewal, NCI
SP1173 <i>set2Δ</i> (<i>S.pombe</i>)	same as above except <i>set2Δ::KanMX</i>	Raghuvar Dronamraju and Brian Strahl, unpublished
KSC1785	<i>MATa-inc ADH4cs::HIS2 ade1 his2 leu2 trp1 ura3</i> (<i>bar1Δ::NATMX</i>)	Nakada <i>et.al</i> Genes and Development, 2003; 17(16) 1957- 1962)

KSC1785set2Δ	same as above except <i>set2Δ::HpHMX</i> and <i>bar1Δ::NA TMX</i>	this study
W303	<i>MATa ade2 can1 his3 leu2 trp1 ura3</i>	Strahl lab
spt16-11	<i>MATa spt16-11 ade2 can1 his3 leu2 lys2 met15 trp1 ura3</i>	David Stillman, University of Utah (DY8107)
set2Δ	<i>MATa ade2 can1 his3 leu2 trp1 ura3 set2Δ::HpHMX</i>	Stephen McDaniel and Brian Strahl, unpublished
spt16-11set2Δ (YSM167)	<i>MATa spt16-11 set2::HpHMX ade2 can1 his3 leu2 ura3</i>	Stephen McDaniel and Brian Strahl, unpublished
W3031A	<i>MATa leu2-3,112 his3-11,15 ade2-1 ura3-1 trp1-1 can1-100</i>	Taschner <i>et.al</i> ; Molecular and Cellular Biology; 2010; 436– 446
JSY1112	<i>MATa leu2-3,112 his3-11,15 ade2-1 ura3-1 trp1-1 can1-100 mec1::HIS3 sml1::TRP1</i>	Taschner <i>et.al</i> ; Molecular and Cellular Biology; 2010; 436– 446
JSY1113	<i>MATa leu2-3,112 his3-11,15 ade2-1 ura3-1 trp1-1 can1-100 chk1 ::HIS3</i>	Taschner <i>et.al</i> ; Molecular and Cellular Biology;

		2010; 436– 446
JSY1114	<i>MATa leu2-3,112 his3-11,15 ade2-1 ura3-1 trp1-1 can1-100 rad53::HIS3 sml1::TRP1</i>	Taschner <i>et.al</i> ; Molecular and Cellular Biology; 2010; 436– 446
JKM139set2Δ	<i>MATa hmrΔ::ADE1 hmlΔ::ADE1 ade1-100 leu2-3,112 lys5 trp1::hisG ura3-52 ade3::GAL-HOset2Δ::KANbar1Δ::NAT</i>	This study
JKM139	<i>MATa hmrΔ::ADE1 hmlΔ::ADE1 ade1-100 leu2-3,112 lys5 trp1::hisG ura3-52 ade3::GAL-Hobar1Δ::NATMX</i>	James Haber, Brandeis University, <i>bar1Δ::NAT</i> was performed in this study.
<i>rad59Δset2Δ</i>	<i>MATa his3Δ0 leu2Δ0 met15Δ0 ura3Δ0 rad59Δ::KANMXset2Δ::NA TMX</i>	This study

Table 6. LIST OF YEAST STRAINS USED IN CHAPTER 3

Strains	Relevant GenotypeSource
BY4741	MAT a (his3-D1 leu2-D0 met15-D0 ura3-D0)
	Open Biosystems
YMP210	MAT a (his3-D1 leu2-D0 met15-D0 ura3-D0), plus pRS316 (<i>CEN6 URA</i>)
	This study
YMP050	MATa (his3-D1 leu2-D0 met15-D0 ura3-D0; htz1D::KanMX4)
	Open Biosystems
YMP295	MATa (his3-D1 leu2-D0 met15-D0 ura3-D0; nap1D::KanMX4)
	Open Biosystems
YMP211	MATa (his3-D1 leu2-D0 met15-D0 ura3-D0; chz1D::KanMX4)
	Open Biosystems
YMP351	MATa (his3-D1 leu2-D0 met15-D0 ura3-D0; swc2D::KanMX4)
	Open Biosystems
YMP179	MATa (his3-D1 leu2-D0 met15-D0 ura3-D0; swr1D::KanMX4)
	Open Biosystems
YMP296	MATa (his3-D1 leu2-D0 met15-D0 ura3-D0; nap1D::KanMX4), plus pRS316 (<i>CEN6 URA</i>)
	This study
YMP293	MATa (his3-D1 leu2-D0 met15-D0 ura3-D0; swr1D::KanMX4), plus pRS316 (<i>CEN6 URA</i>)
	This study

YMP352	MATa (his3-D1 leu2-D0 met15-D0 ura3-D0; swc2D::KanMX4), plus pRS316 (<i>CEN6 URA</i>)	This study
YMP213	MATa his3-D1 leu2-D0 met15-D0 ura3-D0 CHZ1-TAP htz1D::kanMX4	This study
YMP216	MATa his3-D1 leu2-D0 met15-D0 ura3-D0 NAP1-TAP htz1D::kanMX4	This study
YMP077	Isogenic to YMP050, plus pRS316 (<i>CEN6 URA</i>)	This study
YMP065	Isogenic to YMP050, plus pMP008 (<i>CEN6 URA H2A.Z</i>)	This study
YMP286	Isogenic to YMP050, plus pMP115 (<i>CEN6 URA h2a.z L93T</i>)	This study
YMP287	Isogenic to YMP050, plus pMP116 (<i>CEN6 URA h2a.z Y65K</i>)	This study
YMP288	Isogenic to YMP050, plus pMP117 (<i>CEN6 URA h2a.z R48D</i>)	This study
YMP289	Isogenic to YMP050, plus pMP119 (<i>CEN6 URA h2a.z R39D</i>)	This study
YMP290	Isogenic to YMP050, plus pMP120 (<i>CEN6 URA h2a.z D98K</i>)	This study
YMP291	Isogenic to YMP050, plus pMP121 (<i>CEN6 URA h2a.z S53L</i>)	This study
YMP292	Isogenic to YMP050, plus pMP122 (<i>CEN6 URA h2a.z N76M</i>)	This study
YMP298	MATa (his3-D1 leu2-D0 met15-D0 ura3-D0; swr1D::KanMX4 htz1D::NatMX)	This study
YMP300	MATa (his3-D1 leu2-D0 met15-D0 ura3-D0; nap1D::KanMX4)	This study

	htz1D::NatMX)	
YMP301	MATa (his3-D1 leu2-D0 met15-D0 ura3-D0; swc2D::KanMX4 htz1D::NatMX)	This study
YMP307	Isogenic to YMP213, plus pMP008 (<i>CEN6 URA H2A.Z</i>)	This study
YMP308	Isogenic to YMP213, plus pMP115 (<i>CEN6 URA h2a.z L93T</i>)	This study
YMP310	Isogenic to YMP213, plus pMP117 (<i>CEN6 URA h2a.z R48D</i>)	This study
YMP311	Isogenic to YMP213, plus pMP119 (<i>CEN6 URA h2a.z R39D</i>)	This study
YMP313	Isogenic to YMP213, plus pMP121 (<i>CEN6 URA h2a.z S53L</i>)	This study
YMP314	Isogenic to YMP213, plus pMP122 (<i>CEN6 URA h2a.z N76M</i>)	This study
YMP316	Isogenic to YMP216, plus pMP008 (<i>CEN6 URA H2A.Z</i>)	This study
YMP317	Isogenic to YMP216, plus pMP115 (<i>CEN6 URA h2a.z L93T</i>)	This study
YMP319	Isogenic to YMP216, plus pMP117 (<i>CEN6 URA h2a.z R48D</i>)	This study
YMP320	Isogenic to YMP216, plus pMP119 (<i>CEN6 URA h2a.z R39D</i>)	This study
YMP322	Isogenic to YMP216, plus pMP121 (<i>CEN6 URA h2a.z S53L</i>)	This study
YMP323	Isogenic to YMP216, plus pMP122 (<i>CEN6 URA h2a.z N76M</i>)	This study
YMP324	Isogenic to YMP298, plus pRS316 (<i>CEN6 URA</i>)	This study
YMP325	Isogenic to YMP298, plus pMP008 (<i>CEN6 URA H2A.Z</i>)	This study

YMP326	Isogenic to YMP298, plus plasmid pMP115 (<i>CEN6 URA h2a.z L93T</i>)	This study
YMP327	Isogenic to YMP298, plus plasmid pMP116 (<i>CEN6 URA h2a.z Y65K</i>)	This study
YMP328	Isogenic to YMP298, plus plasmid pMP117 (<i>CEN6 URA h2a.z R48D</i>)	This study
YMP329	Isogenic to YMP298, plus plasmid pMP119 (<i>CEN6 URA h2a.z R39D</i>)	This study
YMP330	Isogenic to YMP298, plus plasmid pMP120 (<i>CEN6 URA h2a.z D98K</i>)	This study
YMP331	Isogenic to YMP298, plus plasmid pMP121 (<i>CEN6 URA h2a.z S53L</i>)	This study
YMP332	Isogenic to YMP298, plus plasmid pMP122 (<i>CEN6 URA h2a.z N76M</i>)	This study
YMP333	Isogenic to YMP300, plus plasmid pRS316 (<i>CEN6 URA</i>)	This study
YMP334	Isogenic to YMP300, plus plasmid pMP008 (<i>CEN6 URA H2A.Z</i>)	This study
YMP335	Isogenic to YMP300, plus plasmid pMP115 (<i>CEN6 URA h2a.z L93T</i>)	This study
YMP336	Isogenic to YMP300, plus plasmid pMP116 (<i>CEN6 URA h2a.z</i>)	This study

	<i>Y65K)</i>	
YMP337	Isogenic to YMP300, plus plasmid pMP117 (<i>CEN6 URA h2a.z R48D)</i>	This study
YMP338	Isogenic to YMP300, plus plasmid pMP119 (<i>CEN6 URA h2a.z R39D)</i>	This study
YMP339	Isogenic to YMP300, plus plasmid pMP120 (<i>CEN6 URA h2a.z D98K)</i>	This study
YMP340	Isogenic to YMP300, plus plasmid pMP121 (<i>CEN6 URA h2a.z S53L)</i>	This study
YMP341	Isogenic to YMP300, plus plasmid pMP122 (<i>CEN6 URA h2a.z N76M)</i>	This study
YMP342	Isogenic to YMP301, plus plasmid pRS316 (<i>CEN6 URA)</i>	This study
YMP343	Isogenic to YMP301, plus plasmid pMP008 (<i>CEN6 URA H2A.Z)</i>	This study
YMP344	Isogenic to YMP301, plus plasmid pMP115 (<i>CEN6 URA h2a.z L93T)</i>	This study
YMP345	Isogenic to YMP301, plus plasmid pMP116 (<i>CEN6 URA h2a.z Y65K)</i>	This study
YMP346	Isogenic to YMP301, plus plasmid pMP117 (<i>CEN6 URA h2a.z R48D)</i>	This study

YMP347	Isogenic to YMP301, plus plasmid pMP119 (<i>CEN6 URA h2a.z R39D</i>)	This study
YMP348	Isogenic to YMP301, plus plasmid pMP120 (<i>CEN6 URA h2a.z D98K</i>)	This study
YMP349	Isogenic to YMP301, plus plasmid pMP121 (<i>CEN6 URA h2a.z S53L</i>)	This study
YMP350	Isogenic to YMP301, plus plasmid pMP122 (<i>CEN6 URA h2a.z N76M</i>)	This study

FUNDING SOURCES

This work was funded by a NIH grant to B.D.S. (GM068088)

REFERENCES

- 1 Jha, D. K. & Strahl, B. D. An RNA polymerase II-coupled function for histone H3K36 methylation in checkpoint activation and DSB repair. *Nature communications* **5**, 3965, doi:10.1038/ncomms4965 (2014).
- 2 Jha, D. K., Pfister, S. X., Humphrey, T. C. & Strahl, B. D. SET-ting the stage for DNA repair. *Nature structural & molecular biology* **21**, 655-657, doi:10.1038/nsmb.2866 (2014).
- 3 Lorch, Y., LaPointe, J. W. & Kornberg, R. D. On the displacement of histones from DNA by transcription. *Cell* **55**, 743-744 (1988).
- 4 Kornberg, R. D. & Lorch, Y. Chromatin structure and transcription. *Annual review of cell biology* **8**, 563-587, doi:10.1146/annurev.cb.08.110192.003023 (1992).
- 5 Ong, C. T. & Corces, V. G. Insulators as mediators of intra- and inter-chromosomal interactions: a common evolutionary theme. *Journal of biology* **8**, 73, doi:10.1186/jbiol165 (2009).
- 6 Phillips, J. E. & Corces, V. G. CTCF: master weaver of the genome. *Cell* **137**, 1194-1211, doi:10.1016/j.cell.2009.06.001 (2009).
- 7 Hartwell, L. H. & Kastan, M. B. Cell cycle control and cancer. *Science* **266**, 1821-1828 (1994).
- 8 Nurse, P., Masui, Y. & Hartwell, L. Understanding the cell cycle. *Nature medicine* **4**, 1103-1106, doi:10.1038/2594 (1998).
- 9 Clapier, C. R. & Cairns, B. R. The biology of chromatin remodeling complexes. *Annual review of biochemistry* **78**, 273-304, doi:10.1146/annurev.biochem.77.062706.153223 (2009).
- 10 Beck, D. B. *et al.* Chromatin in the nuclear landscape. *Cold Spring Harbor symposia on quantitative biology* **75**, 11-22, doi:10.1101/sqb.2010.75.052 (2010).

- 11 Margueron, R. & Reinberg, D. Chromatin structure and the inheritance of epigenetic information. *Nature reviews. Genetics* **11**, 285-296, doi:10.1038/nrg2752 (2010).
- 12 Fnu, S. *et al.* Methylation of histone H3 lysine 36 enhances DNA repair by nonhomologous end-joining. *Proceedings of the National Academy of Sciences of the United States of America* **108**, 540-545, doi:10.1073/pnas.1013571108 (2011).
- 13 Cheung, P., Allis, C. D. & Sassone-Corsi, P. Signaling to chromatin through histone modifications. *Cell* **103**, 263-271 (2000).
- 14 Brownell, J. E. & Allis, C. D. Special HATs for special occasions: linking histone acetylation to chromatin assembly and gene activation. *Current opinion in genetics & development* **6**, 176-184 (1996).
- 15 Kuo, M. H. & Allis, C. D. Roles of histone acetyltransferases and deacetylases in gene regulation. *BioEssays : news and reviews in molecular, cellular and developmental biology* **20**, 615-626, doi:10.1002/(SICI)1521-1878(199808)20:8<615::AID-BIES4>3.0.CO;2-H (1998).
- 16 Cheung, W. L., Briggs, S. D. & Allis, C. D. Acetylation and chromosomal functions. *Current opinion in cell biology* **12**, 326-333 (2000).
- 17 Driscoll, R., Hudson, A. & Jackson, S. P. Yeast Rtt109 promotes genome stability by acetylating histone H3 on lysine 56. *Science* **315**, 649-652, doi:10.1126/science.1135862 (2007).
- 18 Voigt, P. & Reinberg, D. Histone tails: ideal motifs for probing epigenetics through chemical biology approaches. *Chembiochem : a European journal of chemical biology* **12**, 236-252, doi:10.1002/cbic.201000493 (2011).
- 19 Campos, E. I. & Reinberg, D. Histones: annotating chromatin. *Annual review of genetics* **43**, 559-599, doi:10.1146/annurev.genet.032608.103928 (2009).
- 20 Wang, Y. *et al.* Linking covalent histone modifications to epigenetics: the rigidity and plasticity of the marks. *Cold Spring Harbor symposia on quantitative biology* **69**, 161-169, doi:10.1101/sqb.2004.69.161 (2004).
- 21 Fischle, W., Wang, Y. & Allis, C. D. Histone and chromatin cross-talk. *Current opinion in cell biology* **15**, 172-183 (2003).

- 22 Jenuwein, T. & Allis, C. D. Translating the histone code. *Science* **293**, 1074-1080, doi:10.1126/science.1063127 (2001).
- 23 Strahl, B. D. & Allis, C. D. The language of covalent histone modifications. *Nature* **403**, 41-45, doi:10.1038/47412 (2000).
- 24 Turner, B. M. Histone acetylation and an epigenetic code. *BioEssays : news and reviews in molecular, cellular and developmental biology* **22**, 836-845, doi:10.1002/1521-1878(200009)22:9<836::AID-BIES9>3.0.CO;2-X (2000).
- 25 Turner, B. M. Cellular memory and the histone code. *Cell* **111**, 285-291 (2002).
- 26 Gardner, K. E., Allis, C. D. & Strahl, B. D. Operating on chromatin, a colorful language where context matters. *Journal of molecular biology* **409**, 36-46, doi:10.1016/j.jmb.2011.01.040 (2011).
- 27 Henikoff, S. & Shilatifard, A. Histone modification: cause or cog? *Trends in genetics : TIG* **27**, 389-396, doi:10.1016/j.tig.2011.06.006 (2011).
- 28 Rando, O. J. Combinatorial complexity in chromatin structure and function: revisiting the histone code. *Current opinion in genetics & development* **22**, 148-155, doi:10.1016/j.gde.2012.02.013 (2012).
- 29 Rothbart, S. B. & Strahl, B. D. Interpreting the language of histone and DNA modifications. *Biochimica et biophysica acta* **1839**, 627-643, doi:10.1016/j.bbagr.2014.03.001 (2014).
- 30 Peterson, C. L. & Tamkun, J. W. The SWI-SNF complex: a chromatin remodeling machine? *Trends in biochemical sciences* **20**, 143-146 (1995).
- 31 Burns, L. G. & Peterson, C. L. Protein complexes for remodeling chromatin. *Biochimica et biophysica acta* **1350**, 159-168 (1997).
- 32 Peterson, C. L. ATP-dependent chromatin remodeling: going mobile. *FEBS letters* **476**, 68-72 (2000).
- 33 Peterson, C. L. & Logie, C. Recruitment of chromatin remodeling machines. *Journal of cellular biochemistry* **78**, 179-185 (2000).

- 34 Fry, C. J. & Peterson, C. L. Chromatin remodeling enzymes: who's on first? *Current biology : CB* **11**, R185-197 (2001).
- 35 Smith, C. L. & Peterson, C. L. ATP-dependent chromatin remodeling. *Current topics in developmental biology* **65**, 115-148, doi:10.1016/S0070-2153(04)65004-6 (2005).
- 36 Swygert, S. G. & Peterson, C. L. Chromatin dynamics: interplay between remodeling enzymes and histone modifications. *Biochimica et biophysica acta* **1839**, 728-736, doi:10.1016/j.bbagr.2014.02.013 (2014).
- 37 Watanabe, S. & Peterson, C. L. The INO80 family of chromatin-remodeling enzymes: regulators of histone variant dynamics. *Cold Spring Harbor symposia on quantitative biology* **75**, 35-42, doi:10.1101/sqb.2010.75.063 (2010).
- 38 Morrison, A. J. & Shen, X. Chromatin remodelling beyond transcription: the INO80 and SWR1 complexes. *Nature reviews. Molecular cell biology* **10**, 373-384, doi:10.1038/nrm2693 (2009).
- 39 Bultman, S. *et al.* A Brg1 null mutation in the mouse reveals functional differences among mammalian SWI/SNF complexes. *Molecular cell* **6**, 1287-1295 (2000).
- 40 Wu, J. I. *et al.* Regulation of dendritic development by neuron-specific chromatin remodeling complexes. *Neuron* **56**, 94-108, doi:10.1016/j.neuron.2007.08.021 (2007).
- 41 Kamakaka, R. T. & Biggins, S. Histone variants: deviants? *Genes & development* **19**, 295-310, doi:10.1101/gad.1272805 (2005).
- 42 Maze, I., Noh, K. M., Soshnev, A. A. & Allis, C. D. Every amino acid matters: essential contributions of histone variants to mammalian development and disease. *Nature reviews. Genetics* **15**, 259-271, doi:10.1038/nrg3673 (2014).
- 43 Happel, N. & Doenecke, D. Histone H1 and its isoforms: contribution to chromatin structure and function. *Gene* **431**, 1-12, doi:10.1016/j.gene.2008.11.003 (2009).
- 44 Wu, R. S., Tsai, S. & Bonner, W. M. Patterns of histone variant synthesis can distinguish G0 from G1 cells. *Cell* **31**, 367-374 (1982).

- 45 Osley, M. A. The regulation of histone synthesis in the cell cycle. *Annual review of biochemistry* **60**, 827-861, doi:10.1146/annurev.bi.60.070191.004143 (1991).
- 46 Meneghini, M. D., Wu, M. & Madhani, H. D. Conserved histone variant H2A.Z protects euchromatin from the ectopic spread of silent heterochromatin. *Cell* **112**, 725-736 (2003).
- 47 Raisner, R. M. *et al.* Histone variant H2A.Z marks the 5' ends of both active and inactive genes in euchromatin. *Cell* **123**, 233-248, doi:10.1016/j.cell.2005.10.002 (2005).
- 48 Zhang, H., Roberts, D. N. & Cairns, B. R. Genome-wide dynamics of Htz1, a histone H2A variant that poises repressed/basal promoters for activation through histone loss. *Cell* **123**, 219-231, doi:10.1016/j.cell.2005.08.036 (2005).
- 49 Shroff, R. *et al.* Distribution and dynamics of chromatin modification induced by a defined DNA double-strand break. *Current biology : CB* **14**, 1703-1711, doi:10.1016/j.cub.2004.09.047 (2004).
- 50 Wu, T. *et al.* Histone Variant H2A.X Deposition Pattern Serves as a Functional Epigenetic Mark for Distinguishing the Developmental Potentials of iPSCs. *Cell stem cell* **15**, 281-294, doi:10.1016/j.stem.2014.06.004 (2014).
- 51 Jin, C. & Felsenfeld, G. Nucleosome stability mediated by histone variants H3.3 and H2A.Z. *Genes & development* **21**, 1519-1529, doi:10.1101/gad.1547707 (2007).
- 52 Wu, G. *et al.* Somatic histone H3 alterations in pediatric diffuse intrinsic pontine gliomas and non-brainstem glioblastomas. *Nature genetics* **44**, 251-253, doi:10.1038/ng.1102 (2012).
- 53 Schwartzenuber, J. *et al.* Driver mutations in histone H3.3 and chromatin remodelling genes in paediatric glioblastoma. *Nature* **482**, 226-231, doi:10.1038/nature10833 (2012).
- 54 Khuong-Quang, D. A. *et al.* K27M mutation in histone H3.3 defines clinically and biologically distinct subgroups of pediatric diffuse intrinsic pontine gliomas. *Acta neuropathologica* **124**, 439-447, doi:10.1007/s00401-012-0998-0 (2012).
- 55 Rinn, J. L. & Chang, H. Y. Genome regulation by long noncoding RNAs. *Annual review of biochemistry* **81**, 145-166, doi:10.1146/annurev-biochem-051410-092902 (2012).

- 56 Lau, E. Non-coding RNA: Zooming in on lncRNA functions. *Nature reviews. Genetics* **15**, 574-575, doi:10.1038/nrg3795 (2014).
- 57 Gupta, R. A. *et al.* Long non-coding RNA HOTAIR reprograms chromatin state to promote cancer metastasis. *Nature* **464**, 1071-1076, doi:10.1038/nature08975 (2010).
- 58 Schaukowitch, K. *et al.* Enhancer RNA Facilitates NELF Release from Immediate Early Genes. *Molecular cell* **56**, 29-42, doi:10.1016/j.molcel.2014.08.023 (2014).
- 59 Dillon, S. C., Zhang, X., Trievel, R. C. & Cheng, X. The SET-domain protein superfamily: protein lysine methyltransferases. *Genome biology* **6**, 227, doi:10.1186/gb-2005-6-8-227 (2005).
- 60 Briggs, S. D. *et al.* Histone H3 lysine 4 methylation is mediated by Set1 and required for cell growth and rDNA silencing in *Saccharomyces cerevisiae*. *Genes & development* **15**, 3286-3295, doi:10.1101/gad.940201 (2001).
- 61 Kim, T. & Buratowski, S. Dimethylation of H3K4 by Set1 recruits the Set3 histone deacetylase complex to 5' transcribed regions. *Cell* **137**, 259-272, doi:10.1016/j.cell.2009.02.045 (2009).
- 62 Tang, Z. *et al.* SET1 and p300 act synergistically, through coupled histone modifications, in transcriptional activation by p53. *Cell* **154**, 297-310, doi:10.1016/j.cell.2013.06.027 (2013).
- 63 Barski, A. *et al.* High-resolution profiling of histone methylations in the human genome. *Cell* **129**, 823-837, doi:10.1016/j.cell.2007.05.009 (2007).
- 64 Rizzardi, L. F., Dorn, E. S., Strahl, B. D. & Cook, J. G. DNA replication origin function is promoted by H3K4 di-methylation in *Saccharomyces cerevisiae*. *Genetics* **192**, 371-384, doi:10.1534/genetics.112.142349 (2012).
- 65 Liu, H. *et al.* Phosphorylation of MLL by ATR is required for execution of mammalian S-phase checkpoint. *Nature* **467**, 343-346, doi:10.1038/nature09350 (2010).
- 66 Faucher, D. & Wellinger, R. J. Methylated H3K4, a transcription-associated histone modification, is involved in the DNA damage response pathway. *PLoS genetics* **6**, doi:10.1371/journal.pgen.1001082 (2010).

- 67 Sollier, J. *et al.* Set1 is required for meiotic S-phase onset, double-strand break formation and middle gene expression. *The EMBO journal* **23**, 1957-1967, doi:10.1038/sj.emboj.7600204 (2004).
- 68 Borde, V. *et al.* Histone H3 lysine 4 trimethylation marks meiotic recombination initiation sites. *The EMBO journal* **28**, 99-111, doi:10.1038/emboj.2008.257 (2009).
- 69 Green, E. M., Mas, G., Young, N. L., Garcia, B. A. & Gozani, O. Methylation of H4 lysines 5, 8 and 12 by yeast Set5 calibrates chromatin stress responses. *Nature structural & molecular biology* **19**, 361-363, doi:10.1038/nsmb.2252 (2012).
- 70 van Leeuwen, F., Gafken, P. R. & Gottschling, D. E. Dot1p modulates silencing in yeast by methylation of the nucleosome core. *Cell* **109**, 745-756 (2002).
- 71 Lazzaro, F. *et al.* Histone methyltransferase Dot1 and Rad9 inhibit single-stranded DNA accumulation at DSBs and uncapped telomeres. *The EMBO journal* **27**, 1502-1512, doi:10.1038/emboj.2008.81 (2008).
- 72 Nguyen, A. T. & Zhang, Y. The diverse functions of Dot1 and H3K79 methylation. *Genes & development* **25**, 1345-1358, doi:10.1101/gad.2057811 (2011).
- 73 Nguyen, A. T. *et al.* DOT1L regulates dystrophin expression and is critical for cardiac function. *Genes & development* **25**, 263-274, doi:10.1101/gad.2018511 (2011).
- 74 Venkatesh, S. & Workman, J. L. Set2 mediated H3 lysine 36 methylation: regulation of transcription elongation and implications in organismal development. *Wiley interdisciplinary reviews. Developmental biology* **2**, 685-700, doi:10.1002/wdev.109 (2013).
- 75 Strahl, B. D. *et al.* Set2 is a nucleosomal histone H3-selective methyltransferase that mediates transcriptional repression. *Molecular and cellular biology* **22**, 1298-1306 (2002).
- 76 Lawrence, M. S. *et al.* Discovery and saturation analysis of cancer genes across 21 tumour types. *Nature* **505**, 495-501, doi:10.1038/nature12912 (2014).
- 77 Youdell, M. L. *et al.* Roles for Ctk1 and Spt6 in regulating the different methylation states of histone H3 lysine 36. *Molecular and cellular biology* **28**, 4915-4926, doi:10.1128/MCB.00001-08 (2008).

- 78 Kizer, K. O. *et al.* A novel domain in Set2 mediates RNA polymerase II interaction and couples histone H3 K36 methylation with transcript elongation. *Molecular and cellular biology* **25**, 3305-3316, doi:10.1128/MCB.25.8.3305-3316.2005 (2005).
- 79 Fuchs, S. M., Kizer, K. O., Braberg, H., Krogan, N. J. & Strahl, B. D. RNA polymerase II carboxyl-terminal domain phosphorylation regulates protein stability of the Set2 methyltransferase and histone H3 di- and trimethylation at lysine 36. *The Journal of biological chemistry* **287**, 3249-3256, doi:10.1074/jbc.M111.273953 (2012).
- 80 Buratowski, S. Progression through the RNA polymerase II CTD cycle. *Molecular cell* **36**, 541-546, doi:10.1016/j.molcel.2009.10.019 (2009).
- 81 Keogh, M. C. *et al.* Cotranscriptional set2 methylation of histone H3 lysine 36 recruits a repressive Rpd3 complex. *Cell* **123**, 593-605, doi:10.1016/j.cell.2005.10.025 (2005).
- 82 Joshi, A. A. & Struhl, K. Eaf3 chromodomain interaction with methylated H3-K36 links histone deacetylation to Pol II elongation. *Molecular cell* **20**, 971-978, doi:10.1016/j.molcel.2005.11.021 (2005).
- 83 Carrozza, M. J. *et al.* Histone H3 methylation by Set2 directs deacetylation of coding regions by Rpd3S to suppress spurious intragenic transcription. *Cell* **123**, 581-592, doi:10.1016/j.cell.2005.10.023 (2005).
- 84 Govind, C. K. *et al.* Phosphorylated Pol II CTD recruits multiple HDACs, including Rpd3C(S), for methylation-dependent deacetylation of ORF nucleosomes. *Molecular cell* **39**, 234-246, doi:10.1016/j.molcel.2010.07.003 (2010).
- 85 Venkatesh, S. *et al.* Set2 methylation of histone H3 lysine 36 suppresses histone exchange on transcribed genes. *Nature* **489**, 452-455, doi:10.1038/nature11326 (2012).
- 86 Smolle, M. *et al.* Chromatin remodelers Isw1 and Chd1 maintain chromatin structure during transcription by preventing histone exchange. *Nature structural & molecular biology* **19**, 884-892, doi:10.1038/nsmb.2312 (2012).
- 87 Pryde, F. *et al.* H3 k36 methylation helps determine the timing of cdc45 association with replication origins. *PloS one* **4**, e5882, doi:10.1371/journal.pone.0005882 (2009).
- 88 Luco, R. F. *et al.* Regulation of alternative splicing by histone modifications. *Science* **327**, 996-1000, doi:10.1126/science.1184208 (2010).

- 89 Guo, R. *et al.* BS69/ZMYND11 Reads and Connects Histone H3.3 Lysine 36 Trimethylation-Decorated Chromatin to Regulated Pre-mRNA Processing. *Molecular cell*, doi:10.1016/j.molcel.2014.08.022 (2014).
- 90 Li, F. *et al.* The histone mark H3K36me3 regulates human DNA mismatch repair through its interaction with MutSalpha. *Cell* **153**, 590-600, doi:10.1016/j.cell.2013.03.025 (2013).
- 91 Pfister, S. X. *et al.* SETD2-dependent histone H3K36 trimethylation is required for homologous recombination repair and genome stability. *Cell reports* **7**, 2006-2018, doi:10.1016/j.celrep.2014.05.026 (2014).
- 92 Bell, O. *et al.* Localized H3K36 methylation states define histone H4K16 acetylation during transcriptional elongation in *Drosophila*. *The EMBO journal* **26**, 4974-4984, doi:10.1038/sj.emboj.7601926 (2007).
- 93 Lhoumaud, P. *et al.* Insulators recruit histone methyltransferase dMes4 to regulate chromatin of flanking genes. *The EMBO journal* **33**, 1599-1613, doi:10.15252/emboj.201385965 (2014).
- 94 Billon, P. & Cote, J. Precise deposition of histone H2A.Z in chromatin for genome expression and maintenance. *Biochimica et biophysica acta* **1819**, 290-302 (2013).
- 95 Yen, K., Vinayachandran, V. & Pugh, B. F. SWR-C and INO80 chromatin remodelers recognize nucleosome-free regions near +1 nucleosomes. *Cell* **154**, 1246-1256, doi:10.1016/j.cell.2013.08.043 (2013).
- 96 Ranjan, A. *et al.* Nucleosome-free region dominates histone acetylation in targeting SWR1 to promoters for H2A.Z replacement. *Cell* **154**, 1232-1245, doi:10.1016/j.cell.2013.08.005 (2013).
- 97 Luk, E. *et al.* Stepwise histone replacement by SWR1 requires dual activation with histone H2A.Z and canonical nucleosome. *Cell* **143**, 725-736, doi:10.1016/j.cell.2010.10.019 (2010).
- 98 Gkikopoulos, T. *et al.* The SWI/SNF complex acts to constrain distribution of the centromeric histone variant Cse4. *The EMBO journal* **30**, 1919-1927, doi:10.1038/emboj.2011.112 (2011).

- 99 Luk, E. *et al.* Chz1, a nuclear chaperone for histone H2AZ. *Molecular cell* **25**, 357-368, doi:10.1016/j.molcel.2006.12.015 (2007).
- 100 Hoeijmakers, J. H. DNA damage, aging, and cancer. *The New England journal of medicine* **361**, 1475-1485, doi:10.1056/NEJMra0804615 (2009).
- 101 Boiteux, S. & Jinks-Robertson, S. DNA repair mechanisms and the bypass of DNA damage in *Saccharomyces cerevisiae*. *Genetics* **193**, 1025-1064, doi:10.1534/genetics.112.145219 (2013).
- 102 Kunkel, T. A. & Erie, D. A. DNA mismatch repair. *Annual review of biochemistry* **74**, 681-710, doi:10.1146/annurev.biochem.74.082803.133243 (2005).
- 103 Symington, L. S. & Gautier, J. Double-strand break end resection and repair pathway choice. *Annual review of genetics* **45**, 247-271, doi:10.1146/annurev-genet-110410-132435 (2011).
- 104 Langerak, P. & Russell, P. Regulatory networks integrating cell cycle control with DNA damage checkpoints and double-strand break repair. *Philosophical transactions of the Royal Society of London. Series B, Biological sciences* **366**, 3562-3571, doi:10.1098/rstb.2011.0070 (2011).
- 105 Chapman, J. R., Taylor, M. R. & Boulton, S. J. Playing the end game: DNA double-strand break repair pathway choice. *Molecular cell* **47**, 497-510, doi:10.1016/j.molcel.2012.07.029 (2012).
- 106 Zimmermann, M., Lottersberger, F., Buonomo, S. B., Sfeir, A. & de Lange, T. 53BP1 regulates DSB repair using Rif1 to control 5' end resection. *Science* **339**, 700-704, doi:10.1126/science.1231573 (2013).
- 107 Di Virgilio, M. *et al.* Rif1 prevents resection of DNA breaks and promotes immunoglobulin class switching. *Science* **339**, 711-715, doi:10.1126/science.1230624 (2013).
- 108 Chapman, J. R. *et al.* RIF1 is essential for 53BP1-dependent nonhomologous end joining and suppression of DNA double-strand break resection. *Molecular cell* **49**, 858-871, doi:10.1016/j.molcel.2013.01.002 (2013).

- 109 Papamichos-Chronakis, M. & Peterson, C. L. Chromatin and the genome integrity network. *Nature reviews. Genetics* **14**, 62-75, doi:10.1038/nrg3345 (2013).
- 110 Tsabar, M. & Haber, J. E. Chromatin modifications and chromatin remodeling during DNA repair in budding yeast. *Current opinion in genetics & development* **23**, 166-173, doi:10.1016/j.gde.2012.11.015 (2013).
- 111 Jazayeri, A., McAINSH, A. D. & JACKSON, S. P. *Saccharomyces cerevisiae* Sin3p facilitates DNA double-strand break repair. *Proceedings of the National Academy of Sciences of the United States of America* **101**, 1644-1649, doi:10.1073/pnas.0304797101 (2004).
- 112 Miller, K. M. *et al.* Human HDAC1 and HDAC2 function in the DNA-damage response to promote DNA nonhomologous end-joining. *Nature structural & molecular biology* **17**, 1144-1151, doi:10.1038/nsmb.1899 (2010).
- 113 Xu, Y., Xu, C. & Price, B. D. Mechanistic links between ATM and histone methylation codes during DNA repair. *Progress in molecular biology and translational science* **110**, 263-288, doi:10.1016/B978-0-12-387665-2.00010-9 (2012).
- 114 Kalocsay, M., Hiller, N. J. & Jentsch, S. Chromosome-wide Rad51 spreading and SUMO-H2A.Z-dependent chromosome fixation in response to a persistent DNA double-strand break. *Molecular cell* **33**, 335-343, doi:10.1016/j.molcel.2009.01.016 (2009).
- 115 Xu, Y. *et al.* Histone H2A.Z controls a critical chromatin remodeling step required for DNA double-strand break repair. *Molecular cell* **48**, 723-733, doi:10.1016/j.molcel.2012.09.026 (2012).
- 116 Hoeijmakers, J. H. DNA damage, aging, and cancer. *N Engl J Med* **361**, 1475-1485, doi:10.1056/NEJMra0804615 (2009).
- 117 Papamichos-Chronakis, M. & Peterson, C. L. Chromatin and the genome integrity network. *Nat Rev Genet* **14**, 62-75, doi:10.1038/nrg3345 (2013).
- 118 Azvolinsky, A., Giresi, P. G., Lieb, J. D. & Zakian, V. A. Highly transcribed RNA polymerase II genes are impediments to replication fork progression in *Saccharomyces cerevisiae*. *Mol Cell* **34**, 722-734, doi:10.1016/j.molcel.2009.05.022 (2009).

- 119 Bermejo, R., Lai, M. S. & Foiani, M. Preventing replication stress to maintain genome stability: resolving conflicts between replication and transcription. *Mol Cell* **45**, 710-718, doi:10.1016/j.molcel.2012.03.001 (2012).
- 120 Strahl, B. D. *et al.* Set2 is a nucleosomal histone H3-selective methyltransferase that mediates transcriptional repression. *Mol Cell Biol* **22**, 1298-1306 (2002).
- 121 Kizer, K. O. *et al.* A novel domain in Set2 mediates RNA polymerase II interaction and couples histone H3 K36 methylation with transcript elongation. *Mol Cell Biol* **25**, 3305-3316, doi:10.1128/MCB.25.8.3305-3316.2005 (2005).
- 122 Xiao, T. *et al.* Phosphorylation of RNA polymerase II CTD regulates H3 methylation in yeast. *Genes Dev* **17**, 654-663, doi:10.1101/gad.1055503 (2003).
- 123 Wagner, E. J. & Carpenter, P. B. Understanding the language of Lys36 methylation at histone H3. *Nat Rev Mol Cell Biol* **13**, 115-126, doi:10.1038/nrm3274 (2012).
- 124 Li, B., Howe, L., Anderson, S., Yates, J. R., 3rd & Workman, J. L. The Set2 histone methyltransferase functions through the phosphorylated carboxyl-terminal domain of RNA polymerase II. *J Biol Chem* **278**, 8897-8903, doi:10.1074/jbc.M212134200 (2003).
- 125 Joshi, A. A. & Struhl, K. Eaf3 chromodomain interaction with methylated H3-K36 links histone deacetylation to Pol II elongation. *Mol Cell* **20**, 971-978, doi:10.1016/j.molcel.2005.11.021 (2005).
- 126 Govind, C. K. *et al.* Phosphorylated Pol II CTD recruits multiple HDACs, including Rpd3C(S), for methylation-dependent deacetylation of ORF nucleosomes. *Mol Cell* **39**, 234-246, doi:10.1016/j.molcel.2010.07.003 (2010).
- 127 Smolle, M. *et al.* Chromatin remodelers Isw1 and Chd1 maintain chromatin structure during transcription by preventing histone exchange. *Nat Struct Mol Biol* **19**, 884-892, doi:10.1038/nsmb.2312 (2012).
- 128 Moore, J. K. & Haber, J. E. Cell cycle and genetic requirements of two pathways of nonhomologous end-joining repair of double-strand breaks in *Saccharomyces cerevisiae*. *Mol Cell Biol* **16**, 2164-2173 (1996).

- 129 Winsor, T. S., Bartkowiak, B., Bennett, C. B. & Greenleaf, A. L. A DNA damage response system associated with the phosphoCTD of elongating RNA polymerase II. *PLoS One* **8**, e60909, doi:10.1371/journal.pone.0060909 (2013).
- 130 Youdell, M. L. *et al.* Roles for Ctk1 and Spt6 in regulating the different methylation states of histone H3 lysine 36. *Mol Cell Biol* **28**, 4915-4926, doi:10.1128/MCB.00001-08 (2008).
- 131 Tsukuda, T., Fleming, A. B., Nickoloff, J. A. & Osley, M. A. Chromatin remodelling at a DNA double-strand break site in *Saccharomyces cerevisiae*. *Nature* **438**, 379-383, doi:nature04148 [pii] 10.1038/nature04148 (2005).
- 132 Bandyopadhyay, S. *et al.* Rewiring of genetic networks in response to DNA damage. *Science* **330**, 1385-1389, doi:10.1126/science.1195618 (2010).
- 133 Guenole, A. *et al.* Dissection of DNA damage responses using multiconditional genetic interaction maps. *Mol Cell* **49**, 346-358, doi:10.1016/j.molcel.2012.11.023 (2013).
- 134 Tompa, R. & Madhani, H. D. Histone H3 lysine 36 methylation antagonizes silencing in *Saccharomyces cerevisiae* independently of the Rpd3S histone deacetylase complex. *Genetics* **175**, 585-593, doi:genetics.106.067751 [pii]10.1534/genetics.106.067751 (2007).
- 135 Lenstra, T. L. *et al.* The specificity and topology of chromatin interaction pathways in yeast. *Mol Cell* **42**, 536-549, doi:10.1016/j.molcel.2011.03.026 (2011).
- 136 Shroff, R. *et al.* Distribution and dynamics of chromatin modification induced by a defined DNA double-strand break. *Curr Biol* **14**, 1703-1711, doi:10.1016/j.cub.2004.09.047 (2004).
- 137 Keogh, M. C. *et al.* A phosphatase complex that dephosphorylates gammaH2AX regulates DNA damage checkpoint recovery. *Nature* **439**, 497-501, doi:nature04384 [pii] 10.1038/nature04384 (2006).
- 138 Tamburini, B. A. & Tyler, J. K. Localized histone acetylation and deacetylation triggered by the homologous recombination pathway of double-strand DNA repair. *Mol Cell Biol* **25**, 4903-4913, doi:10.1128/MCB.25.12.4903-4913.2005 (2005).

- 139 Lin, Y. Y. *et al.* A comprehensive synthetic genetic interaction network governing yeast histone acetylation and deacetylation. *Genes Dev* **22**, 2062-2074, doi:10.1101/gad.1679508 (2008).
- 140 Warmerdam, D. O. & Kanaar, R. Dealing with DNA damage: relationships between checkpoint and repair pathways. *Mutat Res* **704**, 2-11, doi:10.1016/j.mrrev.2009.12.001 (2010).
- 141 Kalocsay, M., Hiller, N. J. & Jentsch, S. Chromosome-wide Rad51 spreading and SUMO-H2A.Z-dependent chromosome fixation in response to a persistent DNA double-strand break. *Mol Cell* **33**, 335-343, doi:10.1016/j.molcel.2009.01.016 (2009).
- 142 Lazzaro, F. *et al.* Histone methyltransferase Dot1 and Rad9 inhibit single-stranded DNA accumulation at DSBs and uncapped telomeres. *Embo J* **27**, 1502-1512, doi:10.1038/emboj.2008.81 (2008).
- 143 Papamichos-Chronakis, M., Krebs, J. E. & Peterson, C. L. Interplay between Ino80 and Swr1 chromatin remodeling enzymes regulates cell cycle checkpoint adaptation in response to DNA damage. *Genes & development* **20**, 2437-2449, doi:10.1101/gad.1440206 (2006).
- 144 van Attikum, H., Fritsch, O. & Gasser, S. M. Distinct roles for SWR1 and INO80 chromatin remodeling complexes at chromosomal double-strand breaks. *Embo J* **26**, 4113-4125, doi:10.1038/sj.emboj.7601835 (2007).
- 145 Wysocki, R. *et al.* Role of Dot1-dependent histone H3 methylation in G1 and S phase DNA damage checkpoint functions of Rad9. *Mol Cell Biol* **25**, 8430-8443, doi:10.1128/MCB.25.19.8430-8443.2005 (2005).
- 146 Grenon, M. *et al.* Docking onto chromatin via the *Saccharomyces cerevisiae* Rad9 Tudor domain. *Yeast* **24**, 105-119, doi:10.1002/yea.1441 (2007).
- 147 Huyen, Y. *et al.* Methylated lysine 79 of histone H3 targets 53BP1 to DNA double-strand breaks. *Nature* **432**, 406-411, doi:10.1038/nature03114 (2004).
- 148 Costelloe, T. *et al.* The yeast Fun30 and human SMARCAD1 chromatin remodellers promote DNA end resection. *Nature* **489**, 581-584, doi:10.1038/nature11353 (2012).

- 149 Chen, X. *et al.* The Fun30 nucleosome remodeller promotes resection of DNA double-strand break ends. *Nature* **489**, 576-580, doi:10.1038/nature11355 (2012).
- 150 Jazayeri, A., McAinsh, A. D. & Jackson, S. P. *Saccharomyces cerevisiae* Sin3p facilitates DNA double-strand break repair. *Proc Natl Acad Sci U S A* **101**, 1644-1649, doi:10.1073/pnas.0304797101 (2004).
- 151 Bird, A. W. *et al.* Acetylation of histone H4 by Esa1 is required for DNA double-strand break repair. *Nature* **419**, 411-415, doi:10.1038/nature01035nature01035 [pii] (2002).
- 152 Miller, K. M. *et al.* Human HDAC1 and HDAC2 function in the DNA-damage response to promote DNA nonhomologous end-joining. *Nat Struct Mol Biol* **17**, 1144-1151, doi:10.1038/nsmb.1899 (2010).
- 153 Symington, L. S. & Gautier, J. Double-strand break end resection and repair pathway choice. *Annu Rev Genet* **45**, 247-271, doi:10.1146/annurev-genet-110410-132435 (2011).
- 154 Ginsburg, D. S., Govind, C. K. & Hinnebusch, A. G. NuA4 lysine acetyltransferase Esa1 is targeted to coding regions and stimulates transcription elongation with Gcn5. *Mol Cell Biol* **29**, 6473-6487, doi:10.1128/MCB.01033-09 (2009).
- 155 Altaf, M. *et al.* NuA4-dependent acetylation of nucleosomal histones H4 and H2A directly stimulates incorporation of H2A.Z by the SWR1 complex. *J Biol Chem* **285**, 15966-15977, doi:10.1074/jbc.M110.117069 (2010).
- 156 Heo, K. *et al.* FACT-mediated exchange of histone variant H2AX regulated by phosphorylation of H2AX and ADP-ribosylation of Spt16. *Mol Cell* **30**, 86-97, doi:10.1016/j.molcel.2008.02.029 (2008).
- 157 Formosa, T. *et al.* Defects in SPT16 or POB3 (yFACT) in *Saccharomyces cerevisiae* cause dependence on the Hir/Hpc pathway: polymerase passage may degrade chromatin structure. *Genetics* **162**, 1557-1571 (2002).
- 158 Biswas, D. *et al.* A role for Chd1 and Set2 in negatively regulating DNA replication in *Saccharomyces cerevisiae*. *Genetics* **178**, 649-659, doi:10.1534/genetics.107.084202 (2008).
- 159 Jin, C. & Felsenfeld, G. Nucleosome stability mediated by histone variants H3.3 and H2A.Z. *Genes Dev* **21**, 1519-1529, doi:10.1101/gad.1547707 (2007).

- 160 Adkins, N. L., Niu, H., Sung, P. & Peterson, C. L. Nucleosome dynamics regulates DNA processing. *Nat Struct Mol Biol* **20**, 836-842, doi:10.1038/nsmb.2585 (2013).
- 161 Aguilera, A. The connection between transcription and genomic instability. *Embo J* **21**, 195-201, doi:10.1093/emboj/21.3.195 (2002).
- 162 Gonzalez-Barrera, S., Garcia-Rubio, M. & Aguilera, A. Transcription and double-strand breaks induce similar mitotic recombination events in *Saccharomyces cerevisiae*. *Genetics* **162**, 603-614 (2002).
- 163 Chai, B., Huang, J., Cairns, B. R. & Laurent, B. C. Distinct roles for the RSC and Swi/Snf ATP-dependent chromatin remodelers in DNA double-strand break repair. *Genes Dev* **19**, 1656-1661, doi:10.1101/gad.1273105 (2005).
- 164 Luger, K., Dechassa, M. L. & Tremethick, D. J. New insights into nucleosome and chromatin structure: an ordered state or a disordered affair? *Nat Rev Mol Cell Biol* **13**, 436-447, doi:nrm3382 [pii] 10.1038/nrm3382 (2012).
- 165 Raisner, R. M. & Madhani, H. D. Patterning chromatin: form and function for H2A.Z variant nucleosomes. *Curr Opin Genet Dev* **16**, 119-124, doi:S0959-437X(06)00027-X [pii]10.1016/j.gde.2006.02.005 (2006).
- 166 Guillemette, B. & Gaudreau, L. Reuniting the contrasting functions of H2A.Z. *Biochem Cell Biol* **84**, 528-535, doi:o06-077 [pii]10.1139/o06-077 (2006).
- 167 Billon, P. & Cote, J. Precise deposition of histone H2A.Z in chromatin for genome expression and maintenance. *Biochim Biophys Acta* **1819**, 290-302, doi:S1874-9399(11)00180-5 [pii]10.1016/j.bbagr.2011.10.004 (2012).
- 168 Allis, C. D., Glover, C. V., Bowen, J. K. & Gorovsky, M. A. Histone variants specific to the transcriptionally active, amitotically dividing macronucleus of the unicellular eucaryote, *Tetrahymena thermophila*. *Cell* **20**, 609-617, doi:0092-8674(80)90307-4 [pii] (1980).
- 169 Santisteban, M. S., Kalashnikova, T. & Smith, M. M. Histone H2A.Z regulates transcription and is partially redundant with nucleosome remodeling complexes. *Cell* **103**, 411-422, doi:S0092-8674(00)00133-1 [pii] (2000).
- 170 Adam, M., Robert, F., Larochelle, M. & Gaudreau, L. H2A.Z is required for global chromatin integrity and for recruitment of RNA polymerase II under specific conditions. *Mol Cell Biol* **21**, 6270-6279 (2001).

- 171 Papamichos-Chronakis, M., Watanabe, S., Rando, O. J. & Peterson, C. L. Global regulation of H2A.Z localization by the INO80 chromatin-remodeling enzyme is essential for genome integrity. *Cell* **144**, 200-213, doi:10.1016/j.cell.2010.12.021 (2011).
- 172 Keogh, M. C. *et al.* The *Saccharomyces cerevisiae* histone H2A variant Htz1 is acetylated by NuA4. *Genes Dev* **20**, 660-665, doi:20/6/660 [pii]10.1101/gad.1388106 (2006).
- 173 Mizuguchi, G. *et al.* ATP-driven exchange of histone H2AZ variant catalyzed by SWR1 chromatin remodeling complex. *Science* **303**, 343-348, doi:10.1126/science.1090701 1090701 [pii] (2004).
- 174 Jensen, K., Santisteban, M. S., Urekar, C. & Smith, M. M. Histone H2A.Z acid patch residues required for deposition and function. *Mol Genet Genomics* **285**, 287-296, doi:10.1007/s00438-011-0604-5 (2011).
- 175 Straube, K., Blackwell, J. S., Jr. & Pemberton, L. F. Nap1 and Chz1 have separate Htz1 nuclear import and assembly functions. *Traffic* **11**, 185-197, doi:TRA1010 [pii] 10.1111/j.1600-0854.2009.01010.x (2010).
- 176 Zhou, Z. *et al.* NMR structure of chaperone Chz1 complexed with histones H2A.Z-H2B. *Nat Struct Mol Biol* **15**, 868-869, doi:nsmb.1465 [pii] 10.1038/nsmb.1465 (2008).
- 177 Natsume, R. *et al.* Structure and function of the histone chaperone CIA/ASF1 complexed with histones H3 and H4. *Nature* **446**, 338-341, doi:nature05613 [pii] 10.1038/nature05613 (2007).
- 178 English, C. M., Adkins, M. W., Carson, J. J., Churchill, M. E. & Tyler, J. K. Structural basis for the histone chaperone activity of Asf1. *Cell* **127**, 495-508, doi:S0092-8674(06)01273-6 [pii] 10.1016/j.cell.2006.08.047 (2006).
- 179 Park, Y. J. & Luger, K. The structure of nucleosome assembly protein 1. *Proc Natl Acad Sci U S A* **103**, 1248-1253, doi:0508002103 [pii] 10.1073/pnas.0508002103 (2006).
- 180 Liu, Y. *et al.* Structural analysis of Rtt106p reveals a DNA binding role required for heterochromatin silencing. *J Biol Chem* **285**, 4251-4262, doi:M109.055996 [pii] 10.1074/jbc.M109.055996 (2010).

- 181 Liu, C. P. *et al.* Structure of the variant histone H3.3-H4 heterodimer in complex with its chaperone DAXX. *Nat Struct Mol Biol* **19**, 1287-1292, doi:nsmb.2439 [pii] 10.1038/nsmb.2439 (2012).
- 182 Elsasser, S. J. *et al.* DAXX envelops a histone H3.3-H4 dimer for H3.3-specific recognition. *Nature* **491**, 560-565, doi:nature11608 [pii] 10.1038/nature11608 (2012).
- 183 Chambers, A. L. *et al.* The INO80 chromatin remodeling complex prevents polyploidy and maintains normal chromatin structure at centromeres. *Genes Dev* **26**, 2590-2603, doi:26/23/2590 [pii] 10.1101/gad.199976.112 (2012).
- 184 Dokholyan, N. V., Buldyrev, S. V., Stanley, H. E. & Shakhnovich, E. I. Discrete molecular dynamics studies of the folding of a protein-like model. *Fold Des* **3**, 577-587 (1998).
- 185 Shirvanyants, D., Ding, F., Tsao, D., Ramachandran, S. & Dokholyan, N. V. Discrete molecular dynamics: an efficient and versatile simulation method for fine protein characterization. *J Phys Chem B* **116**, 8375-8382, doi:10.1021/jp2114576 (2012).
- 186 Ding, F., Tsao, D., Nie, H. & Dokholyan, N. V. Ab initio folding of proteins with all-atom discrete molecular dynamics. *Structure* **16**, 1010-1018, doi:S0969-2126(08)00178-0 [pii] 10.1016/j.str.2008.03.013 (2008).
- 187 Ding, F. & Dokholyan, N. V. Emergence of protein fold families through rational design. *PLoS Comput Biol* **2**, e85, doi:06-PLCB-RA-0120R2 [pii] 10.1371/journal.pcbi.0020085 (2006).
- 188 Brooks, B. R. *et al.* CHARMM: A program for macromolecular energy, minimization, and dynamics calculations. *J. Comput. Chem.* **4**, 187-217 (1983).
- 189 Lazaridis, T. & Karplus, M. Effective energy function for proteins in solution. *Proteins* **35**, 133-152, doi:10.1002/(SICI)1097-0134(19990501)35:2<133::AID-PROT1>3.0.CO;2-N [pii] (1999).
- 190 Shirvanyants, D., Ding, F., Tsao, D., Ramachandran, S. & Dokholyan, N. V. Discrete Molecular Dynamics: An Efficient And Versatile Simulation Method For Fine Protein Characterization. *J Phys Chem B*, doi:10.1021/jp2114576 (2012).

- 191 Anderson, H. C. Molecular dynamics simulations at constant pressure and/or temperature. *Journal of Chemical Physics* **72**, 10 (1980).
- 192 Ding, F. & Dokholyan, N. V. Emergence of protein fold families through rational design. *PLoS Computational Biology* **2**, e85, doi:06-PLCB-RA-0120R2 [pii] 10.1371/journal.pcbi.0020085 (2006).
- 193 Yin, S., Ding, F. & Dokholyan, N. V. Modeling backbone flexibility improves protein stability estimation. *Structure* **15**, 1567-1576, doi:S0969-2126(07)00415-7 [pii] 10.1016/j.str.2007.09.024 (2007).
- 194 Yin, S., Ding, F. & Dokholyan, N. V. Eris: an automated estimator of protein stability. *Nat Methods* **4**, 466-467, doi:nmeth0607-466 [pii] 10.1038/nmeth0607-466 (2007).
- 195 Janke, C. *et al.* A versatile toolbox for PCR-based tagging of yeast genes: new fluorescent proteins, more markers and promoter substitution cassettes. *Yeast* **21**, 947-962, doi:10.1002/yea.1142 (2004).
- 196 Briggs, S. D. *et al.* Histone H3 lysine 4 methylation is mediated by Set1 and required for cell growth and rDNA silencing in *Saccharomyces cerevisiae*. *Genes & Development* **15**, 3286-3295, doi:10.1101/gad.940201 (2001).
- 197 Xiao, T. *et al.* Phosphorylation of RNA polymerase II CTD regulates H3 methylation in yeast. *Genes Dev* **17**, 654-663, doi:10.1101/gad.1055503 (2003).
- 198 Pai, C. C. *et al.* A histone H3K36 chromatin switch coordinates DNA double-strand break repair pathway choice. *Nature communications* **5**, 4091, doi:10.1038/ncomms5091 (2014).
- 199 Carvalho, S. *et al.* SETD2 is required for DNA double-strand break repair and activation of the p53-mediated checkpoint. *eLife* **3**, e02482, doi:10.7554/eLife.02482 (2014).
- 200 Aymard, F. *et al.* Transcriptionally active chromatin recruits homologous recombination at DNA double-strand breaks. *Nature structural & molecular biology* **21**, 366-374, doi:10.1038/nsmb.2796 (2014).